

Enter The DRAGON

Investigating the $^{13}\text{C}(\text{p},\gamma)^{14}\text{N}$ reaction & Using GEANT to test the DRAGON's acceptance

Aaron Matthew Bebington

A dissertation submitted to the Department of Physics at the University of Surrey
in partial fulfilment of the requirements of the degree of Master in Physics

April 2004

Supervised by Professor J. D'Auria (TRIUMF), Dr Chris Ruiz (TRIUMF),
Professor P. Walker (University of Surrey)



Abstract

The $^{13}\text{N}(\text{p},\gamma)^{14}\text{O}$ reaction is important as it determines the breakout from the CNO cycle to the HCNO cycle. Studying the $^{13}\text{C}(\text{p},\gamma)^{14}\text{N}$ reaction was important for the DRAGON facility at TRIUMF for their future analysis of the $^{13}\text{N}(\text{p},\gamma)^{14}\text{O}$ reaction, not only because pure radioactive ion beams of ^{13}N are impossible to create without contamination from ^{13}C due to the very small mass difference between these two elements, but also it was a good test for the DRAGON due to the fact that the $^{13}\text{C}(\text{p},\gamma)^{14}\text{N}$ reaction has been measured before.

Early analysis of the $^{13}\text{C}(\text{p},\gamma)^{14}\text{N}$ reaction data collected by DRAGON, showed that not all the ^{14}N recoils made it through the DRAGON separator to the end detector (an ionization chamber), because they were being clipped due to the large cone angle for this reaction. A GEANT simulation of DRAGON was used to simulate the $^{13}\text{C}(\text{p},\gamma)^{14}\text{N}$ reaction so that it could be compared to see what fraction of the recoils were being lost within the DRAGON due to this clipping, and also to see where the clipping occurred.

The creation of an ionization chamber in the GEANT simulation for the first time, meant that simulations of the $^{13}\text{C}(\text{p},\gamma)^{14}\text{N}$ reaction could test the DRAGON's acceptance also, by simulating different mistunes of the DRAGON's reference tune, in x and y position, x and y angle, and percentage of energy. These mistunes showed that the maximum acceptance for DRAGON is achieved when the beam is not mistuned in x and y position, but mistuned to -0.5% of the energy, and -1.5 mrad and -0.5 mrad in the x and y angular position respectively. They also showed that there is a large acceptance loss, with the maximum acceptance being roughly 78-79%.

“Astrophysics has always been about the extremes of knowledge. Indeed, we look to the skies, in our hope to someday look down on the Universe....”

Daniel West

Acknowledgements

This dissertation marks the end of my university experience (which started all the way back in the September of 1998), with the best piece of work that I have ever done since starting the long road of education 20 years ago. With the harsh reality of adulthood and getting “a proper job” only months away, I’d like to take this opportunity to thank a few people that made this project that I am about to report on possible and enjoyable, as well as a few other friends and family, who have always been there for me over the years.

Firstly, I would like to thank a few people that I meet last year. Dr Chris Ruiz, Dr Alison Laird, Dr Sabine Engel, Dario Gigliotti, and Mike Lamey, for their close help and support, throughout this project, and their friendship during my year at TRIUMF. Also, I like to thank Professor John D’Auria for giving me this excellent opportunity to come to TRIUMF, and experience nuclear astrophysics outside of the classroom.

I wanna also thank all autumn and summer co-op students that came to TRIUMF last year, as well as other TRIUMF employees, for making the whole experience of living and working in Canada a very enjoyable and absolutely amazing one. In particular; Catherine, Shirley, Erika, Jenny, Helen, Mat, Martin, Owen, Roz, Sandi, and Nick. To Herb and Steve for some amazing hikes across British Columbia and for an introduction to racquetball. To Chris, Mike, and Mark, for House Atreides (*“we f-ing rocked the most!”*) and to Dan for getting me into and hooked on volleyball (*“sorry I didn’t like hockey mate, but I’ll always support the Canucks!”*).

A big thankyou has to go to the Physics Department at the University of Surrey, for allowing this kid with lower than average A-level grades, to have the opportunity

to have a shot at a degree. The foundation year that the Physics Department has for students like me, is an excellent way to get more people to come to university who don't quite make the cut. The foundation year was one of the best years of my life, and I made some everlasting friendships. Hasan, Nat, Neil, Darren, and Jules, *"we had some great times guys. I wish we could go back and do it all again"*.

Thanks also to Professor Tony Clough and Dr Paddy Regan for recognizing my determination to do well, and allowing me to transfer onto the MPhys programme. *"I know I'm not a high flyer of a student, and I am truly sorry that my grades have been lower than what you expect of your MPhys students. All I can say is that I did my best"*.

On a good note, I have to give a mention to Dr Jim (Al-Khalili) and Dr Dave (Faux), two of Surrey's best physics lecturers. *"Your enthusiasm and more down-to-earth approaches in your classes, prevented us students from falling asleep (as much!)"*.

I have to obviously give a special mention to the other three Kings. Simon, Chris and Ben, *"you guys are my closest and oldest mates. Thanks for your friendship over the last 12 years. The next round of Guinness is on me!"*.

I gotta thank Hasan again for co-presenting an amazing radio show with me over the last 4 & 1/2 years, and to Andy for filling in for me while I was away in Canada. *"It's gonna be sad to say goodbye to 'Just A Rock Show'"*.

Special thanks go to Amy and Dan, for keeping in close contact with me during my year in Canada on MSN, and for coming to visit us in August. Thanks also for your support and friendship over the last two and a half years, as well as all your help in preparing this dissertation over the last year. *"Dan, you are the best guitarist I've ever known. You are the Widdle-meister! Thanks for letting me be in two bands"*.

with you and play some of those amazing songs that you've composed. It's been an awesome experience". "Amy, we drive each other up the wall, and yet we're still friends. You are such a lovely person, and work really hard. You deserve that special man (although I don't think Mr Brosnan will ever be free)".

Finishing up, I have to give a few special thankyou's.

To my mother for sacrificing her youth to have me. *"You've done a fantastic job raising me and my brothers, Mum. I hope I've made you proud".*

To Martin and Roy, for looking after Mum all these years, while I'll went off to uni to "study"!

To Justine, for bringing my father back into my life. To Dad, for your support whilst at university. And to Lucy, the new light in my life.

Of course, there are loads more friends, family and colleagues that I have to thank, but I'm running out of space. You know who you all are: Thankyou!

And last but not least, I'd like to thank the one person who was always there for me and always close by, throughout my university experience. Without her constant love and support, I would never have come as far as I have. It was her who never lost faith in me, and gave me confidence in myself to knuckle down and do even better than I thought possible. *"Elizabeth, I wish you nothing but happiness for your new life, you deserve at least that. I dedicate this dissertation to you".*

Aaron Bebington (26th April 2004)

Contents

Abstract	i
Quote	ii
Acknowledgements	iii
Contents	vi
List of Figures	viii
List of Tables	xvi
1 Introduction	1
2 Theory	3
2.1 The CNO Cycle	3
2.2 The HCNO Cycle	4
2.3 The Importance of the $^{13}\text{C}(\text{p},\gamma)^{14}\text{N}$ reaction	6
3 Experimental Equipment	7
3.1 TRIUMF	7
3.2 The DRAGON Facility	12
3.3 DRAGON's Ionization Chamber	16
3.4 Tuning The DRAGON	20
4 The $^{13}\text{C}(\text{p},\gamma)^{14}\text{N}$ reaction - Analysis of the DRAGON Data	24

4.1	MIDAS	24
4.2	Calculating the maximum cone angle for the $^{13}\text{C}(\text{p},\gamma)^{14}\text{N}$ reaction	31
4.3	Clipping	35
5	The $^{13}\text{C}(\text{p},\gamma)^{14}\text{N}$ reaction - simulations with GEANT	37
5.1	GEANT	37
5.2	The creation of the DRAGON in GEANT	37
5.3	GEANT BGO simulations	37
5.4	$^{13}\text{C}(\text{p},\gamma)^{14}\text{N}$ input file	39
5.5	Initial $^{13}\text{C}(\text{p},\gamma)^{14}\text{N}$ simulations	43
6	Design of the Ionization Chamber in GEANT	45
6.1	Creating volumes and materials in GEANT	45
6.2	Mylar and Isobutane properties	46
6.3	Initial designs of the ionization chamber (problems and solutions)	47
6.4	SRIM calculations for mylar	53
6.5	Continuation of the ionization chamber simulation	56
7	Testing DRAGON's Acceptance	66
7.1	Rebinning of histograms in GEANT	66
7.2	Effects of the straggling and energy loss in the ionization chamber	66
7.3	Adding colour to GEANT	72
7.4	Acceptance Loss	72
7.5	Final results from months of GEANT simulations	77
8	Conclusions	83

Appendices	86
-------------------	-----------

Bibliography	120
---------------------	------------

List of Figures

1	Graphical representation of the CNO cycle.	4
2	Breakout from the CNO cycle to the Hot CNO cycle, via the $^{13}\text{N}(\text{p},\gamma)^{14}\text{O}$ reaction.	5
3	TRIUMF sits in the forests of UBC, in the beautiful city of Vancouver. (Photo taken before the construction of ISAC-II).	8
4	The world's largest cyclotron, at TRIUMF. This image was taken in 1972 during construction (which started in 1969). The first beam was taken in December 1974.	9
5	A plan view of TRIUMF.	10
6	A 3D cut-away view of the ISAC experimental hall.	11
7	The DRAGON recoil mass separator.	13
8	Inside the gas target box - diagram of the DRAGON's gas target mounting.	14
9	The BGO array, (which surrounds the gas target), and the vacuum pumps.	14
10	The DRAGON, in all its glory!	16
11	The ionization chamber, during construction.	17

12	(from [17]) (a) A similar setup to the inside of the DRAGON's ionization chamber, all ion pairs are formed in the grid-cathode region. (b) The induced pulse that results from the formation of the ion pairs, a distance y from the grid. The rise of the pulse results from the attraction of the electrons, across the grid-anode region. The pulse decays back to zero with a time constant equal to RC	18
13	Location of the ionization chamber. (During the $^{13}\text{C}(p,\gamma)^{14}\text{N}$ reaction run, the ionization chamber would be placed where the DSSSD box is, at the end of the final slit box).	19
14	This CCD image was captured when tuning the gas target to the 544 keV/u ^{13}C ion beam. The Focus box to the left shows an image of the beam spot, and the spectrum to the right shows the relative intensity of the beam.	22
15	Energy histogram of the most energetic coincidence gamma rays, per event, for run 8161.	25
16	Graphical representation of the energy levels in ^{14}N . Shows the incoming Q-value for $^{13}\text{C} + p$, the center-of-mass energy, and the excited level of ^{14}N we were trying to populate.	27
17	Fitting a gaussian curve to an energy peak.	28
18	Passing run 8161 offline through the analyzer and changing the ODB to look at the sum of coincidence gamma rays.	29
19	a two-dimensional energy histogram (from run 8142) of ΔE vs E in the first anode of the ionization chamber.	29
20	Confirmation of recoils and leaky beam. a) attenuated beam tune, b)&d) normal run, c) recoil tune.	30
21	A diagram illustrating the maximum angle of the ^{14}N recoil and associated gamma ray (from the decay of the excited state, $^{14}\text{N}^*$), in the centre-of-mass reference frame. [24]	34

22	The coincidence recoil energy histogram for run 8142, a $^{13}\text{C}(\text{p},\gamma)^{14}\text{N}$ reaction which had an incoming beam energy of 558 keV/u. (Channel 860 on the energy axis, corresponds to ~ 5 MeV).	36
23	Graphical representation (plan view) of DRAGON using GEANT. . .	38
24	GEANT simulation of the probability of how many of the 8 MeV gammas are deposited in x amount of BGO crystal(s).	40
25	GEANT simulation of the BGO gamma array, looking west of the beam direction.	40
26	GEANT simulation of a 3D view of the BGO array.	41
27	Initial simulations of the $^{13}\text{C}(\text{p},\gamma)^{14}\text{N}$ reaction. Under the same parameters of run 8142, a different coincidence recoil energy histogram was found, with a peak energy 1.5 MeV larger than the actual data. .	44
28	The source file loaded before each interactive and batch versions of GEANT.	46
29	A Polyethylene Terephthalate (Mylar) molecule [31].	47
30	An isobutane molecule - 4 hydrogen atoms (blue) and 10 carbon atoms (green). [32].	48
31	Schematic drawing (from [37]) of DRAGON's final focus area.	49
32	Initial design schematic of the simulated ionization chamber. Shows the outer volume (casing) cuts through the entrance tube.	50

33	Problems with GEANT recognizing the mylar window. a) An interactive run shows the tracking of the recoil particle leaving the vacuum entrance tube (ICVT) and passing straight into the isobutane deal layer (ICDL), missing the mylar window (ICMW) all together. b) Moving the mylar window to the middle of the vacuum tube, the interactive run shows that GEANT recognizes a division within the tube, but does not pass the particle through the division (due to no energy loss) and seems to simply ‘skip it’, placing the particle after the division, allowing it to pass to the end of the tube.	52
34	part of the output from an interactive GEANT simulation of a single ^{14}N recoil going around the simulated DRAGON separator. This part of the output, shows the energy of the ^{14}N recoil as it leaves the last quadrupole (Q10 - known as Q14 in GEANT) and enters the simulated ionization chamber. The highlighted box, shows the information of the ^{14}N recoil as it passes through the mylar window (known as ICMW in GEANT).	54
35	the start of a typical SRIM output. This .txt file was the SRIM calculation output for mylar with a thickness of $0.94\ \mu\text{m}$ and a density of $1.39\ \text{g/cm}^3$ (i.e. the properties of DRAGON’s actual mylar window).	55
36	a Microsoft Excel worksheet, used to plot the output of the SRIM calculation, and to calculate the energy loss through mylar. This particular worksheet was used for the SRIM calculation of mylar with a thickness of $0.00282\ \text{cm}$ and a density of $0.04633\ \text{g/cm}^3$ (i.e. the properties of DRAGON’s GEANT simulation of the mylar window for the ionization chamber).	57
37	Code added to the <code>gustep_mitray</code> subroutine to cause straggling to the final energy data.	58

38	Final energy histogram of a simulation (run 32 - Oct 6th) of the $^{13}\text{C}(\text{p},\gamma)^{14}\text{N}$ reaction, showing a double peak structure.	58
39	Shows the positioning of the ^{14}N recoils in the ionization chamber, after a batch run (run 32 - Oct 6th).	59
40	the SRIM input for a stopping range calculation. This particular input is for ^{14}N particles at 5.2 MeV passing through 3 layers (i.e. the first 3 anodes of the ionization chamber) of 5 cm thick isobutane.	59
41	SRIM's graphical representation of the recoils as it calculates the stopping range of, in this case, 500 ^{14}N ions at 6.4 MeV in isobutane.	60
42	The stopping ranges for 5.2 MeV and 6.4 MeV respectively ^{14}N recoils in isobutane, as calculated by SRIM.	61
43	a blow-up diagram of the GEANT simulated ionization chamber (viewed from the top looking down) showing the stopped position of the ^{14}N recoils, and their distance of travel in the isobutane gas.	62
44	an interactive version of the simulation, showing the recoil particle missing the entrance tube to the ionization chamber and passing through the mother volume and into the isobutane.	62
45	Final design schematic of the simulated ionization chamber.	64
46	An interactive simulation, with the final design of the ionization chamber, showing that the recoil passes through the vacuum tube, mylar window, isobutane dead layer, and into the anode region of isobutane.	65
47	A batch simulation, with the final design of the ionization chamber, showing that the recoils all stop in one region (the Anode 2 region) in the ionization chamber.	65
48	The final energy spectrum of the recoils from a GEANT simulation of the $^{13}\text{C}(\text{p},\gamma)^{14}\text{N}$ reaction. This was run 52 which had a mistuned reference tune by 2 mrad in the negative y angular position.	67

49	The data from the histogram (ID15) in figure 48 was rebinned using the modified rescale.f subroutine, to give a more general pattern of the results.	68
50	More code added to the subroutines gustep_mitray.f (a&b) and uhinit.f (c&d) to produce more histograms about the final energy of the recoils. a)&c) is the code added to produce histogram (ID700), which shows the final energy of the recoils minus the straggling effect. b)&d) is the code added to produce histogram (ID710), which shows the energy of the recoils after they have passed round the DRAGON and before they enter the ionization chamber.	69
51	To show the effects of the energy straggling, caused by the ionization chamber, the data from histogram (ID1015) in figure 49 of the final energy of the recoils (with added straggling effects) is overlaid onto new histogram (ID701), which is the final energy of the recoils (no straggling). Both sets of data have been rebinned using the rescale.f subroutine.	70
52	The data from the histogram (ID700) for run 52, is overlaid onto histogram (ID710), to illustrate the amount of energy that the recoils lose as they pass through the mylar window of the ionization chamber. . .	71
53	The commands needed to produce a coloured histogram.	72
54	A coloured histogram, from run 52, using the commands in figure 53. The histogram illustrates the effects of the energy loss through the ionization chamber, and the straggling effects to the data.	73
55	The commands needed to colour in GEANT volumes. In this case, the mother volume of the ionization chamber (ICAC) is being coloured light blue.	74
56	Colouring all the different volumes of DRAGON simulation to distinguish where all the different parts are found.	75

57	This histogram shows the energy of the recoils at the moment of creation in the gas target. Out of 5000 triggered events, 3317 recoils occurred, for this run (run 52). Overlaying this energy data is the rebinned data (to fit with the scale of this data) from histogram (ID710), of the same run (as in figure 52), which is the energy of the recoils after they have passed around the DRAGON and before they enter the ionization chamber.	76
58	The hits.kumac file that was used to read a .end file from the end of each batch simulation (in this case, for run 52).	77
59	Blow-up diagrams of the ‘hits’ around the DRAGON after run 60. Run 60 was set to trigger 50000 events (normal runs were 5000), and was left as a perfect tune.	78
60	Results for the acceptance through the DRAGON, from the GEANT simulation of the $^{13}\text{C}(\text{p},\gamma)^{14}\text{N}$ reaction, by mistuning the reference tune in the x position. Maximum acceptance when reference tune is not mistuned.	79
61	Results for the acceptance through the DRAGON, from the GEANT simulation of the $^{13}\text{C}(\text{p},\gamma)^{14}\text{N}$ reaction, by mistuning the reference tune in the y position. Maximum acceptance when reference tune is not mistuned.	80
62	Results for the acceptance through the DRAGON, from the GEANT simulation of the $^{13}\text{C}(\text{p},\gamma)^{14}\text{N}$ reaction, by mistuning the reference tune in percentage of energy. Maximum acceptance when reference tune is mistuned by -0.5% in energy.	80
63	Results for the acceptance through the DRAGON, from the GEANT simulation of the $^{13}\text{C}(\text{p},\gamma)^{14}\text{N}$ reaction, by mistuning the reference tune in the x angle. Maximum acceptance when reference tune is mistuned by -1.5 mrad in x angular position.	81

64	Results for the acceptance through the DRAGON, from the GEANT simulation of the $^{13}\text{C}(\text{p},\gamma)^{14}\text{N}$ reaction, by mistuning the reference tune in the y angle. Maximum acceptance when reference tune is mistuned by -0.5 mrad in y angular position.	81
----	----------------------------------------------------------------------------------------------------------------------------------------------------------------------------------------------------------------------------------------------------------------------------------------	----

List of Tables

1	Magnet field ratios for a standard DRAGON tune	21
2	Setpoint current ratios for a standard DRAGON tune	21
3	Shows the fractional composition of the elements that make up Polyethylene Terephthalate (Mylar) [30].	46
4	Shows the fractional composition of the elements that make up Isobutane [33].	47

1 Introduction

Being a physicist means you ask questions about everything, but the more you learn and understand, the more and more questions there are to ask.

Questions like “Where did we come from?”, “Why is the world the way it is?”, “How were the atoms that make up our bodies made, and where were these atoms created?”, answers to which lie in understanding the nucleosynthesis of the chemical elements that make up the Universe.

The temperatures in the first three minutes after the Big Bang were hot enough for hydrogen nuclei to fuse together forming small quantities of heavier elements. However, this initial nucleosynthesis only accounts for the next two elements, (helium and a small amount of lithium), up to mass $A = 7$. So how was man, and our world containing elements up to the uranium region, created if this is true? The answers lie in the stars above. For centuries man has looked to the heavens for the truth. What we have found is an answer to where the other chemical elements came from.

Today, we are convinced that elements with mass $A > 7$ come from the nuclear reactions taking place in stars. Quiescent burning can account for some of the elements produced close to the valley of stability. In normal stellar conditions, unstable nuclei decay before they have the chance to react. However, in the high densities and hot temperatures of exploding stars, these decays can be bypassed by radiative proton and alpha capture reactions, whereby a lighter nucleus absorbs a proton or alpha particle forming an excited state of a heavier nucleus, then releases the excess energy through gamma decay.

One site in the Universe where this happens is a nova. In this stellar binary system, a white dwarf star accretes hydrogen rich matter from a younger companion onto its surface. In the hydrogen rich layer on the white dwarf surface (which consists of oxygen and neon), high temperatures are reached leading to the ignition of nuclear fusion processes. This results in an explosion that forms elements up to silicon. Other stellar sites, such as supernovae and x-ray bursters, can produce even higher mass elements through the r-process, s-process, and rp-process.

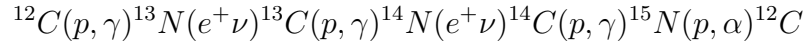
Physicists have modelled novae and have pointed out several important reactions that occur during the explosion which can greatly influence the rate of energy generation and the elements produced, and hence the overall course of the nova. More knowledge of these crucial reactions and their rates will lead us to a better understanding of stellar evolution, element creation, and eventually to the bigger questions of how the Universe evolved and where the elements we are made up of were created.

An important reaction chain at the beginning of exploding novae is the CNO cycle. This thesis will look into the analysis of the $^{13}\text{C}(p,\gamma)^{14}\text{N}$ reaction (which occurs in the CNO cycle) using data obtained using the DRAGON recoil mass separator at TRIUMF's ISAC facility. It will also tell you about the GEANT simulation of the DRAGON and this reaction, as a test to compare with the actual data, and to find out the percentage of acceptance loss through the DRAGON.

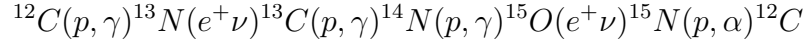
2 Theory

2.1 The CNO Cycle

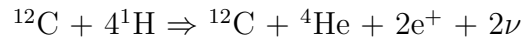
In stars more massive than our Sun, with significant amounts of heavier elements (i.e. Population I stars), the main method of energy production is the fusion of hydrogen in the Carbon-Nitrogen cycle. The CN cycle uses these two elements as catalysts for a sequence of proton captures and beta decays for the production of helium (He). The cycle begins with the radiative proton capture on ^{12}C followed by further proton captures and beta decays:



The (p, α) reaction on ^{15}N ends the cycle because this reaction is more likely than another proton capture. As temperatures rise further to around 10^7 K [1], proton capture on ^{14}N becomes more probable than beta decay. This leads to the Carbon-Nitrogen-Oxygen (CNO) cycle (see figure 1):



Summing the particles before and after one cycle, we see that for one cycle, there is an input of 4 protons and an output of 1 helium nucleus:



Like the CN cycle, the carbon, nitrogen and oxygen nuclei are used as catalysts with their relative abundances remaining unchanged. For both cycles, an initial amount of ^{12}C is required plus a hydrogen-rich environment. [1–3].

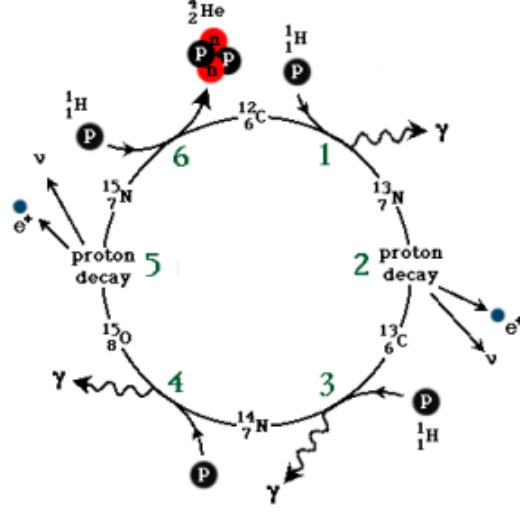


Figure 1: Graphical representation of the CNO cycle.

2.2 The HCNO Cycle

The ‘waiting points’ of the CNO cycle are the nuclei with the longest beta decay lifetimes. Here the cycle must wait for the element to beta decay, if the probability of proton capture is extremely low [1].

If the temperature gets high enough, in the range $0.1\text{-}1.5 \times 10^9 \text{ K}$ [4], proton captures become more probable. Therefore, in the same way the CN cycle transforms to become the CNO cycle by the proton capture reaction $^{14}\text{N}(p,\gamma)^{15}\text{O}$ dominating over the beta decay of ^{14}N , the $^{13}\text{N}(p,\gamma)^{14}\text{O}$ reaction dominates the beta decay of ^{13}N transforming the CNO cycle into what is known as the “hot” CNO (HCNO) cycle (see figure 2).

There is no proton capture on ^{14}O and ^{15}O because the fluorine isotopes ^{15}F and ^{16}F are proton unstable [2]. This means that the rate of energy production is limited by these waiting points at ^{14}O and ^{15}O ($t_{1/2} = 70.6 \text{ s}$ and $t_{1/2} = 122.2 \text{ s}$,

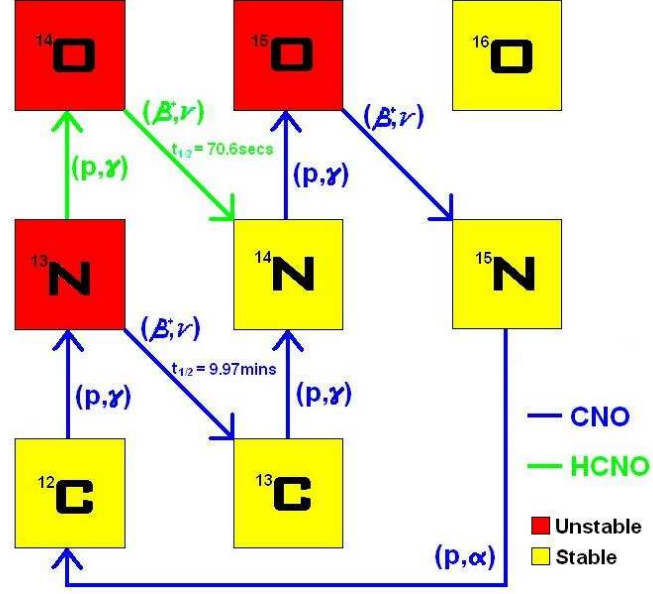


Figure 2: Breakout from the CNO cycle to the Hot CNO cycle, via the $^{13}\text{N}(p,\gamma)^{14}\text{O}$ reaction.

respectively) [1]. The main product material from the HCNO cycle is ^{15}N due to the build up of ^{15}O , the isotope with the longest half life. This is helpful in distinguishing between the CNO and HCNO cycles, using the relative abundances of ^{14}N to ^{15}N . For the CNO cycle, $[^{14}\text{N} / ^{15}\text{N}]$ is about 10^5 , but for the HCNO cycle this value is nearer 0.5 [2].

The HCNO cycle bypasses the beta decay of ^{13}N resulting in the cycle proceeding much quicker than the CNO cycle. The half life of ^{13}N is 9.97 minutes [2], while the half life of ^{14}O is 70.6 seconds. This implies a much larger production rate of helium, and more importantly, a higher energy generation rate.

Again, for this cycle there is an input of 4 protons and an output of 1 helium nucleus.

2.3 The Importance of the $^{13}\text{C}(\text{p},\gamma)^{14}\text{N}$ reaction

The ^{13}N nuclide is very important in the CNO cycle. It is this element that will either beta decay to ^{13}C following the CNO cycle, or proton capture to form ^{14}O changing the cycle to the Hot CNO cycle. This is important for our understanding of novae and supernovae. ^{13}N takes approximately 10 minutes to beta decay, but if the temperature is hot enough, ^{13}N will capture a proton to form ^{14}O , which then beta decays in approximately 70 seconds. This means that the HCNO cycle is much faster and has a higher rate of production of energy. This leads to H and He burning faster, thus resulting in a nova. Consequently the temperature for which there is a change from the CNO to the HCNO cycle is important for our understanding of novae. So what is the relevance of $^{13}\text{C}(\text{p},\gamma)^{14}\text{N}$ reaction?

^{13}N and ^{13}C are very close in mass, in fact they are the two closest mass related elements out of all the elements that make up the Universe [5]. ^{13}N is not a stable element (unlike ^{13}C), and because of the small mass difference between ^{13}N and ^{13}C , a ^{13}N radioactive ion beam will be contaminated with ^{13}C as well. This means that when this radioactive ion beam is eventually used by the DRAGON facility to study the $^{13}\text{N}(\text{p},\gamma)^{14}\text{O}$ reaction, there will be ^{14}N recoils¹ (from the ^{13}C) with the ^{14}O recoils (from the ^{13}N), as well as ^{13}C and ^{13}N leaky beam².

Understanding the $^{13}\text{C}(\text{p},\gamma)^{14}\text{N}$ reaction means that the DRAGONeers can compensate for the ^{14}N recoils and ^{13}C leaky beam when studying the important $^{13}\text{N}(\text{p},\gamma)^{14}\text{O}$ reaction.

¹recoils - a term to describe the product elements from the reaction which occurred in the DRAGON gas target (see section 3.2 The DRAGON Facility)

²leaky beam - a term to describe incoming beam which does not react with the gas target, and makes it through the DRAGON to the end detector with the recoils.

3 Experimental Equipment

3.1 TRIUMF

TRIUMF (TRI-University Meson Facility) is Canada's National Laboratory for Particle and Nuclear Physics, and is situated in Vancouver, on the University of British Columbia campus (figure 3). It is one of three subatomic research facilities in the world that specializes in producing extremely intense beams of particles, and it houses the world's largest cyclotron (figure 4), which accelerates 1000 trillion particles every second. Within the cyclotron, negatively charged hydrogen ions follow an expanding spiral path through it as they are accelerated between the electromagnet's poles guided by the magnetic field, reaching energies of up to 520 MeV³. The acceleration of the ions by the cyclotron is caused by the repeated 'kicks' of electric voltage every half turn, 23 million times per second. After 3000 kicks, the ions are moving at 75% of the speed of light. These intense beams of protons reach the outside edge and are directed out of the cyclotron into pipes (known as beam lines) which lead into experimental areas: the meson hall and the proton hall. In the meson hall, the beam strikes a solid target (carbon, beryllium, copper, or water) which knocks off short-lived pions (known as pi-mesons) from the target atom, which are studied in various experimental stations. In the proton hall, the beam is used directly for analysis and measurements of the properties of nuclei. [6, 7]. (Figure 5).

A beam line is also directed to TISOL (TRIUMF Isotope Separator On-Line). Here, the energetic protons from the cyclotron collide with suitable targets, creating radioactive isotopes, which are separated and directed as a low speed beam of particles

³Beam energies can vary as low as 60 MeV up to 520 MeV. A moving stripping foil inside the cyclotron removes the two electrons from each negatively charged hydrogen ion and allows the remaining protons to channel out of the accelerator. Using more than one stripping foil allows up to three protons beams to be directed out of the cyclotron at the same time, each with different intensities and energies.



Figure 3: TRIUMF sits in the forests of UBC, in the beautiful city of Vancouver. (Photo taken before the construction of ISAC-II).

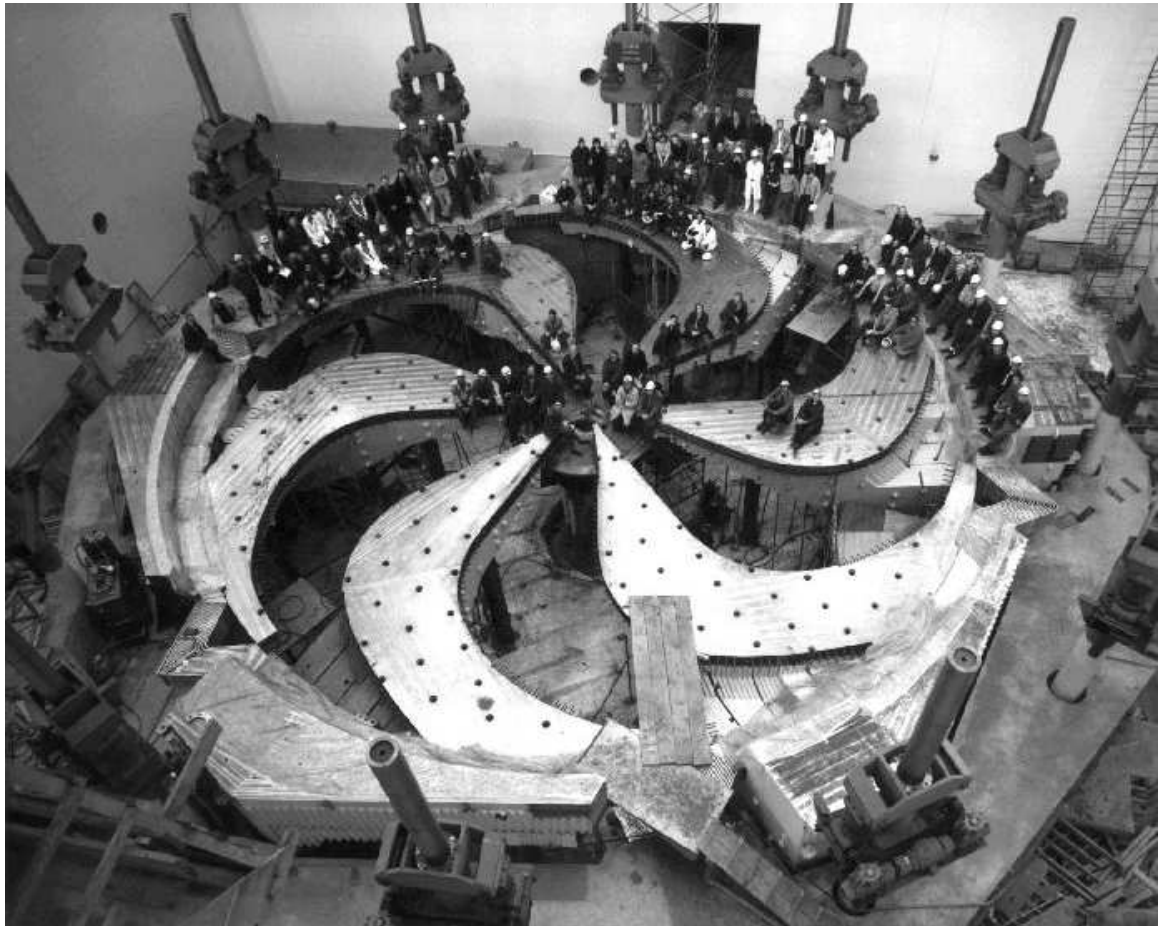


Figure 4: The world's largest cyclotron, at TRIUMF. This image was taken in 1972 during construction (which started in 1969). The first beam was taken in December 1974.

BEAM LINES AND EXPERIMENTAL FACILITIES

ISAC - I & ISAC - II EXPERIMENTAL HALLS

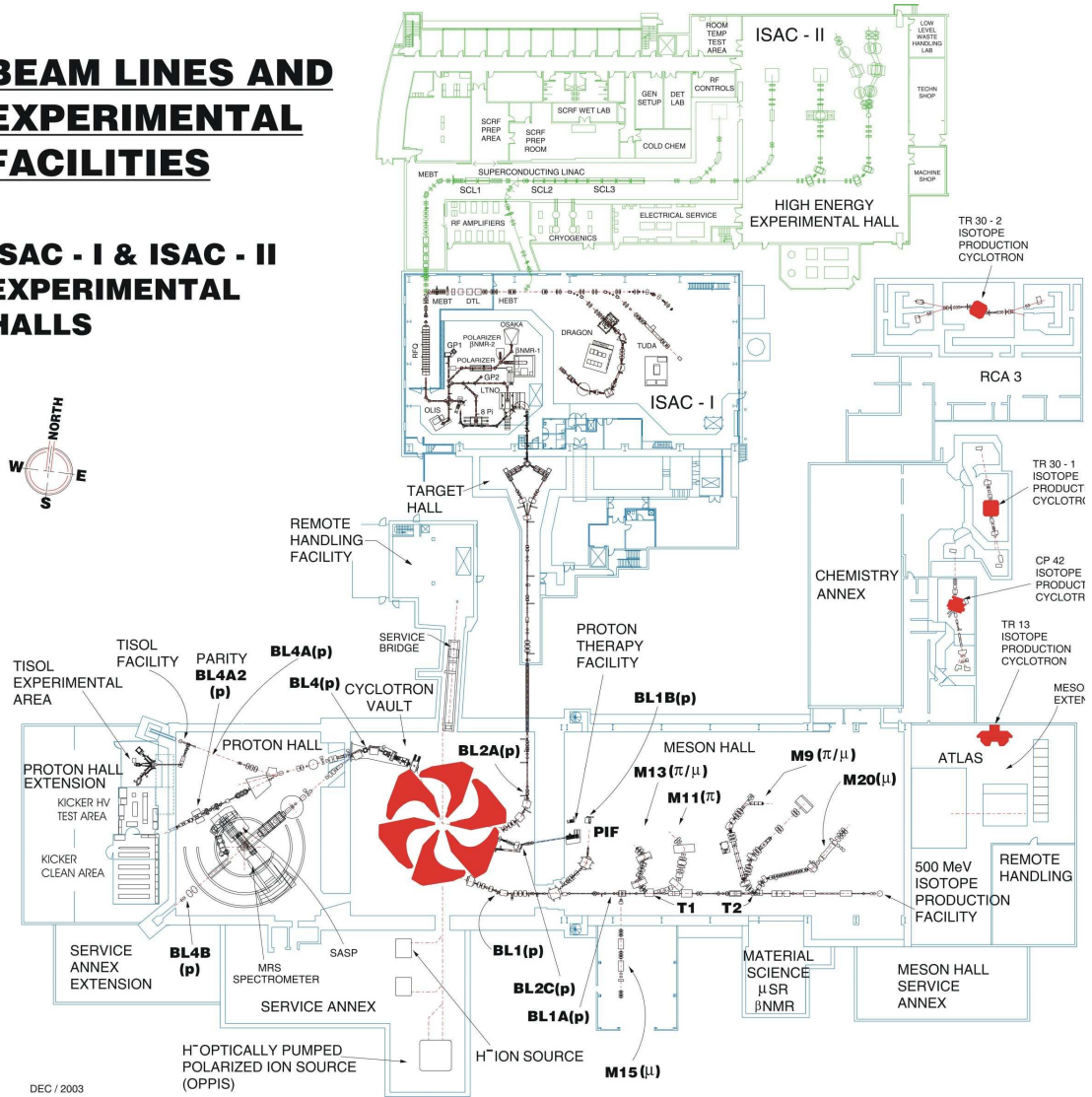


Figure 5: A plan view of TRIUMF.

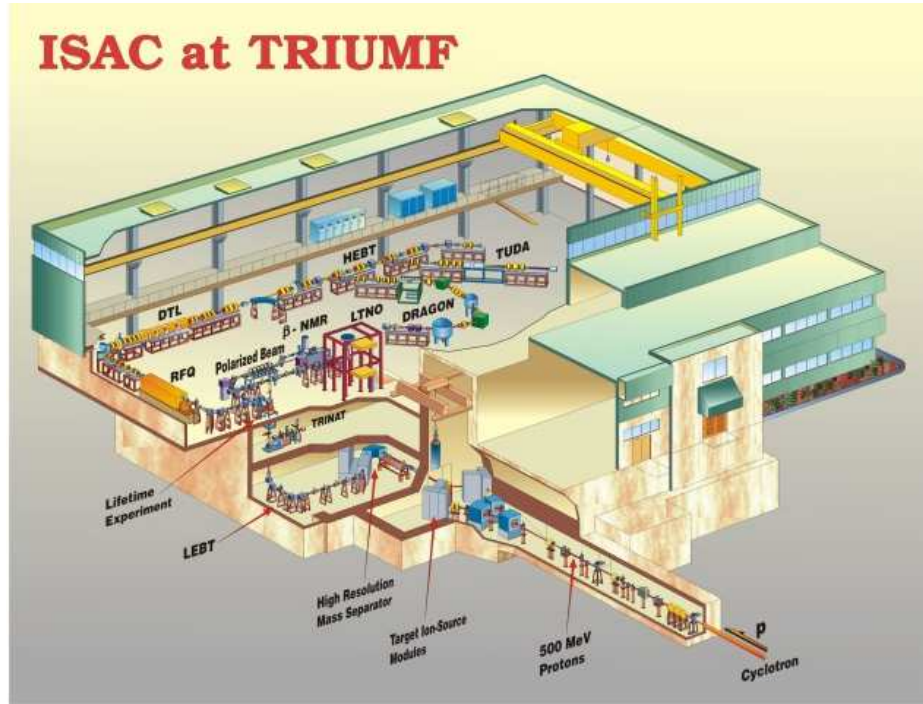


Figure 6: A 3D cut-away view of the ISAC experimental hall.

to the ISAC hall. ISAC (Isotope Separator and ACcelerator) produces a wide range of radioactive ion beams with intensities higher than at any other facility in the world. There are two experimental areas within ISAC: the low and high energy areas. The low energy area uses a non-accelerated, mass separated heavy ion beam for studies in fundamental interactions, nuclear physics, and condensed matter physics. For the high energy area, the beam is passed through the two ISAC accelerators: RFQ (Radio Frequency Quadrupole) and DTL (Drift Tube Linac). Here, beams of masses below 30 amu can be accelerated to energies from 0.15 - 1.5 MeV per mass unit, and are sent in pulses of 1 per 86 nano-seconds to the high energy experiments. This range of energies is the optimal range for studies into the understanding of explosive nucleosynthesis and nuclear astrophysics as a whole, leading to explanations of the evolution of chemical elements in the universe. [8–10]. (Figure 6).

3.2 The DRAGON Facility

DRAGON (Detector of Recoils And Gammas Of Nuclear reactions) [11–13] is on the high energy beam line from the cyclotron at the TRIUMF-ISAC facility, and was designed to measure radiative capture reactions in inverse kinematics using a hydrogen or helium gas target [9]. The DRAGON system (figure 7) is basically a 21 m recoil mass spectrometer⁴ which can create elements via proton or alpha capture reactions and then separate them based on mass. This is achieved in two stages.

The incoming high energy beam line enters DRAGON through a windowless gas target, which has a 12.3 cm effective length (figure 8). A series of pumps are found either side of the entrance and exit to the target, and are used to keep the beam line in vacuum ($\sim 10^{-7}$ Torr) by removing any gas that may leak out of the target. This allows the beam to pass cleanly through the target. Surrounding the target is a closely-packed array of 30 gamma detectors made of BGO (Bismuth Germanium Oxide) scintillation crystals (figure 9). These detect the gamma rays emitted in the nuclear reaction within the gas and measure their energies⁵.

On leaving the gas target, the products (or ‘recoils’) of the nuclear reaction (together with leaky beam) enter the first stage of the mass spectrometer. The mass spectrometer is made up of a series of magnetic dipoles (M), magnetic quadrupoles (Q), magnetic sextupoles (S), and electrostatic dipoles (E), and they are arranged in a two stage mass separation: (QQMSQQQSE)(QQSMQSEQQ). The magnetic dipoles use a magnetic field to separate ions by their charge state through different amounts

⁴21 m from the target center to the end detector.

⁵When a gamma ray enters the BGO crystal, it reacts with an atom inside. This reaction excites an electron to an excited state, and as the excited electron falls back down to a lower energy state it releases its energy in the form of a photon. This is repeated for each atom the gamma ray interacts with, in the BGO, losing some energy each time. The total sum of light (i.e photons) is read by a PMT (Photo-Multiplier Tube) attached at the end of the BGO crystal. The sum of light is proportional to the energy of the gamma ray. [14]

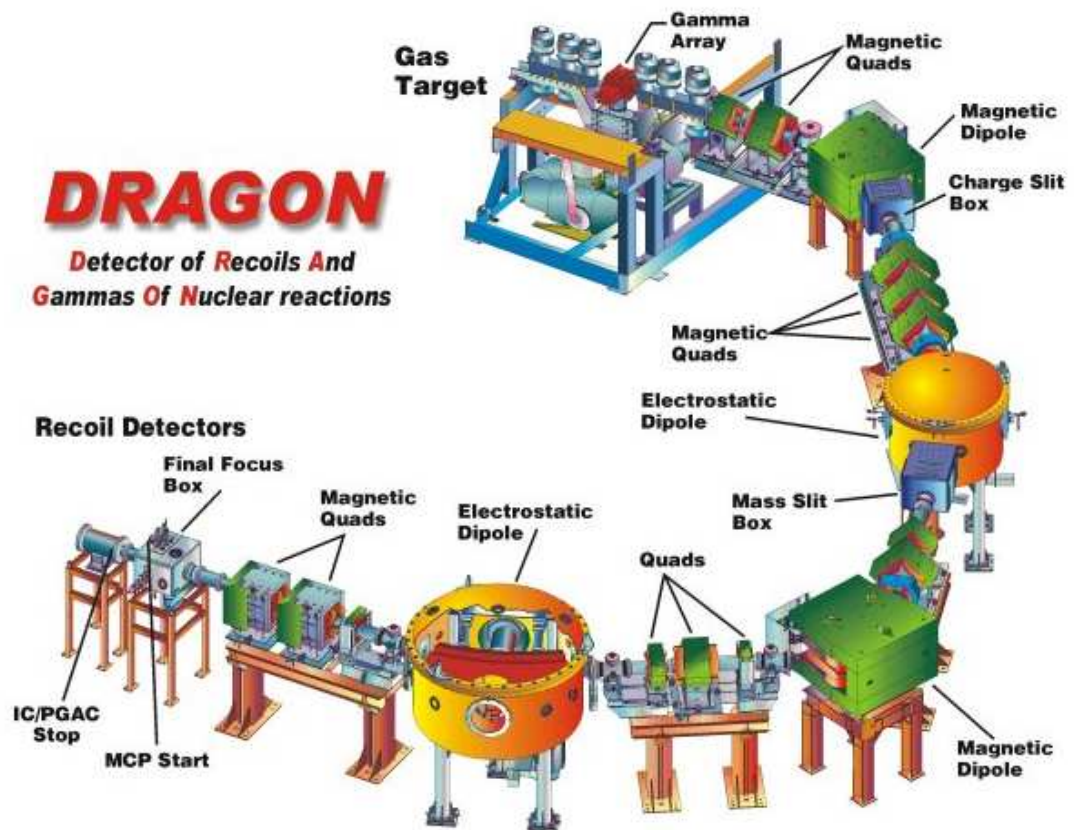


Figure 7: The DRAGON recoil mass separator.

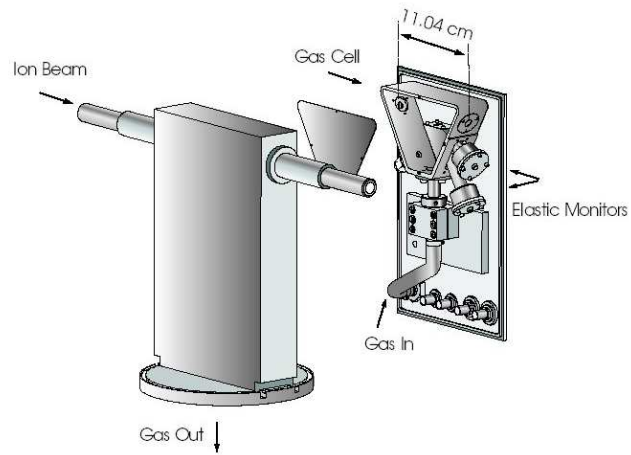


Figure 8: Inside the gas target box - diagram of the DRAGON's gas target mounting.



Figure 9: The BGO array, (which surrounds the gas target), and the vacuum pumps.

of curvature (Eq. 1). The dipoles are set in such a way that it bends the charge state of interest through the charge state slits, while all other charge states are stopped inside the charge slit box.

$$r = \frac{mv}{Bq} \quad (1)$$

The beam and recoil ions leave the magnetic dipoles and carry on downstream with the selected charge state. Both sets of ions have the same momentum and will therefore have different velocities (Eq. 2), and hence, different kinetic energies (Eq. 3). The kinetic energy of the recoils is chosen, and the appropriate voltage is applied to the electrostatic dipoles such that the recoils pass through the mass slits, and the beam ions are stopped in the mass slit box. The ions then pass through the second stage of the mass spectrometer: another magnetic and electrostatic dipole (MD2 and ED2 respectively) to improve the suppression of beam ions with respect to recoil ions.

$$p = mv \quad (2)$$

$$E = \frac{1}{2}mv^2 \quad (3)$$

Currently DRAGON has two main end detectors: a double sided silicon strip detector (DSSSD) and an ionization chamber (IC).

The DSSSD gives data on the number of ions detected, the energy the ions hit the detector with, the position of the ions on the focal plane, and the time-of-flight of the ions. The DSSSD consists of 16 front strips and 16 back strips. Each strip is 3 mm wide, which provides a (256 x 3) mm² pixel area on a 5 cm² detector, giving the x-y position data. [15].

The IC gives the number of counts, and can be used to distinguish different particles as it measures the change in energy (ΔE).

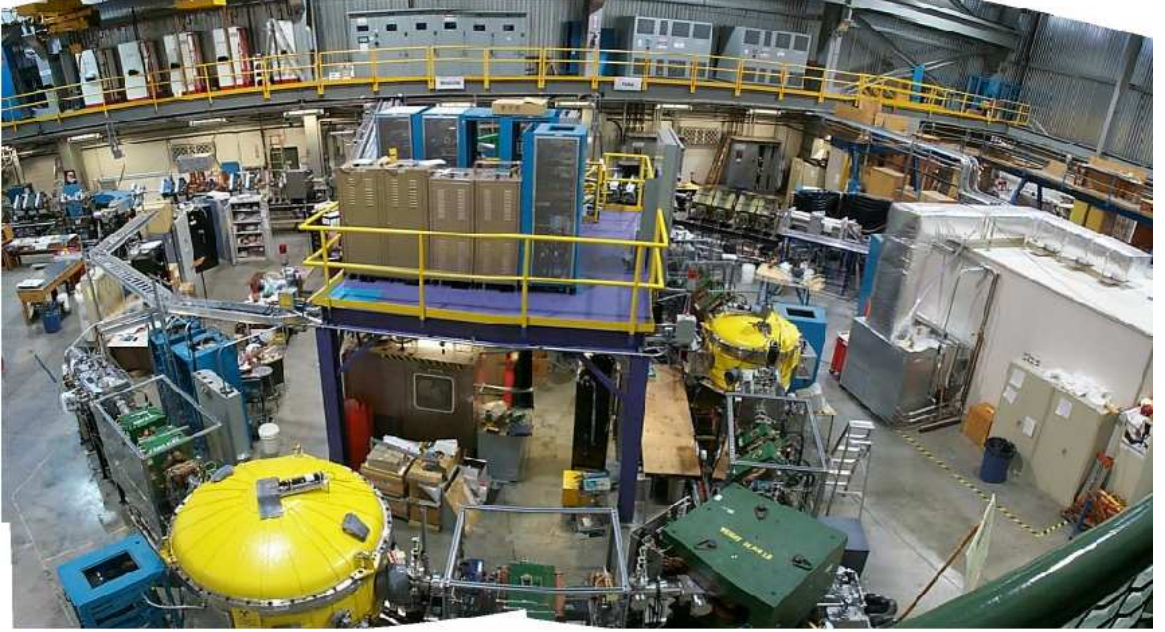


Figure 10: The DRAGON, in all its glory!

3.3 DRAGON's Ionization Chamber

For the $^{13}\text{C}(p,\gamma)^{14}\text{N}$ reaction, DRAGON would use the ionization chamber as its end detector. The ionization chamber is essentially a parallel plate arrangement with a single cathode and several parallel anodes which creates an electric field in between the plates, perpendicular to the beam (figure 11). Separating the anodes from the ionization area of the chamber is a grid of wires, known as a Frisch grid [16], which shields the anodes from the induced charges. Surrounding each of the anode regions are field shaping wires which are kept at a constant fraction of the cathode voltage by a series of resistors, so as to keep the field in the chamber uniform throughout. As the charged particles pass through the isobutane gas in the chamber, they ionize the gas particles creating electrons which are then accelerated in the chamber's electric field. The number of gas particles ionized by an incoming particle is proportional to the type of particle it is, and the energy of that particle. The ionization of the gas

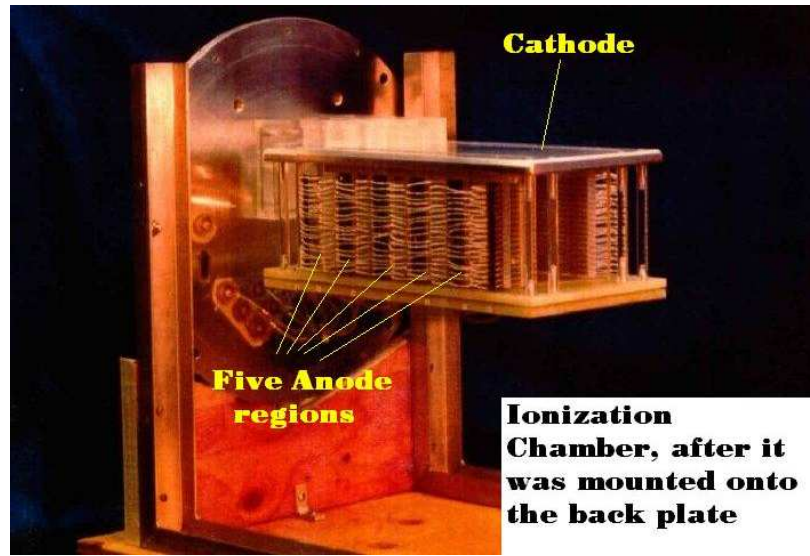


Figure 11: The ionization chamber, during construction.

particles causes a negative induced charge pulse on the Frisch grid and a positive charge pulse on the cathode. The newly created electrons are attracted past the Frisch grid⁶ and are collected at the anodes which creates a second induced charge pulse (however, this time a positive charge) on the Frisch grid and a negative charge pulse on the anode (figure 12). All of these pulses are then read by preamplifiers which isolate them from the large voltages at the electrodes. To summarise, the charge pulses are proportional to the number of electrons created, which is a function of the type of and energy of the incoming particle. The anode signals can be looked at separately to provide the rate of energy loss measurement, and they can be summed to provide the total energy loss measurement. The Frisch grid and the cathode signals can also be looked at to provide independent total energy signals. [18,19]. (Figure 13).

⁶The grid is maintained at an intermediate potential between the anode and cathode, making it as transparent as possible to the electrons [17].

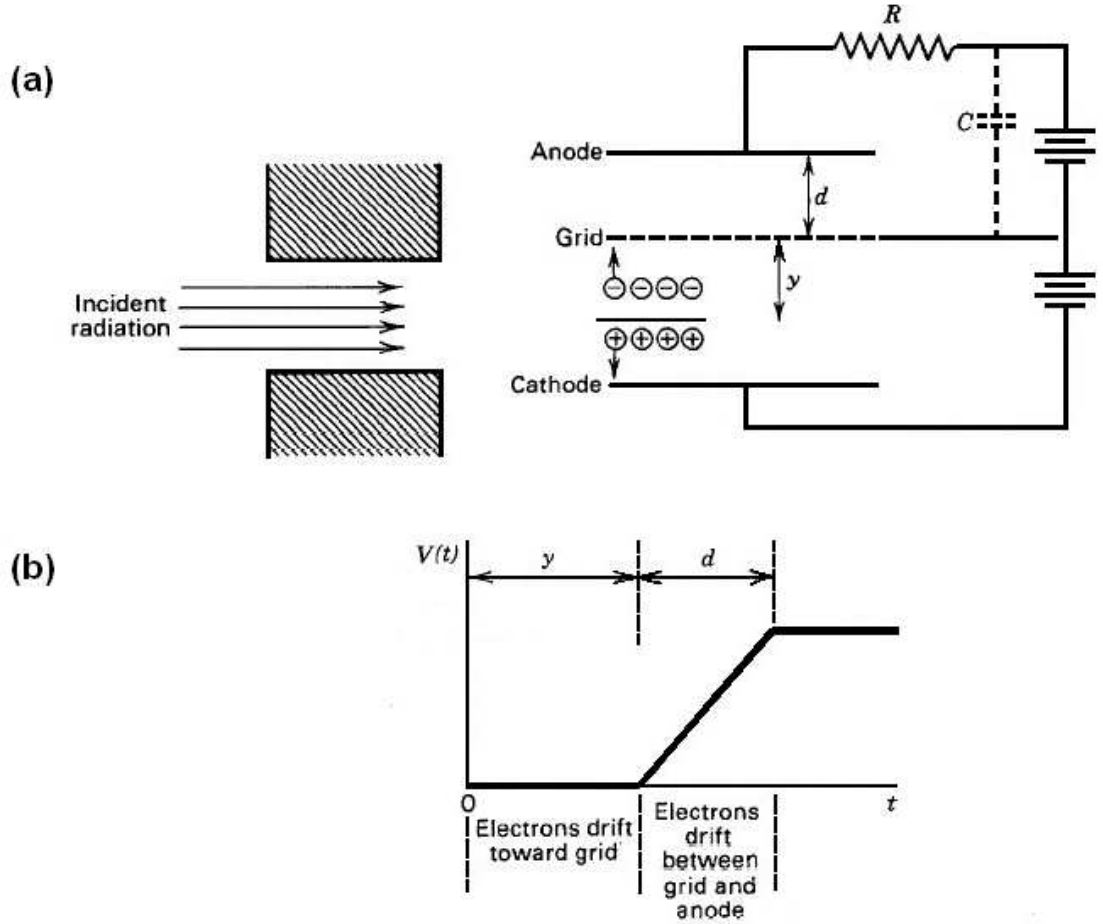


Figure 12: (from [17]) (a) A similar setup to the inside of the DRAGON's ionization chamber, all ion pairs are formed in the grid-cathode region. (b) The induced pulse that results from the formation of the ion pairs, a distance y from the grid. The rise of the pulse results from the attraction of the electrons, across the grid-anode region. The pulse decays back to zero with a time constant equal to RC .

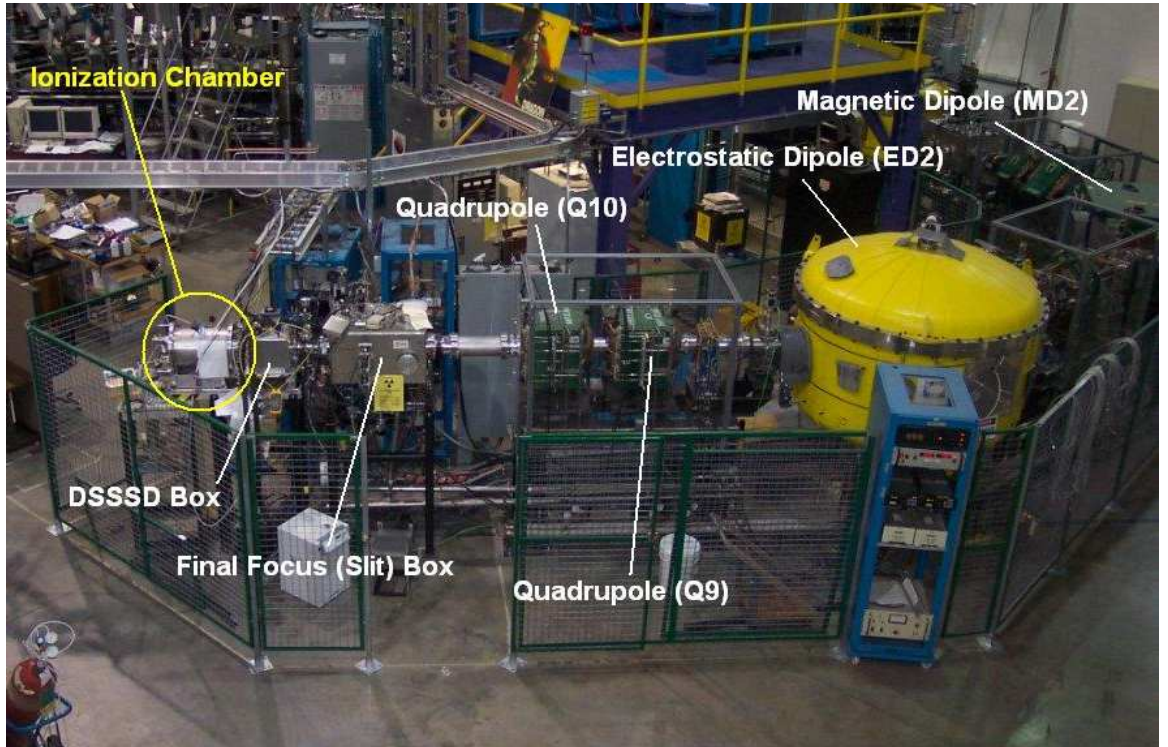


Figure 13: Location of the ionization chamber. (During the $^{13}\text{C}(p,\gamma)^{14}\text{N}$ reaction run, the ionization chamber would be placed where the DSSSD box is, at the end of the final slit box).

3.4 Tuning The DRAGON

Every time DRAGON receives a new beam and/or a new beam energy, the separator must be tuned to allow the recoils of interest to reach the end detector. DRAGON has an EPICS control system, which is an interface, used for modifying magnetic⁷ fields, changing dipole currents, moving slit⁸ positions, etc, to help allow the maximum amount of recoils get through the DRAGON with ease. [21].

Firstly, the tune scaling utility for setting up the tune is used. Either a “good” tune can be recovered from a previous tune, or the settings in Tables 1 and 2 multiplied by the MD1 field or current (which is found by measuring the post-target beam energy for the energy measure to have been valid. Q1 and Q2 fields must have been set in the correct ratio to MD1 field) can be used. [21].

Before tuning the beam through the separator, the beam has to be centred in the horizontal and vertical (in both position and direction) through the middle of the target. This is important for a number of reasons, one of which is that the x-position of the beam at the target affects the apparent beam energy when measured at MD1. By switching quadrupoles Q1 and Q2 on, a CCD⁹ image of the beam in the middle of the target, is observed. Switching Q1 and Q2 off causes the beam to effectively behave as if it is travelling through a 3 m drift space between the target and the charge slits. Therefore, by alternating between having these quadrupoles on and off, the beam position and direction through the target, and the (post-target) beam energy, can be measured. [21].

⁷the DRAGON magnets include two dipoles (MD1-2), ten quadrupoles (Q1-10), four sextupoles (SX1-4), and five steering magnets (SM0-4). [20].

⁸DRAGON has three lots of two-paired (horizontally-moving and vertically-moving) motor-driven slits along the separator, used for centring the beam. [20].

⁹a CCD camera (nicknamed the “Dragon Breathalyzer”) is placed, looking upstream, through an alignment port of MD1. When the beam passes through the gas target, it emits light which can be imaged on the CCD. The CCD is connected to a PC, and two dimensional plots can be made, to measure the width and intensity of the beam spot (see figure 14). [20].

Magnet	Field Ratio
Q1	0.709
Q2	0.677
MD1	1.000
Q3	0.553
Q4	0.735
Q5	0.381
Q6	0.366
Q7	0.512
MD2	1.230
Q8	0.387
Q9	0.238
Q10	0.266

Table 1: Magnet field ratios for a standard DRAGON tune

Magnet	Setpoint Ratio
SX1	0.0528
SX2	0.0112
MD1	1.000
SX3	0.0100
SX4	0.0974

Table 2: Setpoint current ratios for a standard DRAGON tune

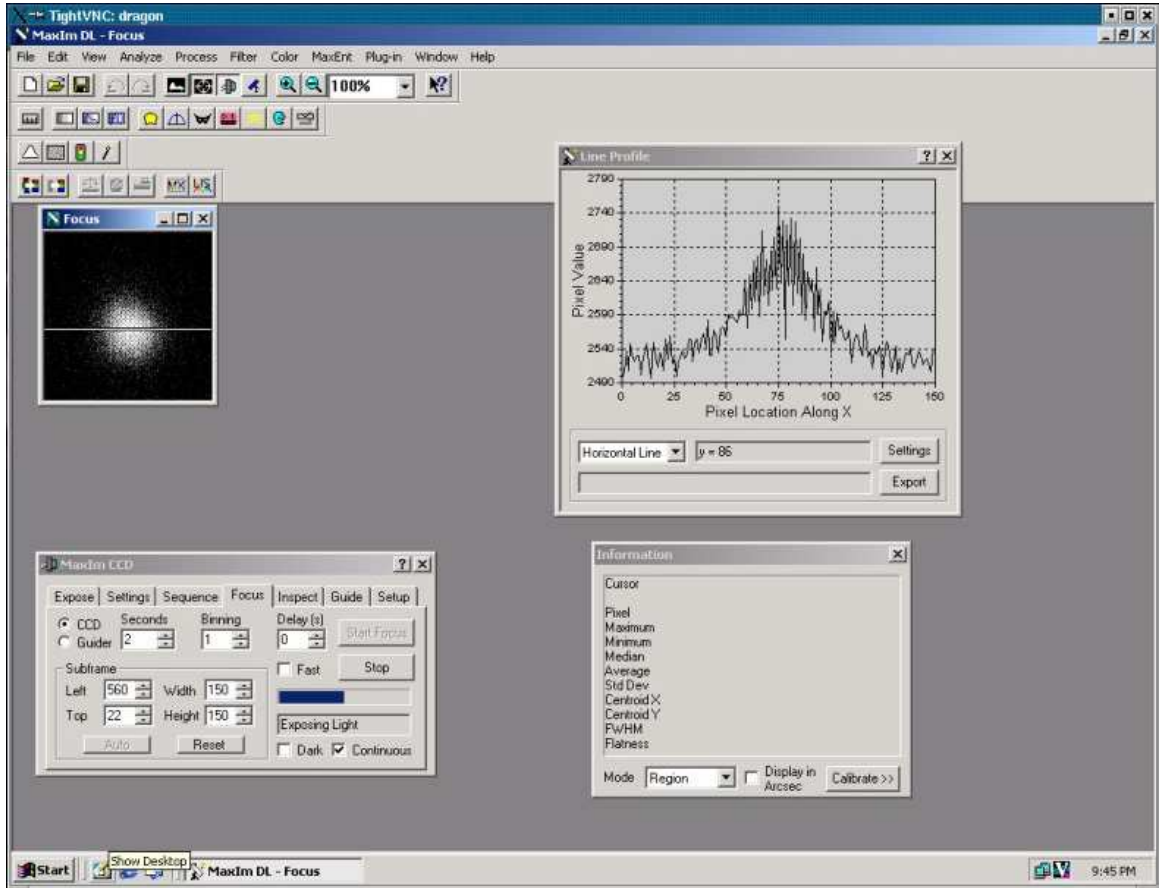


Figure 14: This CCD image was captured when tuning the gas target to the 544 keV/u ^{13}C ion beam. The Focus box to the left shows an image of the beam spot, and the spectrum to the right shows the relative intensity of the beam.

The next step is to tune through the rest of DRAGON. This done by using a tune scaling utility which calculates and sets the DRAGON for certain mass, charge and energy of the ions of interest, scaled from a reference tune. From the charge slits, through the mass slits, and to the final slits, the beam is centred through DRAGON by changing voltages of the ED's, using steering magnets¹⁰ and BCMs¹¹, and adjusting the magnetic fields of the MD's. This procedure is broken up into four EPICS Optics pages by four faraday cups¹². [21].

¹⁰the steering magnets can deflect ions by up to 25 mrad in the x and/or y direction. [20].

¹¹Beam Centring Monitors. DRAGON has six, and each consist of four plates arranged in a 2 x 2 array, mounted on insulators separated by a gap. The BCMs are used with the slits, for further beam positioning. [20].

¹²the faraday cups are placed in various positions along the DRAGON separator, and can be placed in the beam line, not only to prevent the beam reaching the final slits, but to measure the beam current.

4 The $^{13}\text{C}(\text{p},\gamma)^{14}\text{N}$ reaction - Analysis of the DRAGON Data

4.1 MIDAS

The analyzer used for DRAGON is a MIDAS¹³ program which runs: a) online as part of the data acquisition (DAQ), and b) offline to analyze old event-by-event .mid files. This MIDAS analyzer operates as a pipeline to make histograms from event-by-event data, to write these histograms into .hbook (online) or .rz (offline) files, and use PAW++¹⁴ for histogram display. [23]

Offline analysis is different from online analysis, as an offline event stream from the .mid file can be passed through the analyzer many times, whereas the online event stream can only be passed through the analyzer once. Each time the offline event stream is passed through the analyzer, changes to the ODB (Online Data Base) are made to eliminate more and more unwanted background events. Final changes to the ODB are saved, to document the complete analysis. These changes in the ODB also mean that it is possible to look at histograms that are not set up in the online ODB. [23]

For example, figure 15 shows the histogram (ID1001) from the online .hbook file of run number 8161. This $^{13}\text{C}(\text{p},\gamma)^{14}\text{N}$ run lasted for 1700 seconds, and had an incoming beam energy of 543.8 keV/u. Using Eq. 4, the Q-value for this reaction is 7.551 MeV. Eq. 6 gives the center-of-mass energy (E_{cm}). For run 8161 this was 508.6

¹³Maximum Integrated Data Acquisition System - a general purpose system, developed at TRIUMF and the Paul Scherrer Institute (Switzerland) between 1993 and continuing to this day, for event based data acquisition in small to medium scale physics experiments [22].

¹⁴Physics Analysis Workbench - a general purpose portable tool for analysis and presentation of physics data.

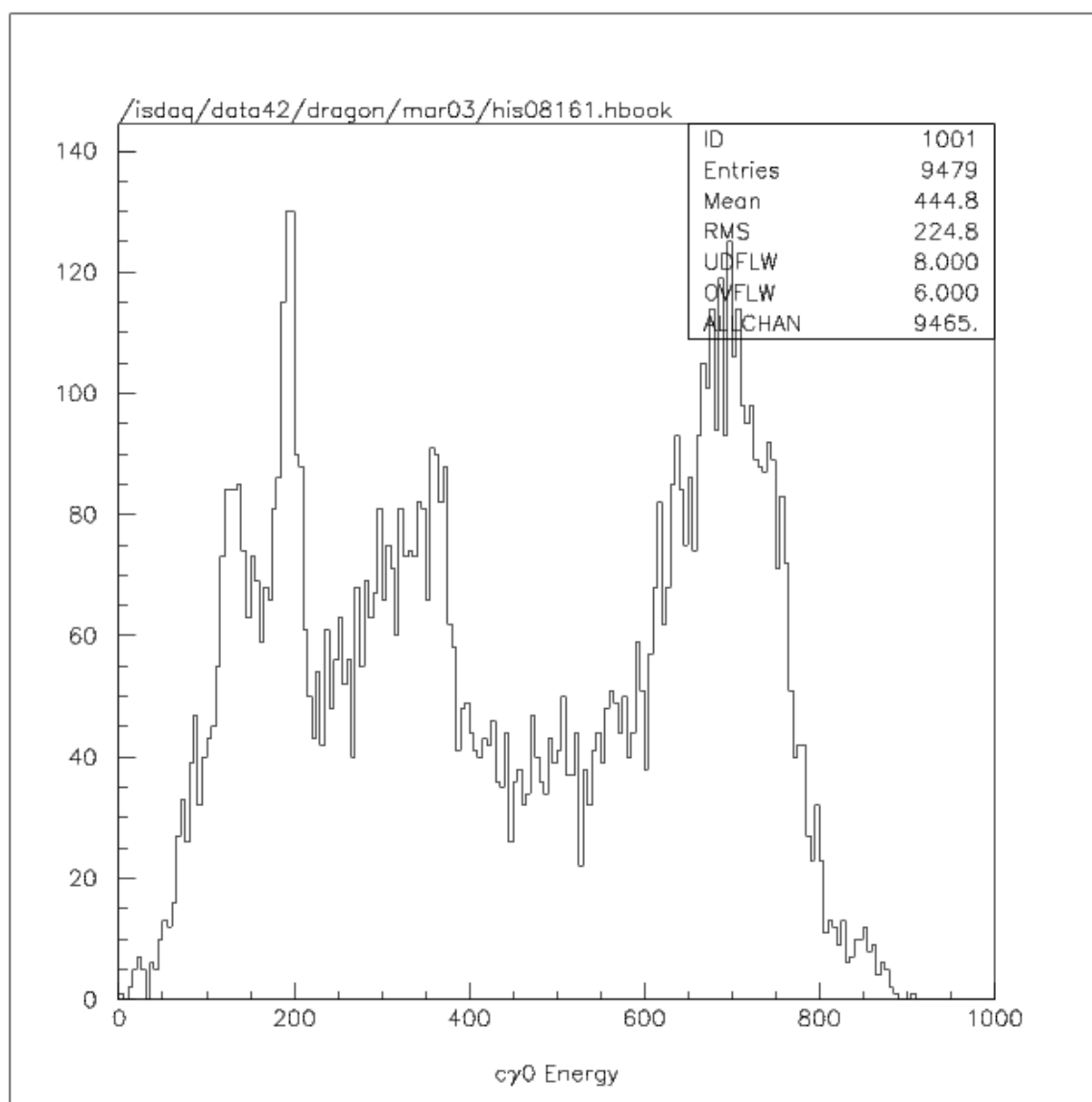


Figure 15: Energy histogram of the most energetic coincidence gamma rays, per event, for run 8161.

keV. Eq. 8 gives the excitation energy (E_x) of the gamma emitted from this reaction. For run 8161, this was 8060 keV (see figure 16).

$$Q = \Delta mc^2 \quad (4)$$

where:

$$\Delta m = m(^{13}\text{C}) + m(^1\text{H}) - m(^{14}\text{N}) \quad (5)$$

$$E_{cm} = \mu E_{beam} \quad (6)$$

where:

$$\mu = \frac{mM}{m + M} \quad (7)$$

$$E_x = Q + E_{cm} \quad (8)$$

Therefore, this coincidence¹⁵ gamma energy histogram for run 8161 has a peak which relates to 8060 keV. As the energy x-axis for these PAW++ histograms were not known, a Gaussian was fitted to the peak. So by knowing the x-axis channel number, it was possible to find a calibration constant for this axis (see figure 17).

Figure 15 is a plot of $c\gamma 0$ energy, where $c\gamma 0$ means that the data put into this histogram is from the most energetic coincidence gamma ray detected by a single BGO, per event, from the BGO gamma detector array. The various other peaks are from either: the cascade gammas to other excited states, or from the main 8060 keV gammas that did not deposit all of their energy into a single BGO. Therefore, by

¹⁵i.e. the data that relates to a recoil heavy ion of ^{14}N as detected by the end detector.

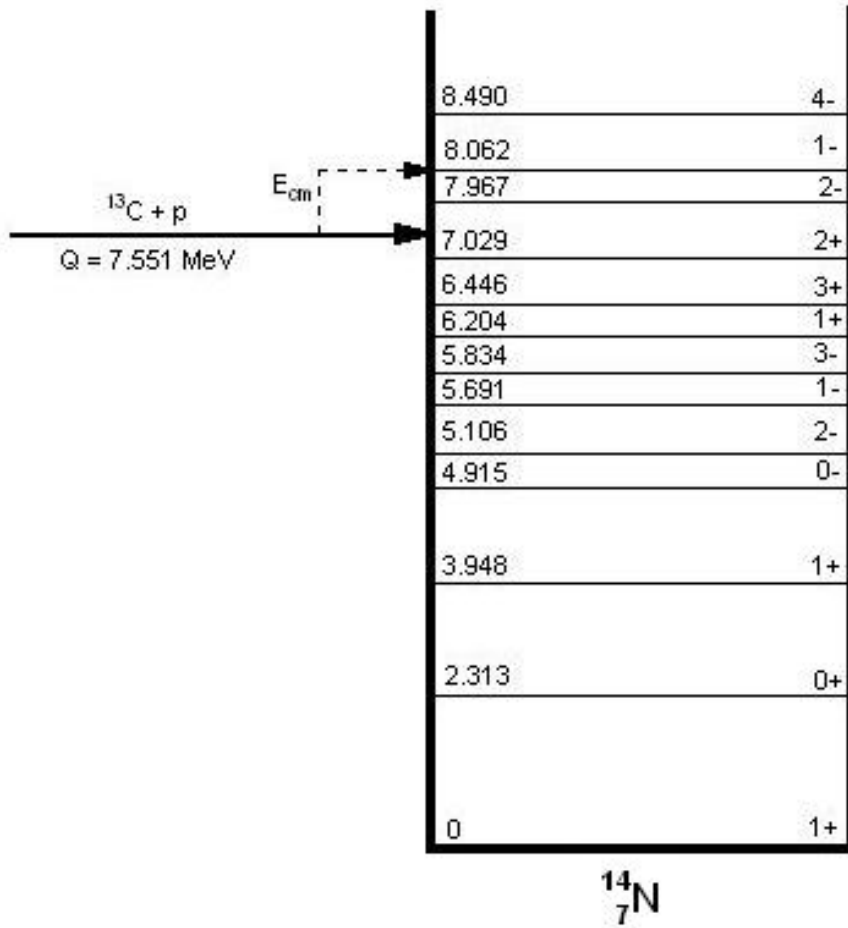


Figure 16: Graphical representation of the energy levels in ^{14}N . Shows the incoming Q-value for $^{13}\text{C} + p$, the center-of-mass energy, and the excited level of ^{14}N we were trying to populate.

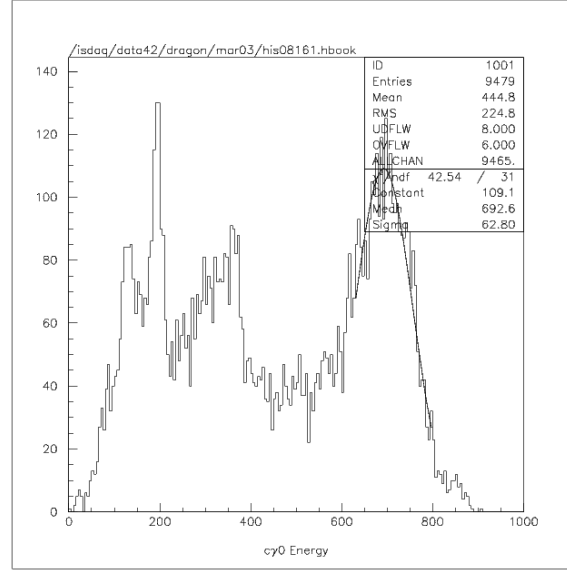


Figure 17: Fitting a gaussian curve to an energy peak.

summing up all the gamma cascades per event, will give, (for this run), the 8060 keV energy peak (see figure 18). This was done by analyzing run 8161 offline and by simply changing the title of the spectrum in the ODB. Also the scale of the x-axis has been changed so that only the relevant data is in the spectrum.

The ionization chamber is made up of four anodes. Looking at the 2D energy histogram of ΔE vs E for the first anode in the ionization chamber (figure 19), it is apparent that there may be leaky beam getting to the end detector. To check what is leaky beam and what is recoils, there were earlier recoil tunes and attenuated beam runs. Figure 20a shows an attenuated beam run, and figure 20c shows a recoil tune. Comparing these two runs to run 8142 (figures 20b&d) shows that the circle in figure 19 is actually leaky beam. Therefore, a cut could be made in further analysis, to only include the recoil data.

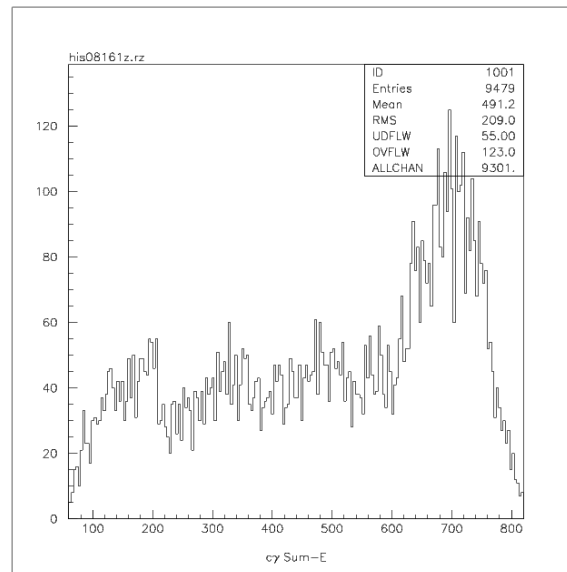


Figure 18: Passing run 8161 offline through the analyzer and changing the ODB to look at the sum of coincidence gamma rays.

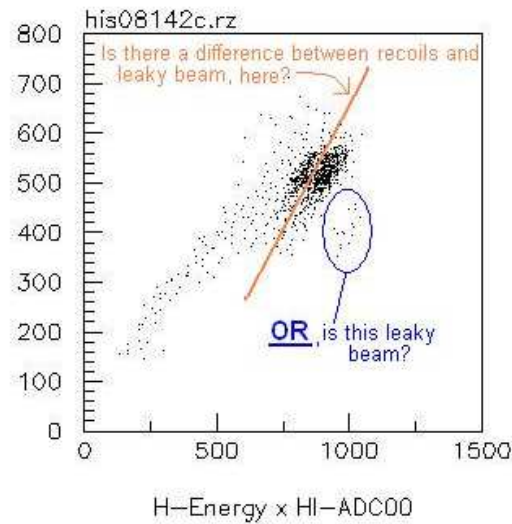


Figure 19: a two-dimensional energy histogram (from run 8142) of ΔE vs E in the first anode of the ionization chamber.

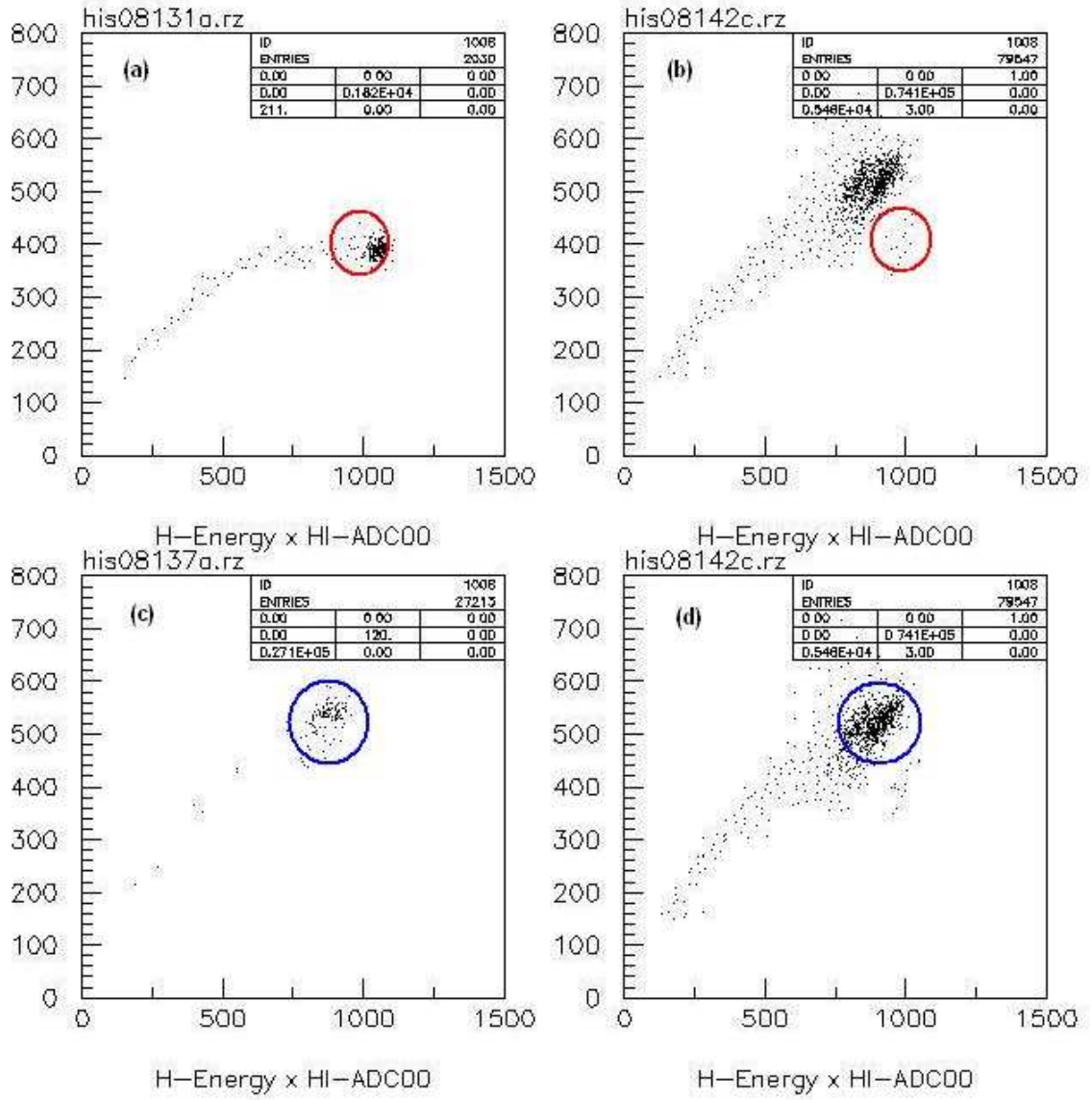


Figure 20: Confirmation of recoils and leaky beam. a) attenuated beam tune, b)&d) normal run, c) recoil tune.

4.2 Calculating the maximum cone angle for the $^{13}\text{C}(p,\gamma)^{14}\text{N}$ reaction

The total energy in any nuclear reaction is conserved (i.e. energy going in equals energy coming out). Therefore for the $^{13}\text{C}(p,\gamma)^{14}\text{N}$ reaction:

$$m(^{13}\text{C}) + T(^{13}\text{C}) + m(^1\text{H}) + T(^1\text{H}) = [m(^{14}\text{N}) + E_x] + T(^{14}\text{N}) \quad (9)$$

Since the hydrogen target is at rest in the laboratory frame:

$$T(^1\text{H}) = 0 \quad (10)$$

Non-relativistically:

$$T(^{13}\text{C}) = \frac{m(^{13}\text{C}) + m(^1\text{H})}{m(^1\text{H})} E_{cm} \quad (11)$$

The centre-of-mass energy (E_{cm}) is related to the excitation energy (E_x) of the recoiling nucleus:

$$E_{cm} = E_x - Q \quad (12)$$

where E_x is equal to:

$$E_x = E_\gamma = 8.062 \text{ MeV} \quad (13)$$

and the Q-value (Q) is equal to:

$$Q = \Delta mc^2 = [m(^{13}\text{C}) + m(^1\text{H}) - m(^{14}\text{N})]c^2 \quad (14)$$

Note

$$1u = 931.4943 \text{ MeV}/c^2 \quad (15)$$

$$m(^{13}\text{C}) = 13.0033548u = 12112.5514 \text{ MeV}/c^2 \quad (16)$$

$$m(^1\text{H}) = 1.00782503u = 938.7833 \text{ MeV}/c^2 \quad (17)$$

$$m(^{14}\text{N}) = 14.0030740u = 13043.7842 \text{ MeV}/c^2 \quad (18)$$

Substituting Eq. 15, 16, 17, 18 into Eq. 14, gives a Q-value equal to:

$$Q = 7.551 \text{ MeV} \quad (19)$$

Substituting Eq. 19 and Eq. 13 into Eq. 12, gives a centre-of-mass equal to:

$$E_{cm} = 0.511 \text{ MeV} \quad (20)$$

Substituting Eq. 16, 17, 18 and 20 into Eq. 11, gives a kinetic energy for ^{13}C to be:

$$T(^{13}\text{C}) = 7.104 \text{ MeV} \quad (21)$$

Rearranging Eq. 9 gives:

$$T(^{14}\text{N}) = m(^{13}\text{C}) + m(^1\text{H}) - m(^{14}\text{N}) + T(^{13}\text{C}) - E_x \quad (22)$$

In natural units, $c = 1$. This means that Eq. 22 becomes:

$$T(^{14}\text{N}) = Q + T(^{13}\text{C}) - E_x = 6.593 \text{ MeV} \quad (23)$$

The energy-squared equation:

$$E^2 = m^2c^4 + p^2c^2 \quad (24)$$

therefore becomes:

$$E^2 = m^2 + p^2 \quad (25)$$

The relativistic velocity is given by:

$$\nu = \frac{p}{E} \quad (26)$$

By substituting the RHS of Eq. 9 into Eq. 25 and rearranging it, gives:

$$p^2 = [[m(^{14}\text{N}) + E_x] + T(^{14}\text{N})]^2 - [m(^{14}\text{N}) + E_x]^2 \quad (27)$$

Therefore, by substituting Eq. 27 into Eq. 26, and by using Eq. 13, 18, 23, the velocity of the excited ^{14}N is found to be:

$$\nu = \frac{p}{E} = \frac{\sqrt{\{[m(^{14}\text{N}) + E_x] + T(^{14}\text{N})\}^2 - [m(^{14}\text{N}) + E_x]^2}}{[m(^{14}\text{N}) + E_x] + T(^{14}\text{N})} = 0.03177c \quad (28)$$

The relativistic gamma equation is:

$$\gamma = \left[\sqrt{1 - \frac{\nu^2}{c^2}} \right]^{-1} \quad (29)$$

If $c = 1$, and by substituting Eq. 31 into Eq. 29, then gamma becomes:

$$\gamma = 1.000505 \quad (30)$$

We assume that the recoil moves at 90 degrees to the z-axis in the centre-of-mass frame (figure 21) where:

$$\nu = 0.03177c \quad (31)$$

and

$$\nu_1^{cm} = \frac{p^{cm}}{E_1^{cm}} = \frac{E_\gamma}{\sqrt{[m(^{14}\text{N})]^2 + [E_\gamma]^2}} \quad (32)$$

To find the (cone) angle on the laboratory frame, we have to use:

$$\tan \theta_1 = \gamma^{-1} \sin \theta_1^{cm} \left(\frac{\nu}{\nu_1^{cm}} + \cos \theta_1^{cm} \right)^{-1} \quad (33)$$

From figure 21:

$$\theta_1^{cm} = 90^\circ \quad (34)$$

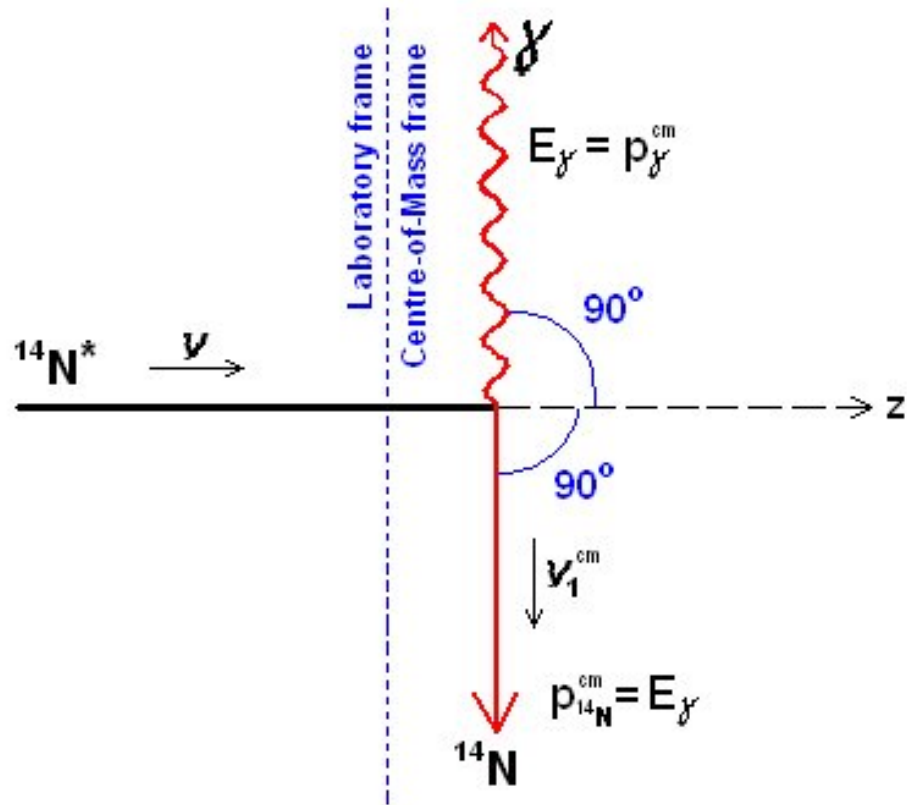


Figure 21: A diagram illustrating the maximum angle of the ^{14}N recoil and associated gamma ray (from the decay of the excited state, $^{14}\text{N}^*$), in the centre-of-mass reference frame. [24]

Substituting Eq. 32 and 34 into Eq. 33, and using Eq. 13, 18, 31, and 30,

$$\tan \theta_1 = \gamma^{-1} \left(\frac{\nu}{\nu_1^{cm}} \right)^{-1} = \frac{E_\gamma}{\nu \gamma \sqrt{[m(^{14}\text{N})]^2 + [E_\gamma]^2}} = 0.01944 \quad (35)$$

Therefore, the maximum cone angle of the $^{13}\text{C}(\text{p},\gamma)^{14}\text{N}$ reaction, is:

$$\theta_1 = \tan^{-1} 0.01944 = 19.4 \text{ mrad} \quad (36)$$

(Equations from [24]).

4.3 Clipping

The $^{13}\text{N}(\text{p},\gamma)^{14}\text{O}$ requires quite high sensitivity, so the $^{13}\text{C}(\text{p},\gamma)^{14}\text{N}$ reaction was used to probe the DRAGON not only because it has similar properties, but because it had been measured before by King et al [25]. However, from analysis of our $^{13}\text{C}(\text{p},\gamma)^{14}\text{N}$ run, it was observed that the ^{14}N recoils were being “clipped” in the target box. Pure angular clipping¹⁶ would cause a trough in the coincidence recoil peak, (i.e. giving two peaks), which is what was observed (see figure 22). However, the lower energy recoil peak should be the same height as the higher energy recoil peak. But this was not seen, and it was believed that the difference in height maybe due to an energy asymmetry correlation problem, whereby low energy recoils were not being focused at the focal point of the end detector. [24].

To find out what percentage of recoils were not making it to the end detector, work started on a GEANT simulation of the DRAGON and this reaction to see what fraction of the recoils were being cut off, so that it would be possible calculate the required parameters such as the yield.

¹⁶the $^{13}\text{C}(\text{p},\gamma)^{14}\text{N}$ reaction has large maximum cone angle of approximately 19 mrad (eq. 36), which is beyond the design limits of DRAGON (which is approximately 16 mrad) Therefore, some recoils will not make it through the beam line, but are “clipped”, staying in the gas target box. [24].

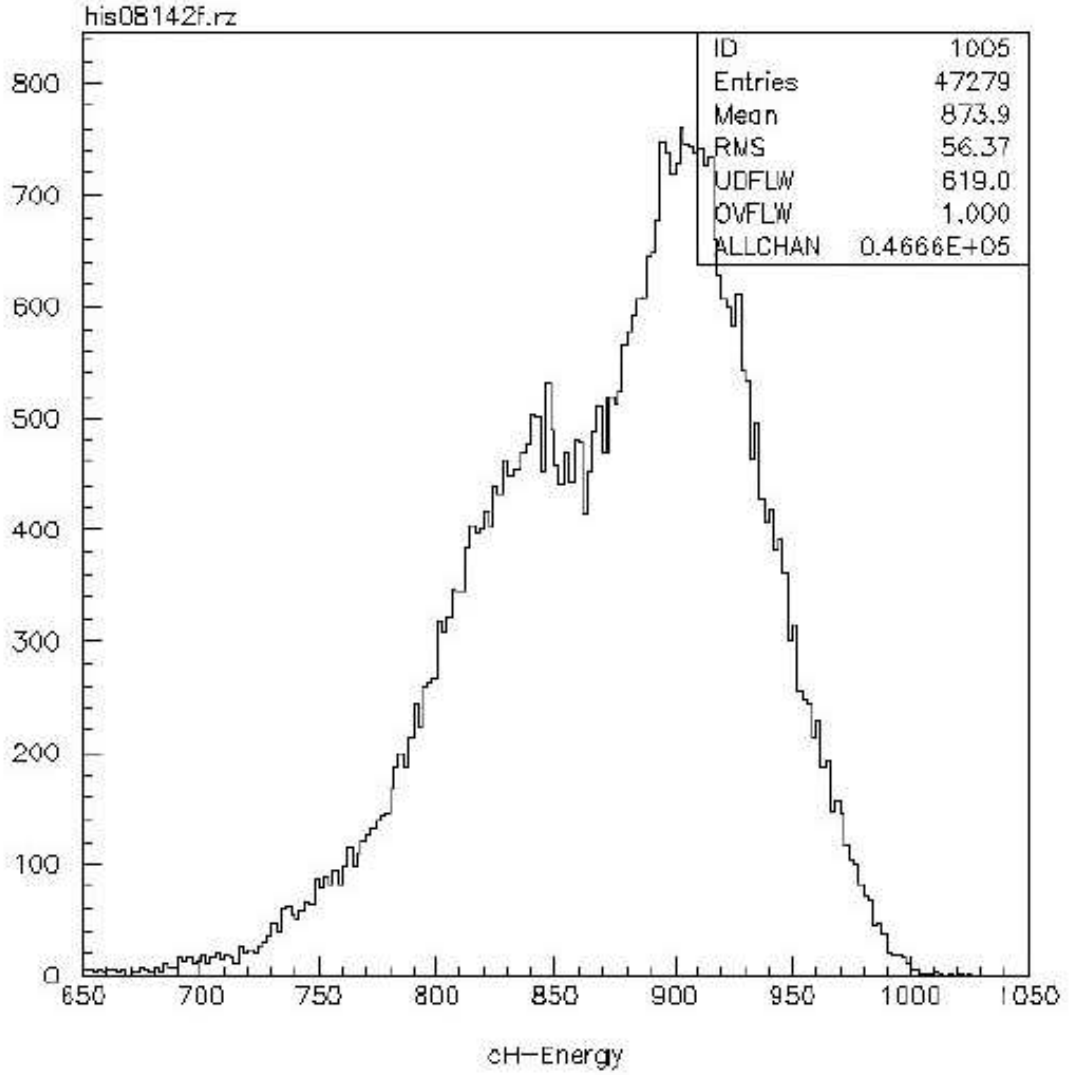


Figure 22: The coincidence recoil energy histogram for run 8142, a $^{13}\text{C}(p,\gamma)^{14}\text{N}$ reaction which had an incoming beam energy of 558 keV/u. (Channel 860 on the energy axis, corresponds to ~ 5 MeV).

5 The $^{13}\text{C}(\text{p},\gamma)^{14}\text{N}$ reaction - simulations with GEANT

5.1 GEANT

GEANT is a Detector Description and Simulation Tool. It is a program that simulates the way in which elementary particles pass through matter. It was originally designed for High Energy Physics but is also today used in medical and biological sciences, and astronautics. The main applications of GEANT for High Energy Physics are the tracking of particles through an experimental setup, for the simulation of detector response, and the graphical illustration of the setup and of the particle trajectories. [26].

5.2 The creation of the DRAGON in GEANT

A GEANT representation of the DRAGON was originally created by P.Gumplinger in the late 1990's, and was later modified by C.Ruiz in early 2003 (see figure 23). Modifications included:

- adding beampipes throughout the DRAGON to correctly simulate acceptance losses for large cone angle reactions.
- adding the capability to plot out a graphical model of the DRAGON, where events (recoils) were being lost due to acceptance losses.
- adding automatic setup of GEANT particles including beam particle, resonant particle and all excited states of the recoil, from a user defined input file. [24].

5.3 GEANT BGO simulations

Due to the many excited energy states of ^{14}N (see figure 16), and hence the large amount of cascading gamma rays, the GEANT analysis of $^{13}\text{C}(\text{p},\gamma)^{14}\text{N}$ started by concentrating solely on the 8 MeV ground state gamma emitted in this reaction, which could be compared with the paper of King et al [25]. But how would it be

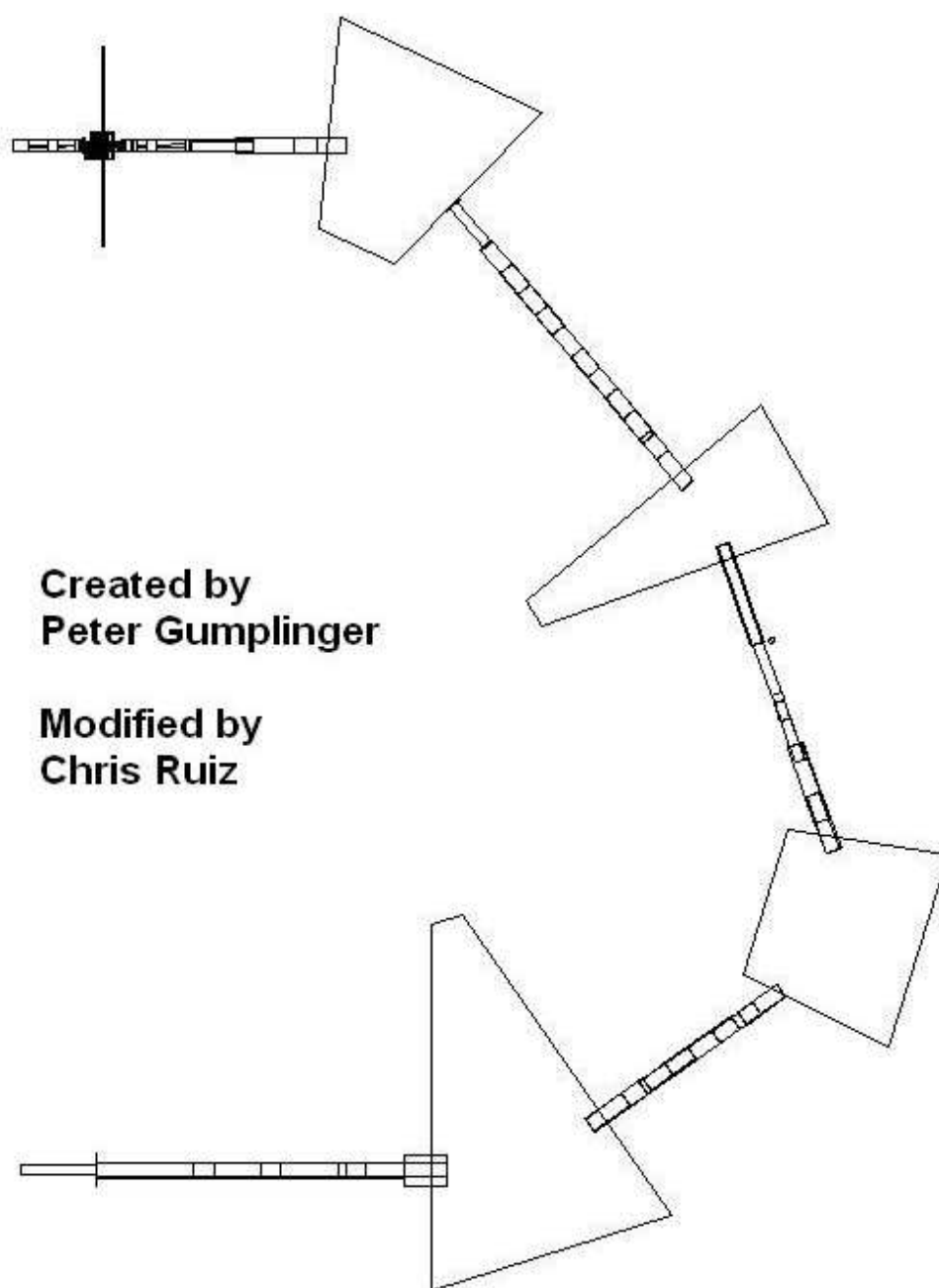


Figure 23: Graphical representation (plan view) of DRAGON using GEANT.

possible to separate out the ground state gammas from the cascading ones?

The GEANT simulation of DRAGON's BGO array was used to calculate the percentage of 8 MeV gammas that deposited all of their energy in a single BGO (figure 24). 82.2% of the number of "hits" made in a single BGO were registered by the PMTs as 8 MeV gammas. Other hits were probably due to random gammas, or 8 MeV gammas which only deposited some of their energy before escaping out of the BGO array. The BGO gamma array only covers 92% of the solid angle from the gas target (figure 25), meaning that some gammas escape completely. Of the gammas that did register, 85.3% deposited their entire energy in a single BGO, and 13.9% deposited their energy in both a BGO and its neighbour. [14].

Therefore, a method was needed to be incorporated into the analyzer, such that an event triggering a BGO, which is then followed by a trigger in a neighbouring BGO, registers as an event of interest. But what classifies as a neighbouring BGO? As seen in figures 25 and 26, the BGO gamma array is very complex.

To simplify, the GEANT BGO simulation of DRAGON's gamma detector array was updated to use a cuboid technique, where by if a BGO fires and another fires a certain distance away, which is within the cuboid, then it classes as a neighbouring BGO. [14].

5.4 $^{13}\text{C}(p,\gamma)^{14}\text{N}$ input file

Using the c12pg.dat input file created by C.Ruiz as a backbone, a GEANT input file for this reaction, known as c13pg.dat (see Appendix A), was created.

From the Table Of Isotopes, information about the excited states of ^{14}N up to

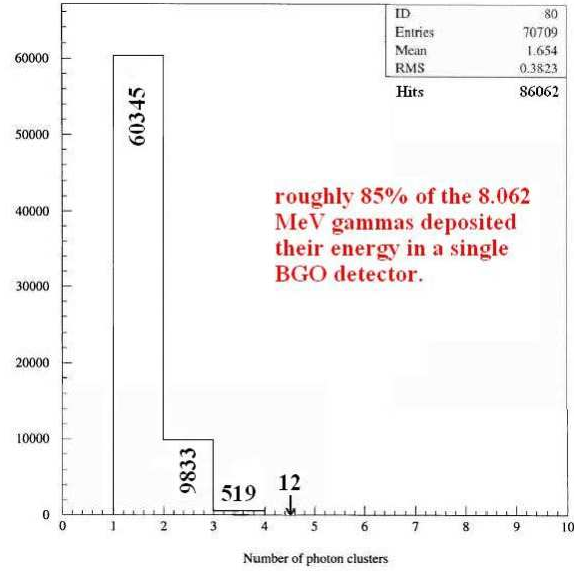


Figure 24: GEANT simulation of the probability of how many of the 8 MeV gammas are deposited in x amount of BGO crystal(s).

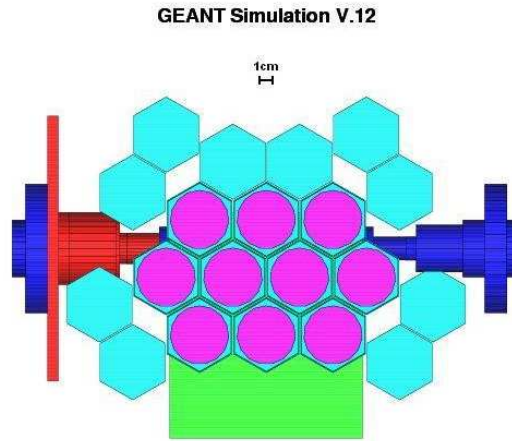


Figure 25: GEANT simulation of the BGO gamma array, looking west of the beam direction.

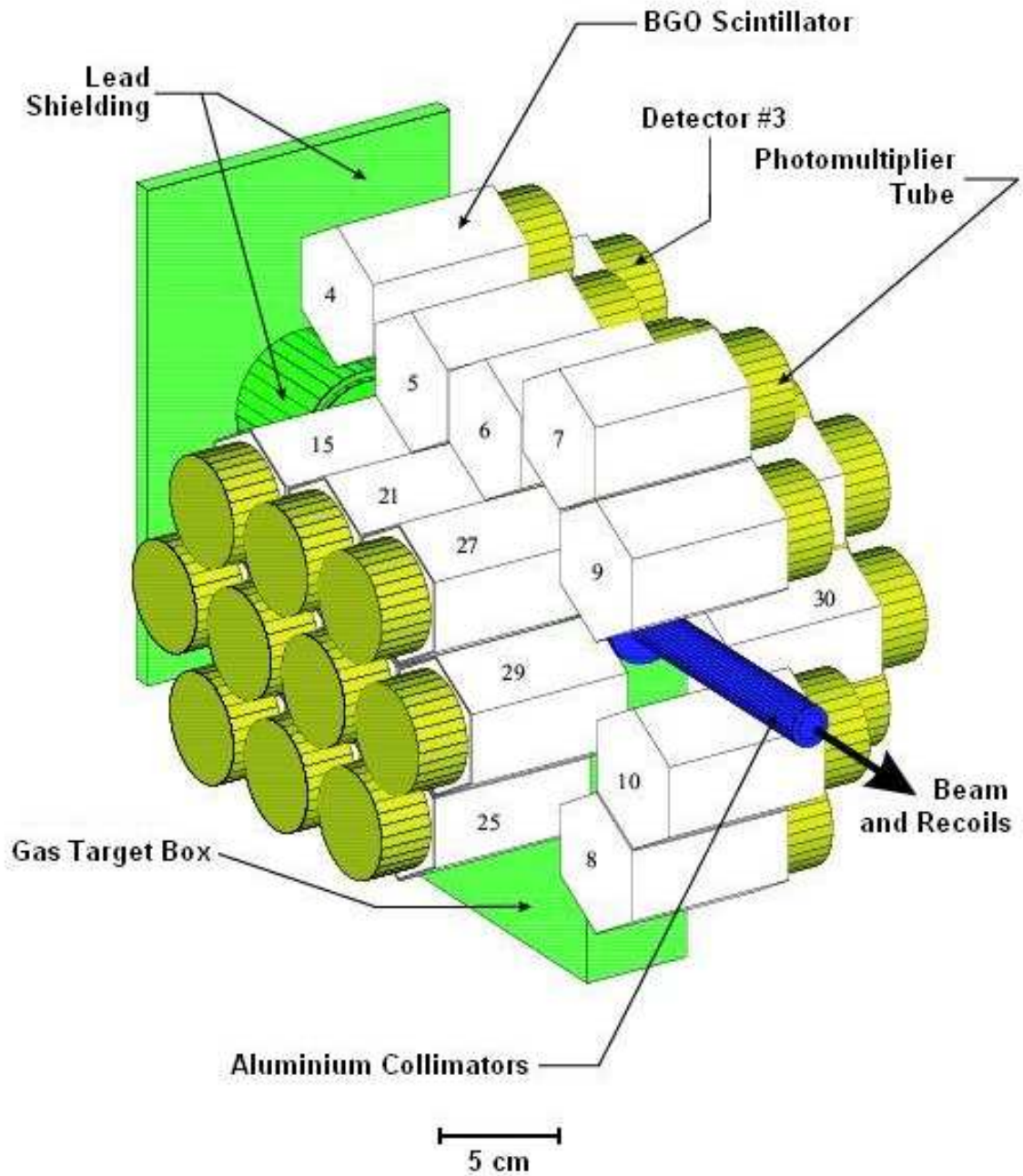


Figure 26: GEANT simulation of a 3D view of the BGO array.

and including the 8.062 MeV excited state were put into the input file. The 8.062 MeV state is the 11th excited state in ^{14}N from the ground state. The Table Of Isotopes included the percentage probabilities of what excited state of ^{14}N decayed to which other excited state in ^{14}N . The Table Of Isotopes also included the lifetimes of some of the excited states. The states that were not given a lifetime, the total resonance width (Γ) was given. The lifetime (τ) of the state was calculated using Eq. 37.

$$\tau = \frac{\hbar}{\Gamma} \quad (37)$$

(where $\hbar = 6.582 \times 10^{-16}$ eV.s)

For the 8.062 MeV, the value from King et al., $\Gamma_{tot} = 38.4 \pm 0.3$ keV, was used.

The “beam_mass_excess” and the “recoil_mass_excess” were found from [27] and [28] respectively. The “resenerg” is the resonance energy, which is found using Eq. 38. E_x is the energy of the excited case, which will be 8.062 MeV.

$$E_{res} = E_x - Q \quad (38)$$

The “gam_width” is the gamma width, which for the 8.062 MeV state, was found from [29] to be $\Gamma_\gamma = 9.9 \pm 2.5$ eV. The “part_width” was calculated using Eq. 39.

$$\Gamma_\alpha = \Gamma_{tot} - \Gamma_\gamma \quad (39)$$

The “spin_stat_frac” was calculated using Eq. 40.

$$\omega = \frac{(2J + 1)}{(2I_1 + 1)(2I_2 + 1)} \quad (40)$$

where J is the spin of the resonance state, I_1 is the spin of the projectile, and I_2 is the spin of the target. The spin of ^{13}C ground state is equal to $1/2^-$. The spin of ^1H ground state is equal to $1/2$. The spin of the 8.062 MeV excited state in ^{14}N is equal to 1^- .

If $\text{I}_1 = 1/2^-$, and $\text{I}_2 = 1/2^+$, then the two possible s values are $s = 1^-, 0^-$. To find “ell” (ℓ), we have to use Eq. 41.

$$|\mathbf{J}| = |\ell + \mathbf{s}| = |\ell + \mathbf{I}_1 + \mathbf{I}_2| \quad (41)$$

Therefore, if $\ell = 0$ then $J^\pi = 1^-, 0^-$, or if $\ell = 1$ then $J^\pi = 0^+, 1^+, 2^+$. For the 8.062 MeV state, $J^\pi = 1^-$, and therefore, $\ell = 0$.

All this data was put into the c13pg.dat file and before a simulation was run, this file was called.

5.5 Initial $^{13}\text{C}(\text{p},\gamma)^{14}\text{N}$ simulations

By creating an input file for the $^{13}\text{C}(\text{p},\gamma)^{14}\text{N}$ reaction, it was now possible to simulate this reaction through DRAGON to compare with the actual data. Figure 22 is an energy histogram of one of the best runs from the $^{13}\text{C}(\text{p},\gamma)^{14}\text{N}$ experiment. It had an incoming beam energy of 558 keV/u and gas pressure of 2 Torr. It has a rough peak energy of 5 MeV. Simulating the same conditions with the DRAGON GEANT simulation gave a peak energy of 6.55 MeV (see figure 27). The DRAGON group believed this 1.5 MeV energy loss happened as the recoils pass through the entrance window (a mylar foil) of the ionization chamber. As a test of the effect, work began on creating an ionization chamber within GEANT for the DRAGON simulation¹⁷. Other motivation for simulating the ionization chamber were to: a) get a proper estimate of energy straggling, b) find out what anode the recoil ion stops in, c) get a proper energy spectrum, d) compare with the real data and estimate the acceptance loss, e) simulate the correct geometry features of the energy loss, f) test recoils in different pressures within the ionization chamber.

¹⁷The ionization chamber had not been included in the simulation before this point, and one had never been created with GEANT. It was the job of the author to create one.

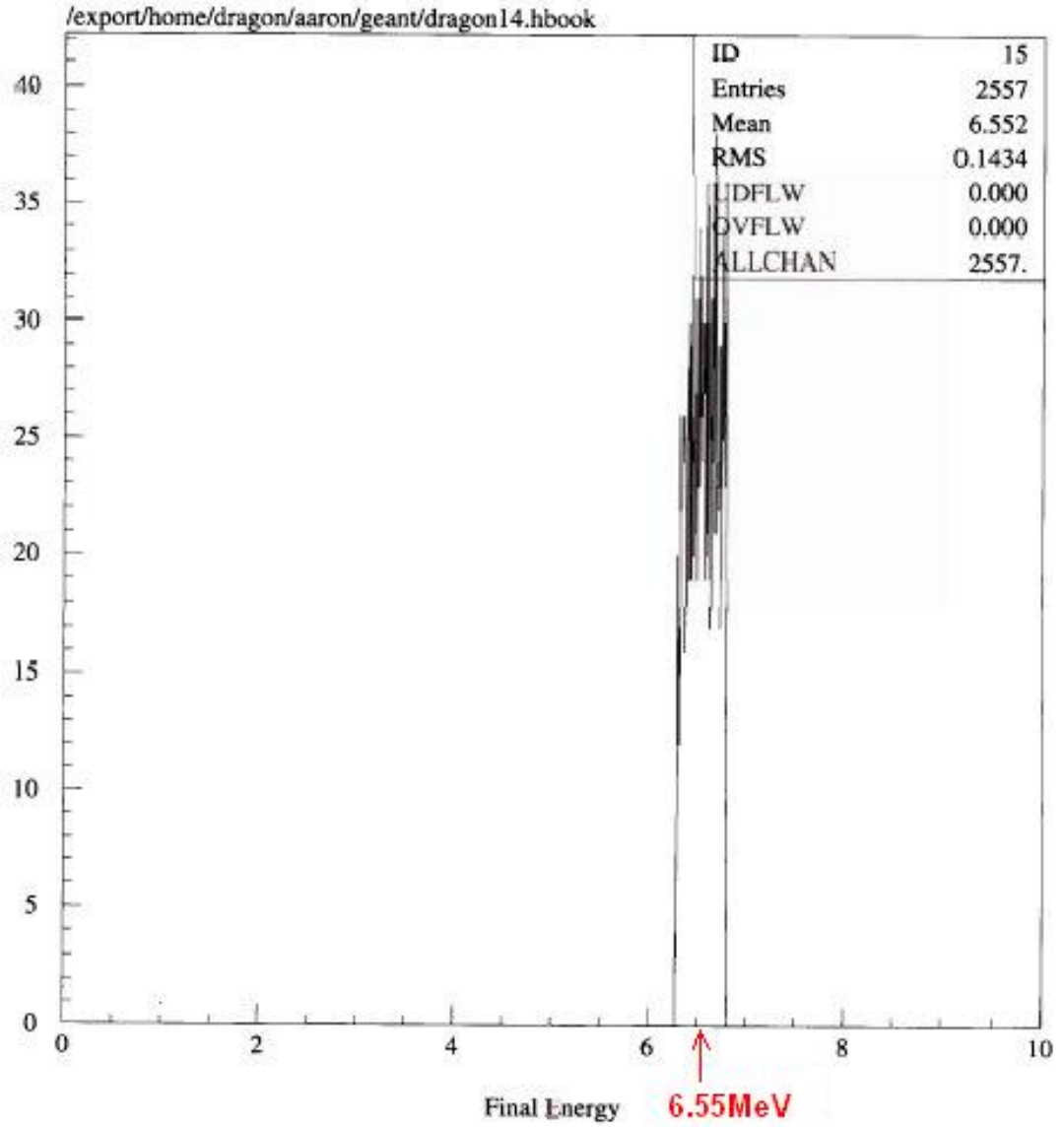


Figure 27: Initial simulations of the $^{13}\text{C}(p,\gamma)^{14}\text{N}$ reaction. Under the same parameters of run 8142, a different coincidence recoil energy histogram was found, with a peak energy 1.5 MeV larger than the actual data.

6 Design of the Ionization Chamber in GEANT

6.1 Creating volumes and materials in GEANT

To create volumes and materials in GEANT, the interactive version¹⁸ of GEANT must be firstly run. Once within this version, volumes are created by filling in various command windows about the name, size, type, material, and position of the volume. Once completed, the GEANT volume can be viewed.

If a material is required that is not specified in GEANT already (such as isobutane and mylar), then that material can be create in a similar way to creating volumes. The information needed is the density, mixture of elements and their weight ratios, and their atomic A and Z numbers.

Once happy with the volumes and materials that have been created, they can be inserted into the simulation. The GEANT simulation of DRAGON is very large, and calls many subroutines. These new volumes and materials need to be updated in some of these routines. The new materials, isobutane and mylar, were updated in subroutines ‘ugmate’ (used to define tracking materials) and ‘ugstmed’ (used to define tracking mediums). (See Appendix B and C, respectively).

A new subroutine, ‘ugeo_ionc’, was created in the main subroutine ‘ugeom_mitray’. In ‘ugeo_ionc’, the ionization chamber was defined. Here, the new volumes are defined, positioned, and called into the main simulation.

¹⁸GEANT can be run in two versions - interactive and batch. The interactive version of GEANT allows the user to track a single particle through the experimental setup. The batch version allows the user to simulate any number of reactions within the experimental setup. Before each interactive and batch run of GEANT, a source file is loaded, to present the input files (see figure 28).

```

[dragon]> source setup.csh
Setting environment variables...
MITRAY=dragon_2001b.dat
FFCARD=dragon_2003.ffcards
INPUT=c13pg.dat
[dragon]> dsbatch

```

Figure 28: The source file loaded before each interactive and batch versions of GEANT.

COMPOSITION OF MYLAR:	
Atomic element and number	Fraction by weight
Hydrogen (1)	0.041959
Carbon (6)	0.625017
Oxygen (8)	0.333025

Table 3: Shows the fractional composition of the elements that make up Polyethylene Terephthalate (Mylar) [30].

6.2 Mylar and Isobutane properties

Mylar

Once a particle enters the ionization chamber, it enters an entrance tube, which, like the separator tubes, is full of vacuum. At the end of this entrance tube, the recoil particles have to penetrate a window (foil) made of Mylar. Mylar, its full name being Polyethylene Terephthalate (figure 29), has a density of 1.39 g/cm^3 [30] and is made up of hydrogen, carbon, and oxygen. The ratio of these three elements in Mylar are shown in Table 3.

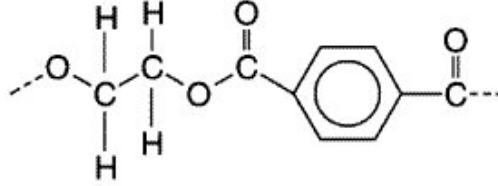


Figure 29: A Polyethylene Terephthalate (Mylar) molecule [31].

COMPOSITION OF ISOBUTANE: $\text{CH}(\text{CH}_3)_3$		
Atomic element	No. of atoms per isobutane molecule	% per molecule
Hydrogen	4	0.7143
Carbon	10	0.2857

Table 4: Shows the fractional composition of the elements that make up Isobutane [33].

Isobutane

Once through the Mylar window, the recoils enter a ‘dead layer’ of isobutane gas. An isobutane molecule (figure 30) is made up as shown in Table 4 . The density of isobutane at standard temperature and pressure (STP) is 0.00267 g/cm^3 [34].

6.3 Initial designs of the ionization chamber (problems and solutions)

Schematic drawings of the DRAGON’s ionization chamber had been found to be slightly inaccurate [35]. The ionization chamber contains a mylar window (foil) positioned at the end of the entrance tube. This foil keeps the isobutane gas inside the ionization chamber. Directly behind the mylar window is a 2 mm isobutane dead

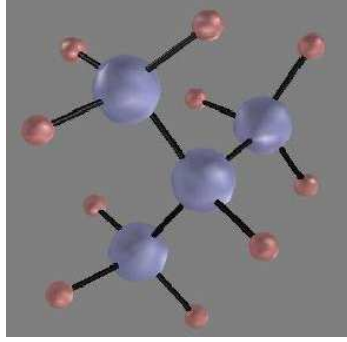


Figure 30: An isobutane molecule - 4 hydrogen atoms (blue) and 10 carbon atoms (green). [32].

layer. The anode region is found directly behind the dead layer. [35].

Not being able to open up the casing of the ionization chamber to check the measurements, the dimensions of the ionization chamber in the schematic diagram had to be assumed to be correct. One dimension that was possible to check, was the length of the entrance tube. This was found to be roughly 49 mm longer than the schematic diagram (a length of 10.5 cm).

The thickness of the mylar window was found from [36] to be 120 - 140 $\mu\text{g}/\text{cm}^2$. Knowing the density of mylar, the thickness of the window was calculated to be $(9.4 \pm 0.7) \times 10^{-5} \text{ cm}$ ($\sim 0.9 \pm 0.1 \mu\text{m}$).

The positioning of the ionization chamber in the ‘WRLD’ volume¹⁹, was found from the schematic drawing of the DRAGON’s final focus area (figure 31). The distance from the front face of the horizontal final slits to the ionization chamber’s window was measured/calculated to be 61.96 cm. This worked out to be a distance of 73.41 cm to the centre of the ionization chamber, from the final slits, which is the distance needed for the simulation. [37].

¹⁹This is the main volume where the GEANT experimental setup (in this case, the DRAGON) was created (figure 23)

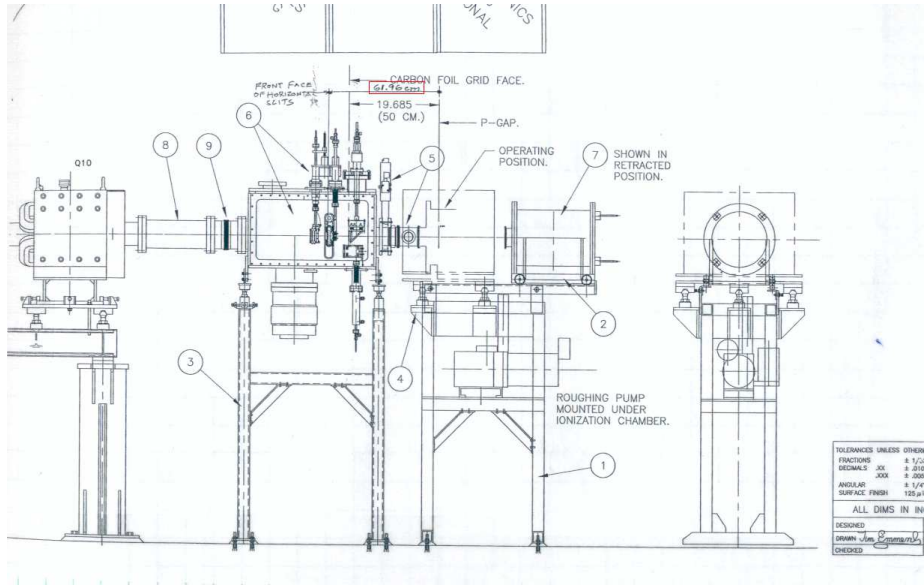


Figure 31: Schematic drawing (from [37]) of DRAGON's final focus area.

Initial problems with the design of the ionization chamber were firstly with the entrance tube. The space inside the tube was not defined as anything, so that once a particle entered it, the medium was not defined, and hence GEANT could not compute the tracking. The solution was to create a solid aluminium entrance tube, and place a slightly thinner solid vacuum tube inside of that. However, now the particle would enter the tube, but would not get to the end because the aluminium casing for the ionization chamber was cutting through the tube (see figure 32).

As the recoils particles never have any interference with the outside edge of the ionization chamber, it was totally plausible to make the aluminium casing encompass the entire tube. By doing this, the entrance tube could be deleted, only having the vacuum tube for the particles to travel through.

These changes to the ionization chamber simulation were made in the `ugeom_mitray.f` file, under a subroutine known as `'ugeo_ionc'`, which defined the (simple) ionization chamber.

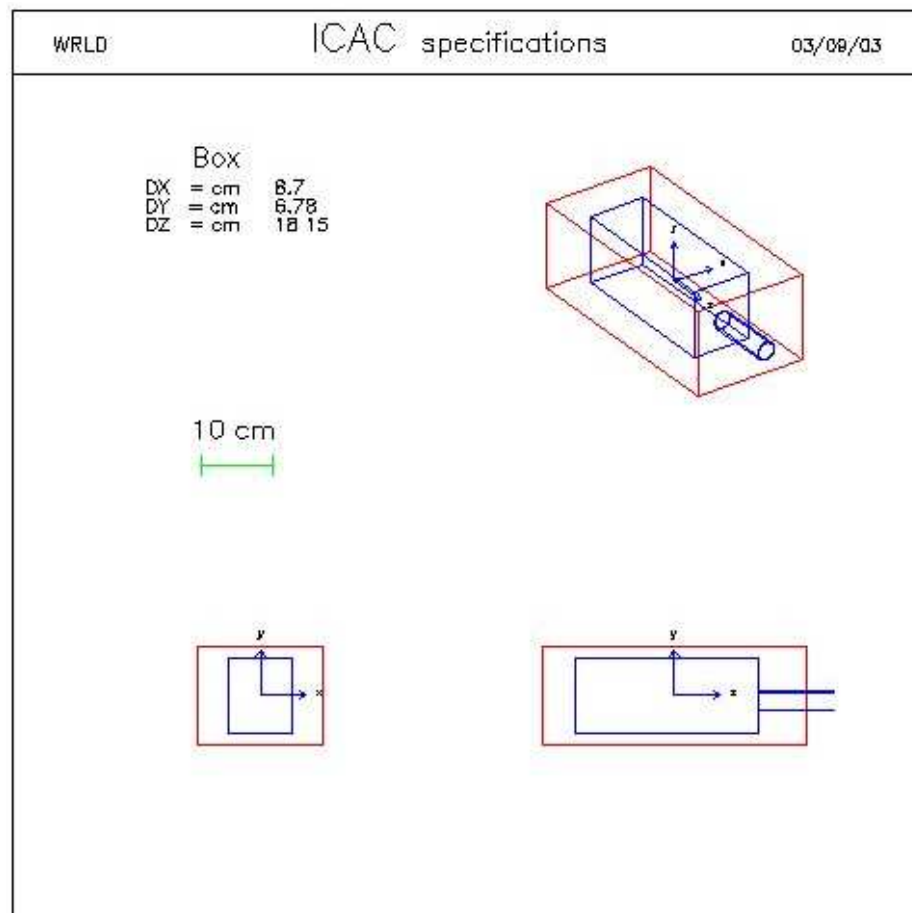


Figure 32: Initial design schematic of the simulated ionization chamber. Shows the outer volume (casing) cuts through the entrance tube.

There were still problems with the tracking of particles through the ionization chamber, with the recoil still not being able to make it to the end on the entrance tube. To try and understand the simulation, volumes were moved around, volumes were deleted from the ionization chamber, changes were made to material densities, etc. In doing so, a few errors were adjusted, only to come across others.

GEANT volumes are given ONLY or MANY flags. The aluminium casing (ICAC) which holds all of the ionization chamber volumes, is known as a ‘mother’ volume. The volumes inside ICAC are known as ‘daughter’ volumes. In GEANT, daughter volumes can overlap the mother volumes. However, if a daughter volume overlaps another daughter volume, then it is given a MANY flag (for example, some of DRAGON’s beam pipes overlap the dipoles). All other volumes are given an ONLY flag. It was suggested that a better way to construct the ionization chamber in the simulation was that the mother volume, ICAC, should be made of vacuum, and that the entrance tube should encompass the vacuum tube again. [38].

The two subroutines that deal with the output histograms, `gustep_mitray.f` and `uhinit.f` (see Appendix D and E, respectively), had to be updated so that the final energy spectrum would show the energy of the recoils in the ionization chamber.

The first few batch simulations of the $^{13}\text{C}(\text{p},\gamma)^{14}\text{N}$ reaction, showed that the recoils all stopped in the anode 1 region of the ionization chamber (expected anode was number 3). The reason for this was found later to be that the density of isobutane was given in STP and not the pressure in the actual ionization chamber. Standard pressure is 760 Torr and the pressure in the ionization chamber during the experiment was 14.6 Torr. So in the simulation, the material density was changed accordingly. Running an interactive simulation showed that the particle now stopped in the anode 2-3 region, which is what was expected.

It was noted during the interactive GEANT simulations that the Mylar window was not being recognized by GEANT, and the particle was carrying on through the

a)

X	Y	Z	R	NAME	NUMBER	SLENG	STEP	DESTEP	GEKIN	MECHANISMS
-1024.4609	0.8944	91.5523	1024.4613	Q14	14	1952.0723	0.4059	0.0	eV	6.716 MeV FIEL
-1024.4613	0.8940	91.5040	1024.4617	Q14	14	1952.1206	0.0483	0.0	eV	6.716 MeV FIEL NEXT
-1024.4613	0.8940	91.5040	1024.4617	WRLD	1	1952.1206	0.0000	0.0	eV	6.716 MeV NULL
-1026.1208	-0.4909	-96.7754	1026.1210	WRLD	1	2140.4124	188.2917	0.0	eV	6.716 MeV NEXT
-1026.1208	-0.4909	-96.7754	1026.1210	ICVT	1	2140.4124	0.0000	0.0	eV	6.716 MeV NULL
-1026.2134	-0.5681	-107.2725	1026.2135	ICVT	1	2150.9131	10.5008	0.0	eV	6.716 MeV NEXT
-1026.2134	-0.5681	-107.2755	1026.2135	ICDL	1	2150.9131	0.0000	0.0	eV	6.716 MeV NULL
-1026.2134	-0.5681	-107.2808	1026.2135	ICDL	1	2150.9185	0.0054	1.1	keV	6.715 MeV LOSS MULS

b)

X	Y	Z	R	NAME	NUMBER	SLENG	STEP	DESTEP	GEKIN	MECHANISMS
-1024.4609	0.8944	91.5523	1024.4613	Q14	14	1952.0723	0.4059	0.0	eV	6.716 MeV FIEL
-1024.4613	0.8940	91.5040	1024.4617	Q14	14	1952.1206	0.0483	0.0	eV	6.716 MeV FIEL NEXT
-1024.4613	0.8940	91.5040	1024.4617	WRLD	1	1952.1206	0.0000	0.0	eV	6.716 MeV NULL
-1026.1208	-0.4909	-96.7754	1026.1210	WRLD	1	2140.4124	188.2917	0.0	eV	6.716 MeV NEXT
-1026.1208	-0.4909	-96.7754	1026.1210	ICVT	1	2140.4124	0.0000	0.0	eV	6.716 MeV NULL
-1026.1671	-0.5295	-102.0255	1026.1672	ICVT	1	2145.6628	5.2505	0.0	eV	6.716 MeV NEXT
-1026.1671	-0.5295	-102.0255	1026.1672	ICVT	1	2145.6628	0.0000	0.0	eV	6.716 MeV NULL
-1026.2134	-0.5681	-107.2756	1026.2135	ICVT	1	2150.9133	5.2504	0.0	eV	6.716 MeV NEXT
-1026.2134	-0.5681	-107.2756	1026.2135	ICDL	1	2150.9133	0.0000	0.0	eV	6.716 MeV NULL
-1026.2134	-0.5681	-107.2809	1026.2135	ICDL	1	2150.9187	0.0054	1.1	keV	6.715 MeV LOSS MULS

Figure 33: Problems with GEANT recognizing the mylar window. a) An interactive run shows the tracking of the recoil particle leaving the vacuum entrance tube (ICVT) and passing straight into the isobutane dead layer (ICDL), missing the mylar window (ICMW) all together. b) Moving the mylar window to the middle of the vacuum tube, the interactive run shows that GEANT recognizes a division within the tube, but does not pass the particle through the division (due to no energy loss) and seems to simply ‘skip it’, placing the particle after the division, allowing it to pass to the end of the tube.

vacuum tube into the isobutane dead layer, without losing any energy through the window (figure 33a). This meant that particles were not entering the anode region of the ionization chamber at the correct energy. Changing the tracking precision to the maximum preciseness had no effect. Moving the mylar window to the middle of the vacuum tube showed that GEANT would recognize a division in the tube, and notes the energy at this position. However it seemed to then place the particle back into the vacuum tube, after the window, and carry on to the end of the tube, into the ionization chamber (figure 33b).

No matter what was tried, it seemed that the window was just too thin for GEANT to recognize it. Most of the volumes in the DRAGON GEANT simulation are metres and centimetres, but the mylar window is less than a micrometre thick. Through trial and error, it was found that the window had to be around 0.002-3 cm thick (roughly 30 times thicker than its current value) for it to be recognized by GEANT. If the window was 30 times thicker, the particles would never make it through the window. If the window was 30 times thicker, and 30 times less dense, the particles would make it through, but was the energy loss and straggling effects the same as the original window?

6.4 SRIM calculations for mylar

To test that by increasing the mylar window thickness by 30 times, and decreasing the density of mylar by 30 times, had no effect on the energy loss, SRIM (Stopping and Range of Ions in Matter) was used to calculate the energy loss of five thousand 6716 keV ^{14}N recoils through both types of mylar.

The GEANT interactive simulation run previously with the new thicker less dense window, showed a ^{14}N recoil enter the mylar window (ICMW) with 6716 keV energy, and leave the window with 5508 keV energy (figure 34). This worked out to be a loss of 1206 keV energy through the mylar window.

The first SRIM calculation was done for the original mylar window, which had a thickness of 0.94 μm and a density of 1.39 g/cm³. The output of SRIM on all five thousand events was sent to an output text file, which contained information on the energy and position of each event (figure 35). The energy information from this text file was copied into a Microsoft Excel document, and a histogram was plotted. Next, the mean, error, sigma (standard deviation), and normalization needed to be specified, (which Microsoft Excel can solve for you). To find the values of a Gaussian

X	Y	Z	R	NAME	NUMBER	SLENG	STEP	DESTEP	GEKIN	MECHANISMS
-1024.4574	0.8974	91.9581	1024.4578	Q14	14	1951.6664	0.4059	0.0 eV	6.716 MeV	FIEL
-1024.4609	0.8944	91.5523	1024.4613	Q14	14	1952.0723	0.4059	0.0 eV	6.716 MeV	FIEL
-1024.4613	0.8940	91.5040	1024.4617	Q14	14	1952.1206	0.0483	0.0 eV	6.716 MeV	FIEL NEXT
-1024.4613	0.8940	91.5040	1024.4617	WRLD	1	1952.1206	0.0000	0.0 eV	6.716 MeV	NULL
-1026.1208	-0.4909	-96.7754	1026.1210	WRLD	1	2140.4124	188.2917	0.0 eV	6.716 MeV	NEXT
-1026.1208	-0.4909	-96.7754	1026.1210	ICVT	1	2140.4124	0.0000	0.0 eV	6.716 MeV	NULL
-1026.2134	-0.5681	-107.2727	1026.2135	ICVT	1	2150.9104	10.4980	0.0 eV	6.716 MeV	NEXT
-1026.2134	-0.5681	-107.2727	1026.2135	ICMW	1	2150.9104	0.0000	0.0 eV	6.716 MeV	NULL
-1026.2144	-0.5681	-107.2756	1026.2145	ICMW	1	2150.9133	0.0028	1.2 MeV	5.508 MeV	SCOR NEXT LOSS MULS
-1026.2144	-0.5681	-107.2756	1026.2145	ICDL	1	2150.9133	0.0000	0.0 eV	5.508 MeV	NULL
-1026.2144	-0.5681	-107.2810	1026.2145	ICDL	1	2150.9187	0.0054	1.7 keV	5.506 MeV	LOSS MULS
-1026.2144	-0.5681	-107.2863	1026.2145	ICDL	1	2150.9241	0.0054	5.0 keV	5.501 MeV	LOSS MULS
-1026.2144	-0.5681	-107.2917	1026.2145	ICDL	1	2150.9294	0.0054	3.7 keV	5.498 MeV	LOSS MULS

Figure 34: part of the output from an interactive GEANT simulation of a single ^{14}N recoil going around the simulated DRAGON separator. This part of the output, shows the energy of the ^{14}N recoil as it leaves the last quadrupole (Q10 - known as Q14 in GEANT) and enters the simulated ionization chamber. The highlighted box, shows the information of the ^{14}N recoil as it passes through the mylar window (known as ICMW in GEANT).

plot, Eq. 42 was used.

$$G = norm \times e^{-\left[\frac{(E_A - mean)^2}{2(sigma)^2}\right]} \quad (42)$$

where E_A is the energy of the recoil.

The energy loss was calculated using Eq. 43.

$$E_{loss} = E_{in} - mean \quad (43)$$

where $E_{in} = 6716 \text{ keV}$

This exact same process was done for the second SRIM calculation, for the new mylar window, which had a thickness of 0.00282 cm and a density of 0.04633 g/cm³.

The energy loss through mylar at a thickness of 0.94 μm and a density of 1.39 g/cm³ (the properties of DRAGON's actual mylar window for the ionization chamber) was calculated to be 1.2247 MeV.

Figure 35: the start of a typical SRIM output. This .txt file was the SRIM calculation output for mylar with a thickness of $0.94 \mu\text{m}$ and a density of 1.39 g/cm^3 (i.e. the properties of DRAGON's actual mylar window).

The energy loss through mylar at a thickness of 0.00282 cm and a density of 0.04633 g/cm³ (the properties of DRAGON's GEANT simulation of the mylar window for the ionization chamber) was calculated to be 1.2251 MeV (figure 36).

6.5 Continuation of the ionization chamber simulation

After the SRIM calculations found no significant difference in energy loss between the two types of mylar window, GEANT simulations of the ionization chamber went ahead. Straggling effects were included to the simulation of the ionization chamber, to simulate the energy spread effect.

From the data of the $^{13}\text{C}(\text{p},\gamma)^{14}\text{N}$ reaction with the DRAGON, the full-width-half-maximum (FWHM) of the total energy deposited in the ionization chamber, was found to be 0.858657 [19]. This gave a standard deviation (σ) of 0.365386 (see Eq. 44).

$$\sigma = \frac{FWHM}{2.35} \quad (44)$$

Using this value of σ and a subroutine found from [39], and modifying it, the code in figure 37 was added into GEANT to the `gustep_mitray.f` file to create the straggling effects.

The simulated batch runs showed a double peak in the final energy spectrum (figure 38), which was expected, but showed two regions of recoils stopping in the ionization chamber (figure 39), which was not expected.

These two regions of recoils were believed to be the result of the high and low energy recoils. To prove this, the average peak energies were taken to be 5.2 MeV and 6.4 MeV (see figure 38), and used in SRIM to calculate the stopping ranges of ^{14}N at these energies in isobutane (at the correct density for the ionization chamber), (see figures 40 and 41).

SRIM showed that the two different energies of ^{14}N recoils stop 2 cm apart (figure 42), which corresponded with the two regions in GEANT (figure 43). The stopping

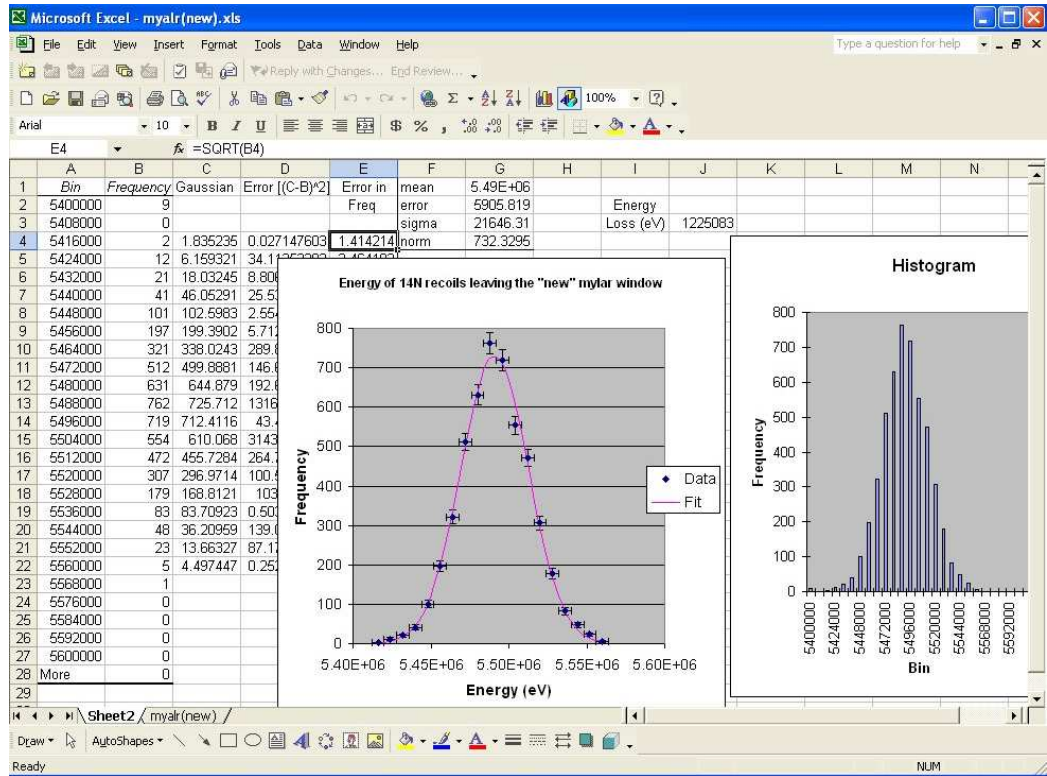


Figure 36: a Microsoft Excel worksheet, used to plot the output of the SRIM calculation, and to calculate the energy loss through mylar. This particular worksheet was used for the SRIM calculation of mylar with a thickness of 0.00282 cm and a density of 0.04633 g/cm³ (i.e. the properties of DRAGON's GEANT simulation of the mylar window for the ionization chamber).

```

C. *****
C. ***Adding ionization chamber straggling effects.***
C.
      CALL granor(rndm(1),rndm(2))
      sigma = 0.365386
      trec = trec + (sigma*rndm(2))
C. *****

```

Figure 37: Code added to the `gustep_mitray` subroutine to cause straggling to the final energy data.

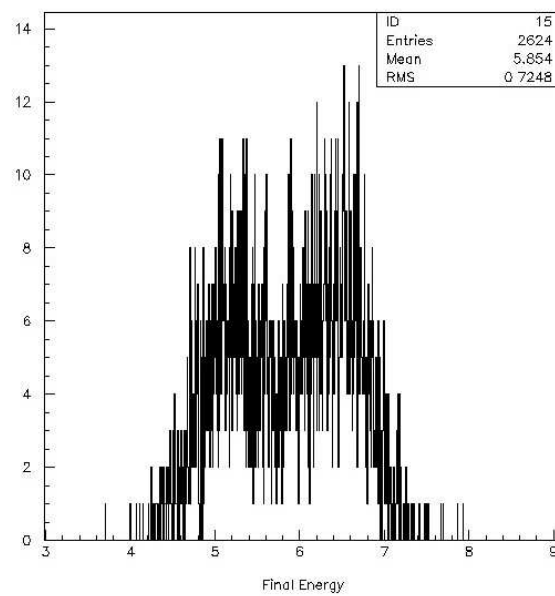


Figure 38: Final energy histogram of a simulation (run 32 - Oct 6th) of the $^{13}\text{C}(p,\gamma)^{14}\text{N}$ reaction, showing a double peak structure.

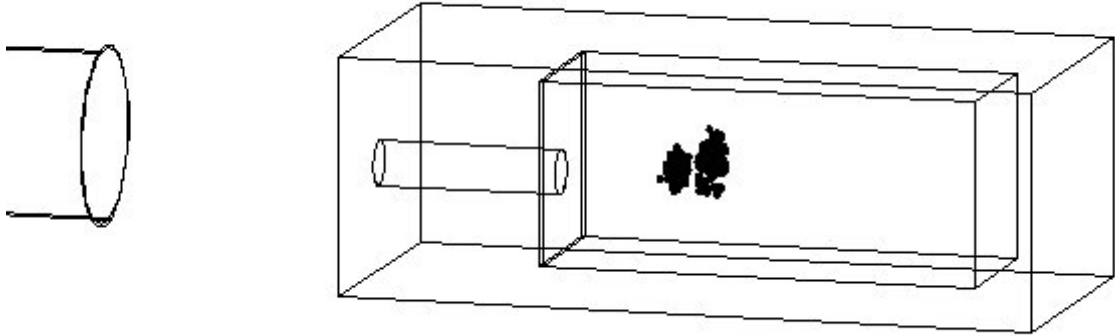


Figure 39: Shows the positioning of the ^{14}N recoils in the ionization chamber, after a batch run (run 32 - Oct 6th).

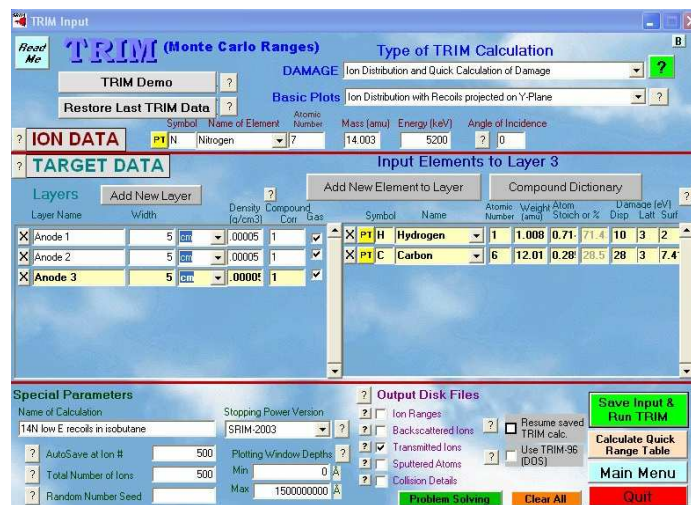


Figure 40: the SRIM input for a stopping range calculation. This particular input is for ^{14}N particles at 5.2 MeV passing through 3 layers (i.e. the first 3 anodes of the ionization chamber) of 5 cm thick isobutane.

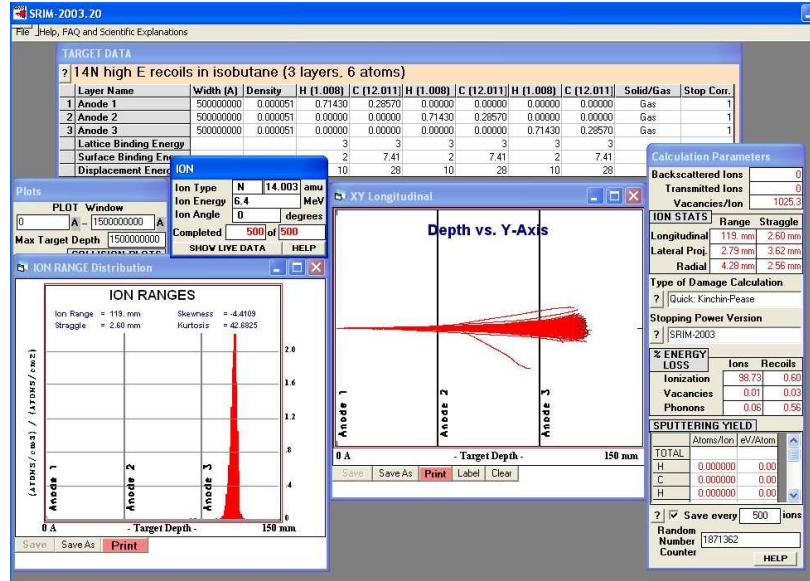


Figure 41: SRIM's graphical representation of the recoils as it calculates the stopping range of, in this case, 500 ^{14}N ions at 6.4 MeV in isobutane.

distances are different, but SRIM calculations of energy loss are more complex than the GEANT calculations.

Although, this proved that the two regions of recoils shown in the ionization chamber were of different energies, it was still puzzling why there were two regions of recoils rather than one continuous region.

The solution was discovered later while running some interactive simulations. While tracking a recoil through the simulation to the end detector, it was observed that the recoil missed the entrance tube, and passed straight through the ionization chamber, into the isobutane (figure 44). It had been recommended by [38] making the mother volume of the ionization chamber out of vacuum, because that would better simulate the particle effect if they were to escape out of the isobutane anode region, rather than a solid aluminium casing. However, in doing so, recoils which are not travelling along the centre of the beam line through the separator, could miss the

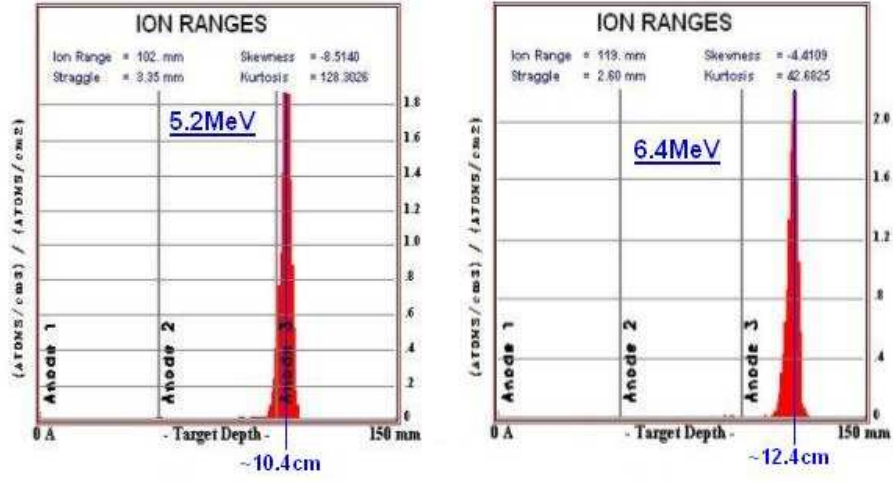


Figure 42: The stopping ranges for 5.2 MeV and 6.4 MeV respectively ^{14}N recoils in isobutane, as calculated by SRIM.

ionization chamber.

Also, it was noted that the entrance tube of the ionization chamber, was slightly off centre in the y-direction of the ionization chamber, and because the ionization chamber ‘sits’ in the centre of the beam line, the entrance tube does not.

The mother volume was changed back to being made of aluminium and the entrance tube was no longer needed with the vacuum tube, and so was deleted. The ionization chamber was moved up in the y-direction by 0.75 cm, so that the tube was in the centre of the beam line.

It was at this point, during the remodification of the ionization chamber in GEANT, while doing a scale drawing of the changes made to the ionization chamber, that it became apparent that the entrance tube in the simulation was not 5 cm in diameter as it should be. Earlier in the design of the ionization chamber in GEANT, it was realized that GEANT volumes had to be specified in half lengths. So all lengths were halved, including the radiuses of the tubes. If the radius of the entrance tube

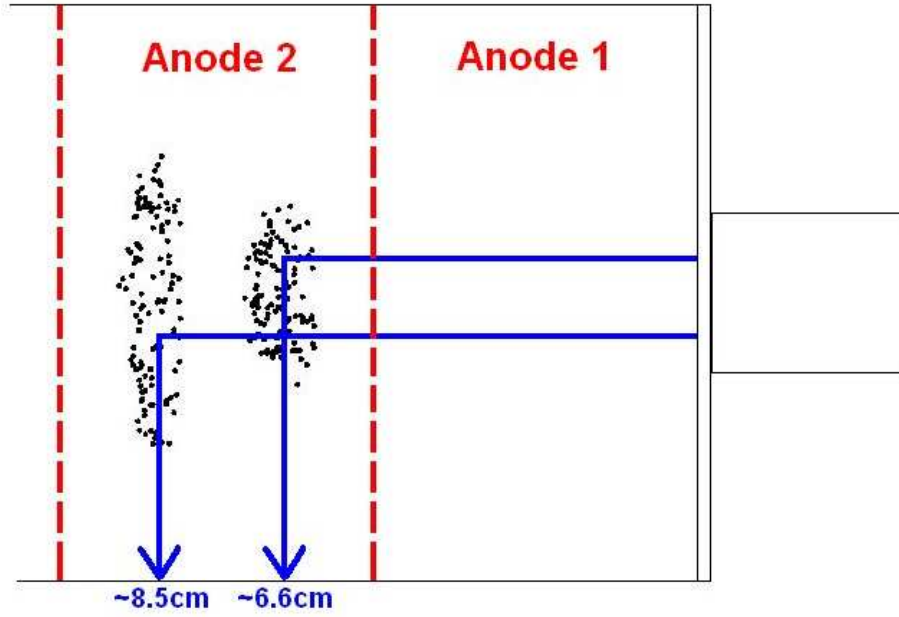


Figure 43: a blow-up diagram of the GEANT simulated ionization chamber (viewed from the top looking down) showing the stopped position of the ^{14}N recoils, and their distance of travel in the isobutane gas.

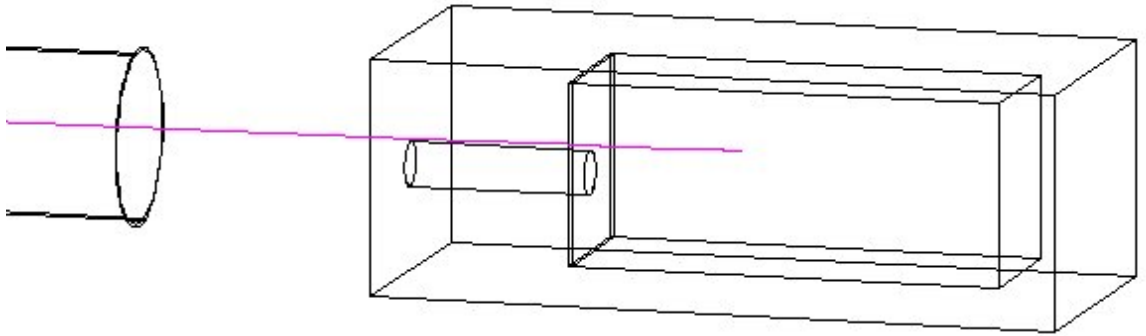


Figure 44: an interactive version of the simulation, showing the recoil particle missing the entrance tube to the ionization chamber and passing through the mother volume and into the isobutane.

had not been inaccurate, then the discovery of the ionization chamber being off centre to the beam line, would have gone unnoticed.

With the radius of the entrance tube adjusted to its correct dimension, the final design of the ionization chamber was now complete (figure 45). Interactive and batch simulations of GEANT were run; the interactive version showing that the recoil made it into the ionization chamber via the tube and mylar window (figure 46), and the batch version showing that the recoils only stop in one region of isobutane gas (figure 47).

The reason that the recoils were stopping in two regions in previous batch simulations was believed to be because that some recoils passed through the tube, and hence through the window, losing roughly 1.2 MeV of energy and stopping roughly 6.6 cm after the dead layer. The second region would have been formed from recoils that missed the tube and window, passing straight through the dead layer into the isobutane, not losing the 1.2 MeV of energy, and hence stopping roughly 8.5 cm after the dead layer. SRIM showed that the recoils with 6.4 MeV stop 2 cm further than 5.2 MeV recoils, but the reason there were 6.4 MeV recoils in the isobutane was because they had not lost any energy through the window, because they had not passed through it.

Appendix F shows the GEANT code for the `ugeo_ionc` subroutine of the final design of the ionization chamber.

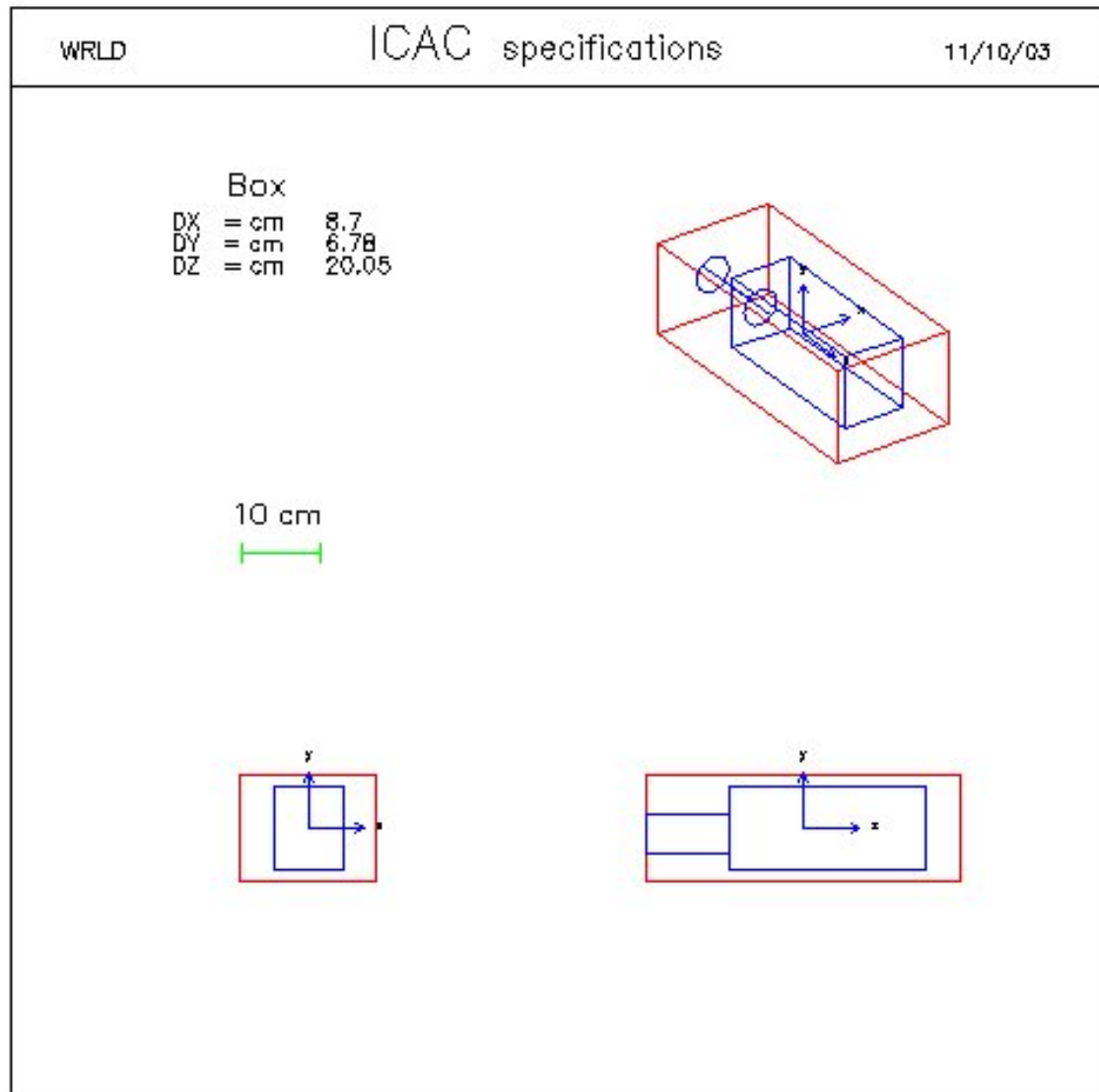


Figure 45: Final design schematic of the simulated ionization chamber.

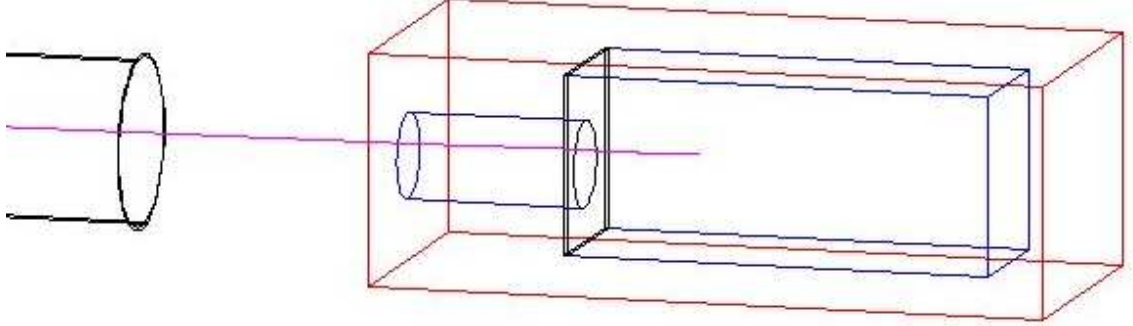


Figure 46: An interactive simulation, with the final design of the ionization chamber, showing that the recoil passes through the vacuum tube, mylar window, isobutane dead layer, and into the anode region of isobutane.

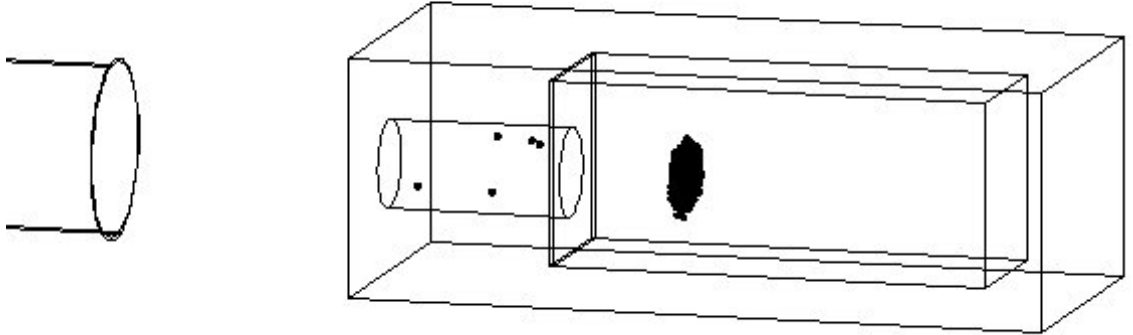


Figure 47: A batch simulation, with the final design of the ionization chamber, showing that the recoils all stop in one region (the Anode 2 region) in the ionization chamber.

7 Testing DRAGON's Acceptance

Now that the simulation had proven to work correctly, the next step was to use the simulations for mistuning the reference tune of DRAGON. The reference tune is a perfect tune of the incoming beam to DRAGON, which allows the beam to pass through the DRAGON with maximum efficiency. The beam (in the GEANT simulation) can be mistuned from the reference tune by x and y position, x and y angle, and percentage of energy.

7.1 Rebinning of histograms in GEANT

Figure 48 shows the final energy histogram for run 52. Run 52 was mistuned by 2 mrad in the negative y angular position. The spectrum is very “spiky” and therefore a method was needed to rebin the data in such a way that a general outline of the final energy was plotted. Using the `rescale.f` subroutine found from [40], this was modified to rebin the data (see Appendix G). Now, after the original histogram is plotted, `rescale.f` can be called to plot another version of this histogram, which can be rebinned to produce a more general spectrum. It can also be used to change the x-axis so that only the region of interest is plotted (see figure 49).

7.2 Effects of the straggling and energy loss in the ionization chamber

As a comparison, code was added to the subroutines `gustep_mitray.f` and `uhinit.f` to create a histogram (ID700) of the final energy without the straggling (see figure 50a and 50c). Using `rescale.f`, histogram (ID700) was rebinned and the region of interest was selected, to produce histogram (ID701). The data from histogram (ID1015) in figure 49 was then overlaid onto the new histogram (ID701), so that the effects of the energy spread (straggling) from the ionization chamber, could be observed (see

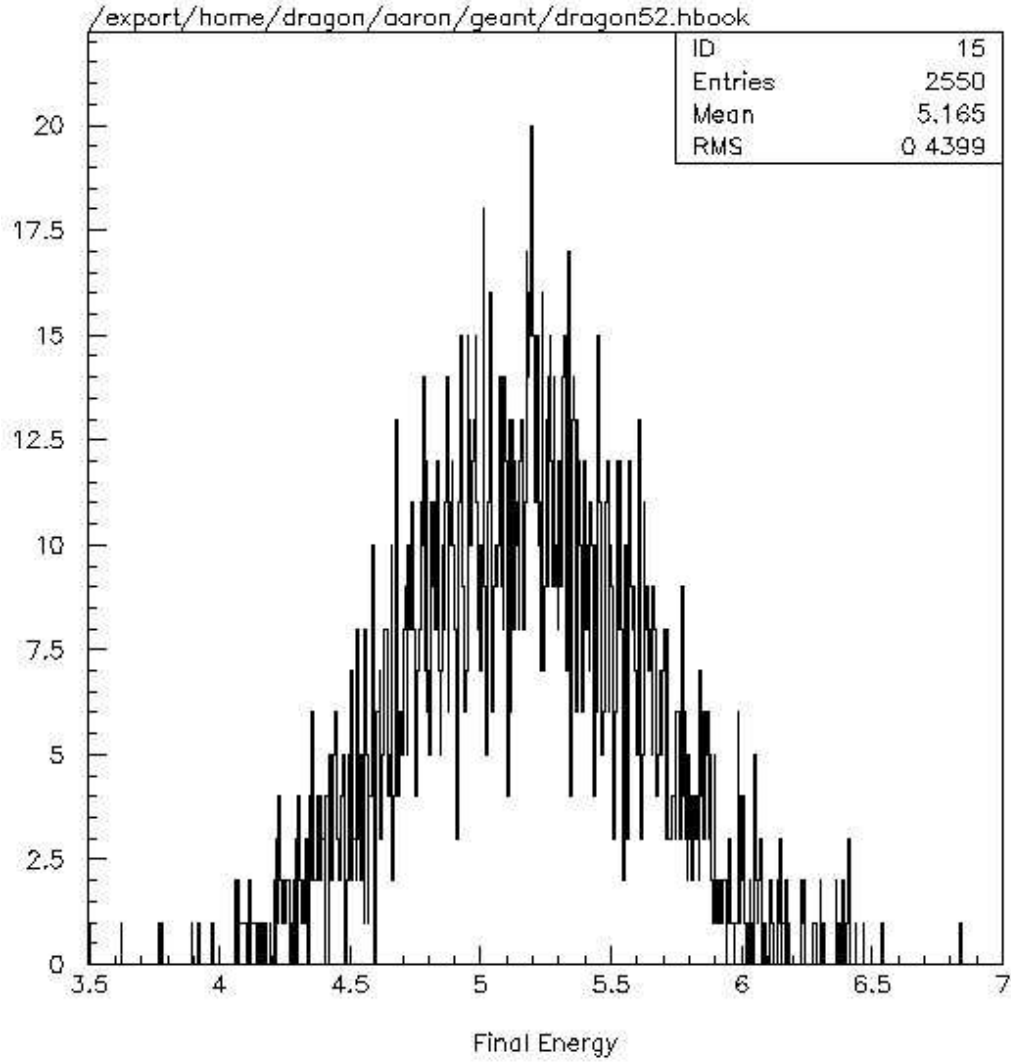


Figure 48: The final energy spectrum of the recoils from a GEANT simulation of the $^{13}\text{C}(p,\gamma)^{14}\text{N}$ reaction. This was run 52 which had a mistuned reference tune by 2 mrad in the negative y angular position.

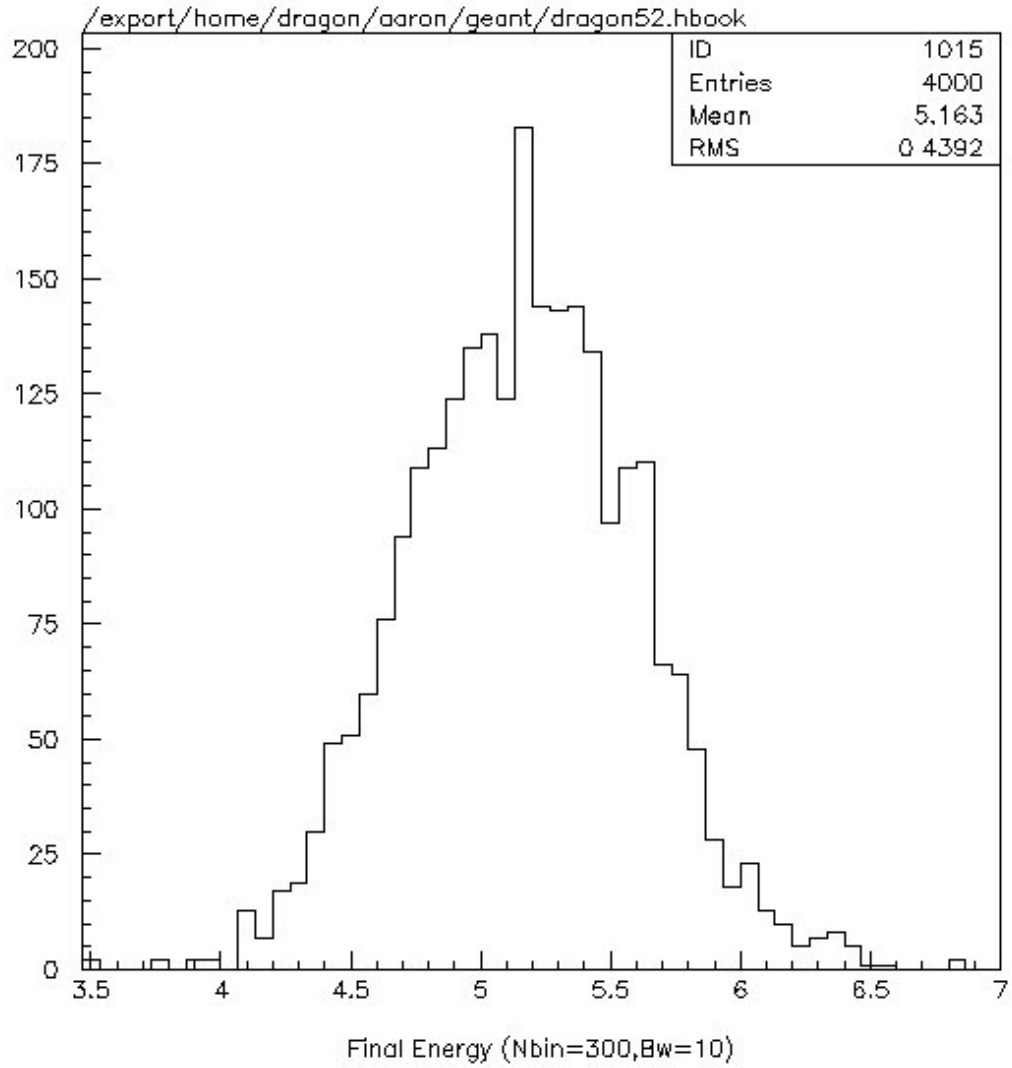


Figure 49: The data from the histogram (ID15) in figure 48 was rebinned using the modified `rescale.f` subroutine, to give a more general pattern of the results.

```

a) C. *****
C. ***call final energy spectrum with no straggling***
C.
C.         CALL hfill(700,trec,0.0,1.0)
C. *****

b) C.
C. *** If particle has entered the vacuum (entrance) tube of the IC
C.
C.         If(chname_nlevel.eq.'ICVT' .and. in_new_vol.eq.1 )then
C.             CALL hfill(710,trec,0.0,1.0)
C.         Endif
C.

c) C. Final Energy with no straggling effects (15.10.03):
C.     CALL hbook1(700,'Final Energy (no straggling)',4000,0.0,20.0,0.0)

d) C. Energy entering the ionization chamber (22.10.03):
C.     CALL hbook1(710,'Energy entering IC',4000,0.0,20.0,0.0)

```

Figure 50: More code added to the subroutines `gustep_mitray.f` (a&b) and `uhinit.f` (c&d) to produce more histograms about the final energy of the recoils. a)&c) is the code added to produce histogram (ID700), which shows the final energy of the recoils minus the straggling effect. b)&d) is the code added to produce histogram (ID710), which shows the energy of the recoils after they have passed round the DRAGON and before they enter the ionization chamber.

figure 51). Code was later added to the same two subroutines (see figure 50b and 50d) to plot a histogram showing the energy of the recoils before they enter the ionization chamber. With this new histogram (ID710), it was possible to illustrate the amount of energy loss that occurs as the recoils pass through the mylar window of the ionization chamber into the isobutane gas (see figure 52).

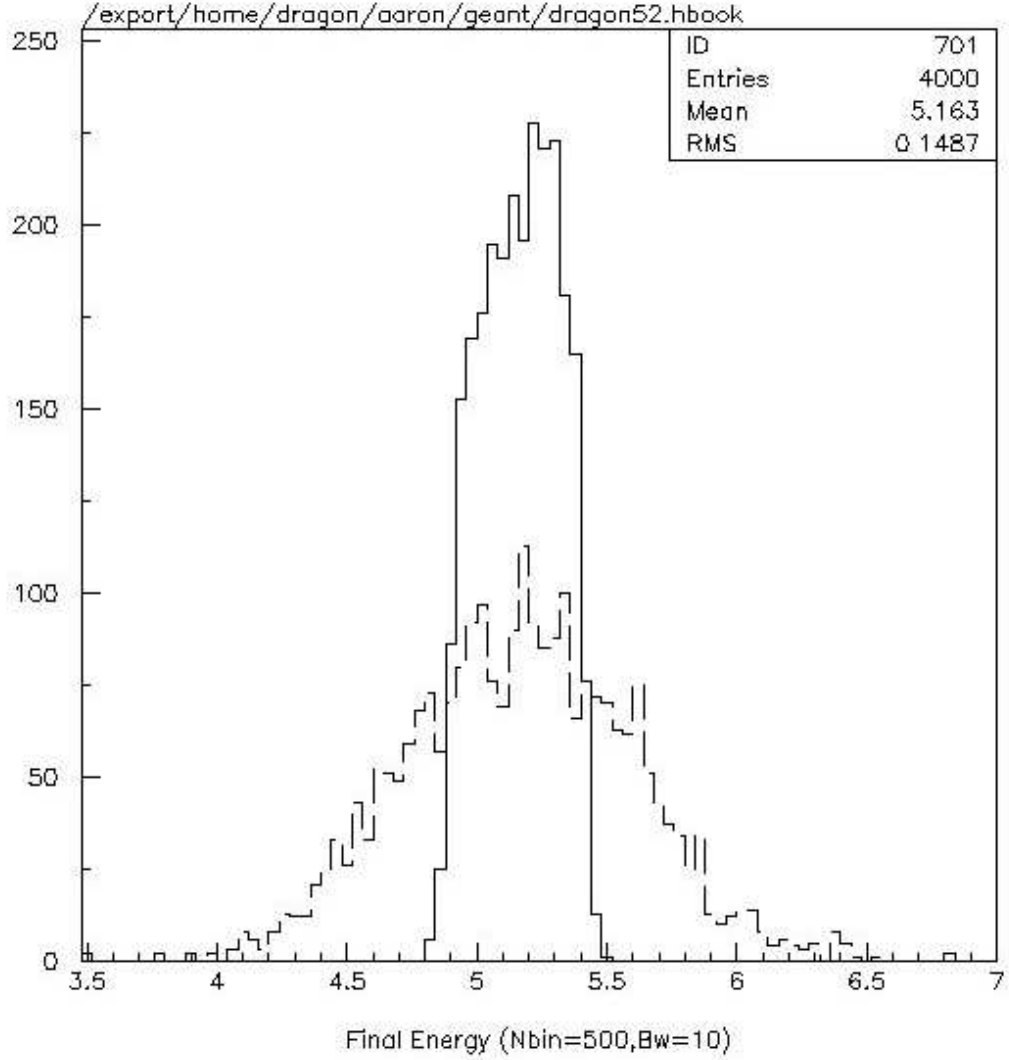


Figure 51: To show the effects of the energy straggling, caused by the ionization chamber, the data from histogram (ID1015) in figure 49 of the final energy of the recoils (with added straggling effects) is overlaid onto new histogram (ID701), which is the final energy of the recoils (no straggling). Both sets of data have been rebinned using the rescale.f subroutine.

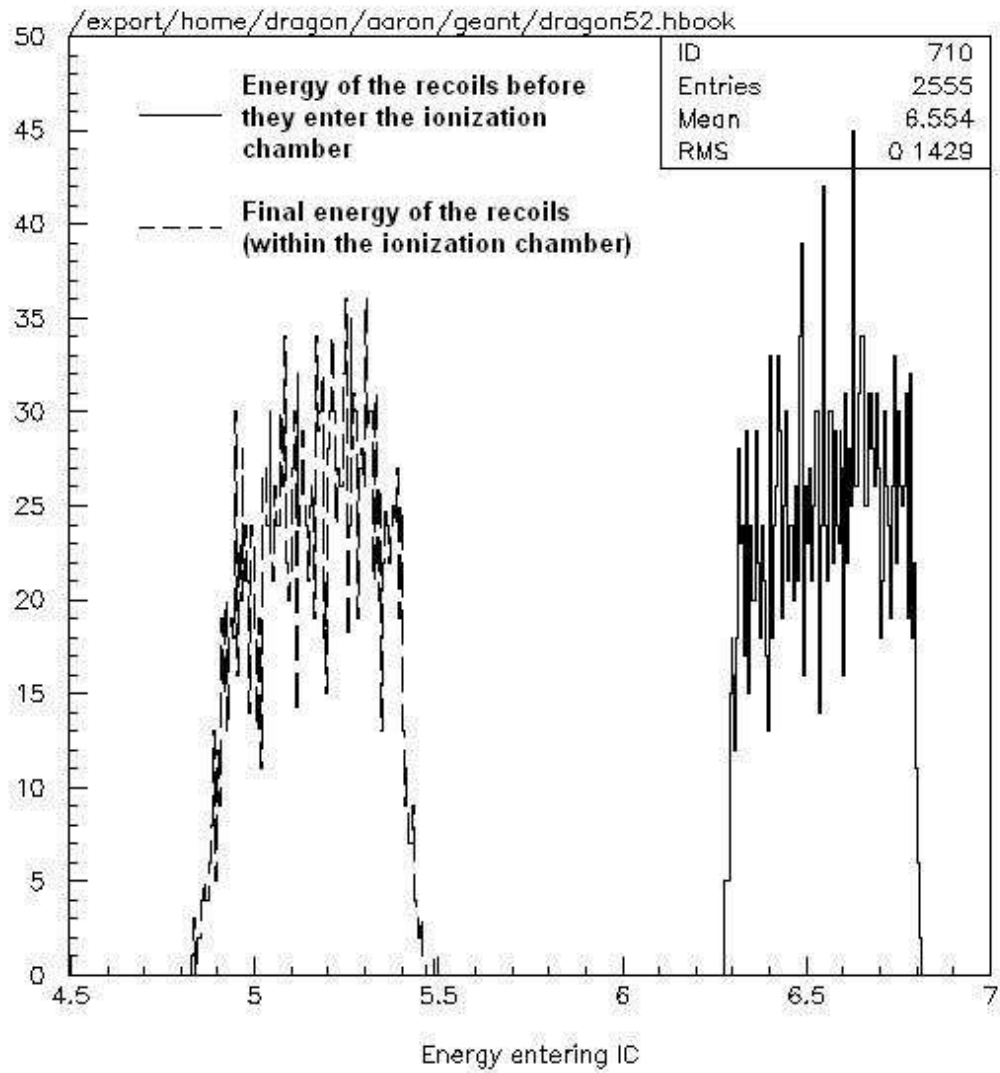


Figure 52: The data from the histogram (ID700) for run 52, is overlaid onto histogram (ID710), to illustrate the amount of energy that the recoils lose as they pass through the mylar window of the ionization chamber.


```

GEANT> set hcol 1001
GEANT> set bcol 1007
GEANT> h/pl 710 (70:150)
GEANT> set hcol 1004
GEANT> h/pl 700 s
GEANT> set hcol 1002
GEANT> h/pl 15 s

```

1 (the histogram is filled), 0 (only the border is drawn)

Border colour (if the histogram is filled)
[0 for no border]

Inside colour (if histogram is filled),
border colour (if not filled).

plot histogram 710 between channels 70 and 150

plot the data from histogram 700 into histogram 710

1=black
2=red
3=green
4=blue
5=yellow
6=purple
7=light blue
8=white

Figure 53: The commands needed to produce a coloured histogram.

7.3 Adding colour to GEANT

To colour histograms in GEANT, a SET command was used, which can specify both the border and the inside colour for the histogram (HCOL) and the box (BCOL). For an example, see figures 53 and 54.

It was also possible to colour in GEANT volumes, using the DOPT and SATT commands. See figures 55 and 56.

7.4 Acceptance Loss

The GEANT simulation was able to plot an energy histogram of the recoils as they occur, in the centre of DRAGON's gas target. To get a representation of the loss of the recoils through the DRAGON, this histogram was overlaid with the data for the final energy of the recoils before they enter the ionization chamber (see figure 57).

From figure 57, the shift down in the y-axis of the data corresponds to the acceptance loss through the DRAGON. The overlaid data (from figure 52) corresponds to 2555 recoils that make it through the DRAGON. If 3317 recoils were created, this gives an acceptance of 77%. The reasoning for the shift in energy in the x-axis of

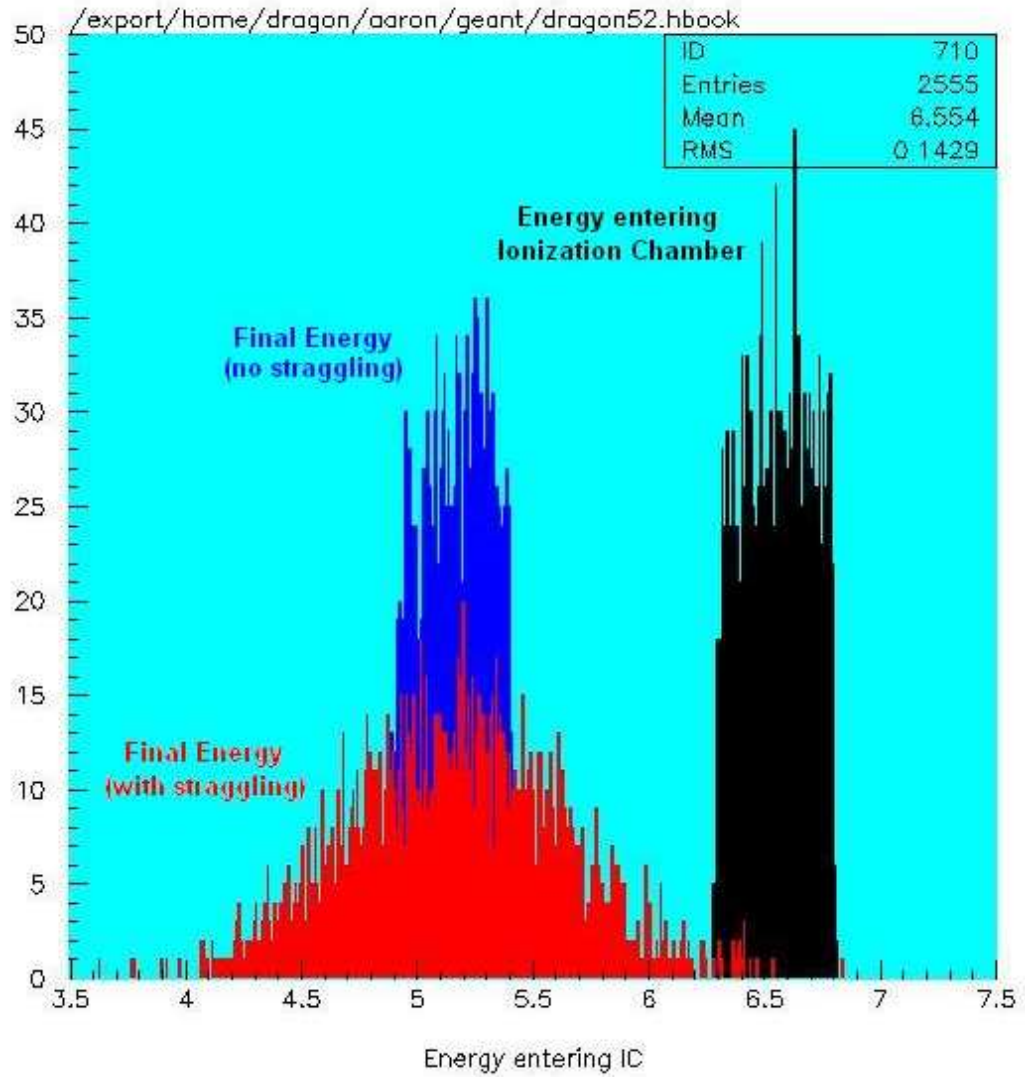


Figure 54: A coloured histogram, from run 52, using the commands in figure 53. The histogram illustrates the effects of the energy loss through the ionization chamber, and the straggling effects to the data.

```

GEANT> dopt 'shad' 'on'
GEANT> satt 'icvt' 'lsty' 7
GEANT> satt 'icac' 'colo' 7
GEANT> satt 'icac' 'fill' 7

```

precision of circular volumes (max=7)
 colours volume icac (7=light blue)
 shadow effect on volume (max=7)

All volumes are transparent, until the following code is typed in, which fills the volumes:

```

GEANT> dopt 'hide' 'on'

```

Figure 55: The commands needed to colour in GEANT volumes. In this case, the mother volume of the ionization chamber (ICAC) is being coloured light blue.

the recoils once through the DRAGON, is from the loss of energy as the recoils pass through gas in the target before they enter the vacuum of the DRAGON. (The target is 12.3 cm in length, and the simulation triggers the events in the centre of the target).

After each batch simulation, information about the positioning of the recoils final place of rest and their energy, was saved as a .end file. Creating a hits.kumac file to read the .end file of interest (figure 58) was used to illustrate the ‘hits’ around the DRAGON (or a specific GEANT volume of interest - such as the ionization chamber) of the recoils created in the gas target (see figure 59).

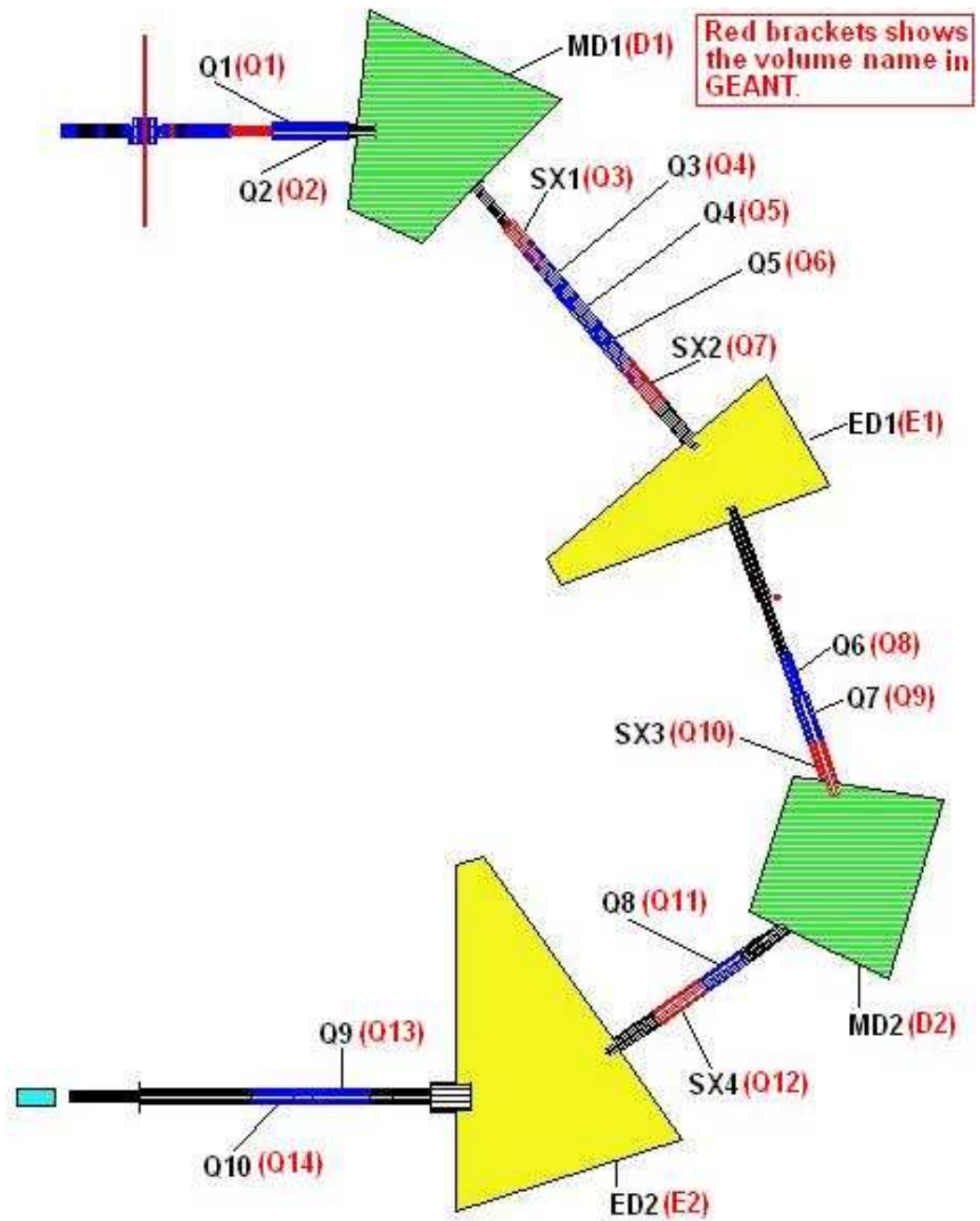


Figure 56: Colouring all the different volumes of DRAGON simulation to distinguish where all the different parts are found.

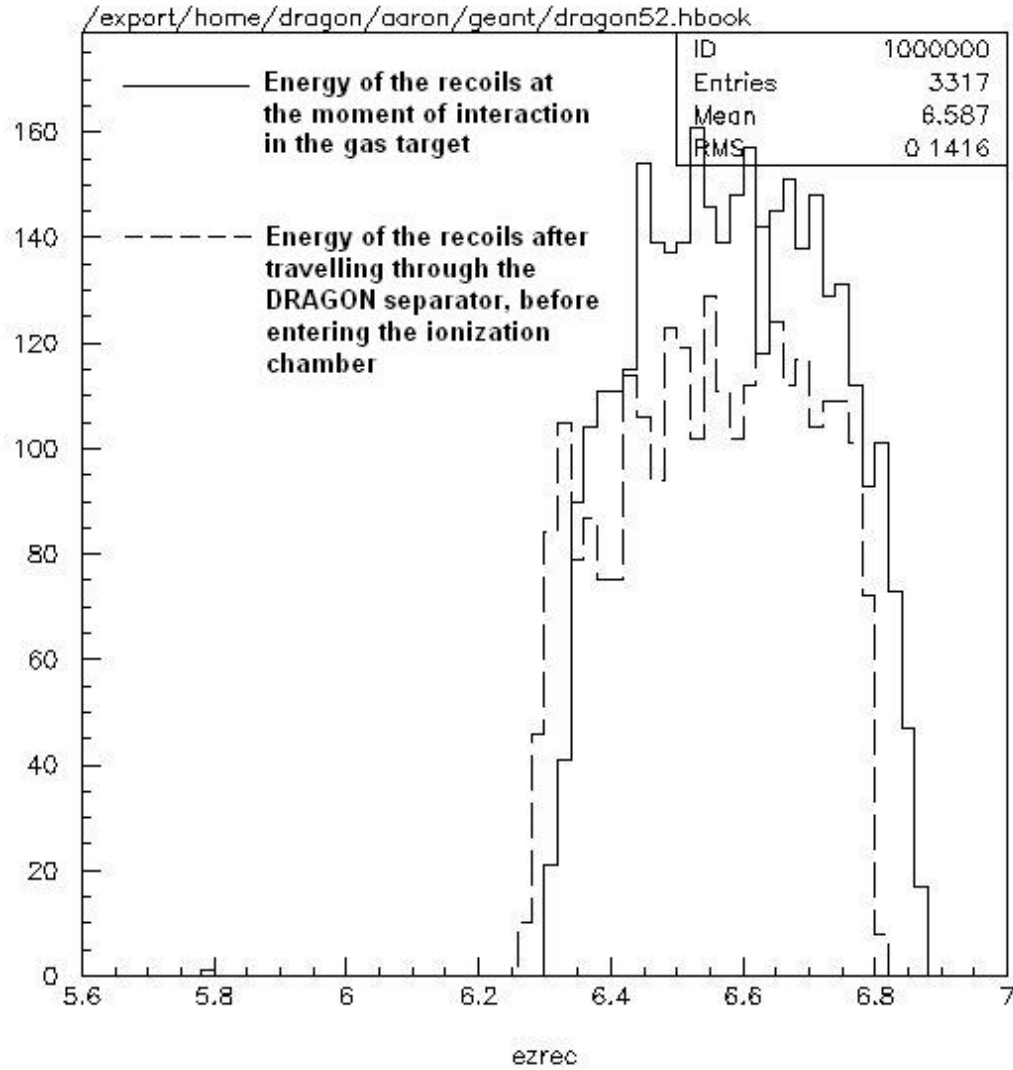


Figure 57: This histogram shows the energy of the recoils at the moment of creation in the gas target. Out of 5000 triggered events, 3317 recoils occurred, for this run (run 52). Overlaying this energy data is the rebinned data (to fit with the scale of this data) from histogram (ID710), of the same run (as in figure 52), which is the energy of the recoils after they have passed around the DRAGON and before they enter the ionization chamber.

```

emacs@lin01a.triumf.ca
Buffers Files Tools Edit Search Mule Help

MACRO HITS
mess "Drawing hit points"
vec/read x,y,z,e /home8/dragon/aaron/geant/dragon52.end
CALL GDCOL(2)
do i= 1, 3317
CALL GDAHIT(x([i]),y([i]),z([i]),850,0.1)
enddo
CALL GDCOL(1)

```

Figure 58: The hits.kumac file that was used to read a .end file from the end of each batch simulation (in this case, for run 52).

7.5 Final results from months of GEANT simulations

With over 40 different GEANT simulations done of the $^{13}\text{C}(p,\gamma)^{14}\text{N}$ reaction with DRAGON, for different mistunes of the reference tune, (in x and y position, x and y angular position, and percentage of energy, of the incoming beam), the acceptance of DRAGON was calculated. The acceptance from each simulation was place into a Mircosoft Excel file, and the acceptance for the five different types of mistunes were plotted. The acceptance, A , of DRAGON was calculated from the recoil data of each simulation using Eq. 45.

$$A = \frac{E_{final}}{E_{recoil}} \quad (45)$$

where E_{recoil} is the number of recoils created in the gas target, and E_{final} is the number of recoils that come to rest in the ionization chamber. (The error in the acceptance

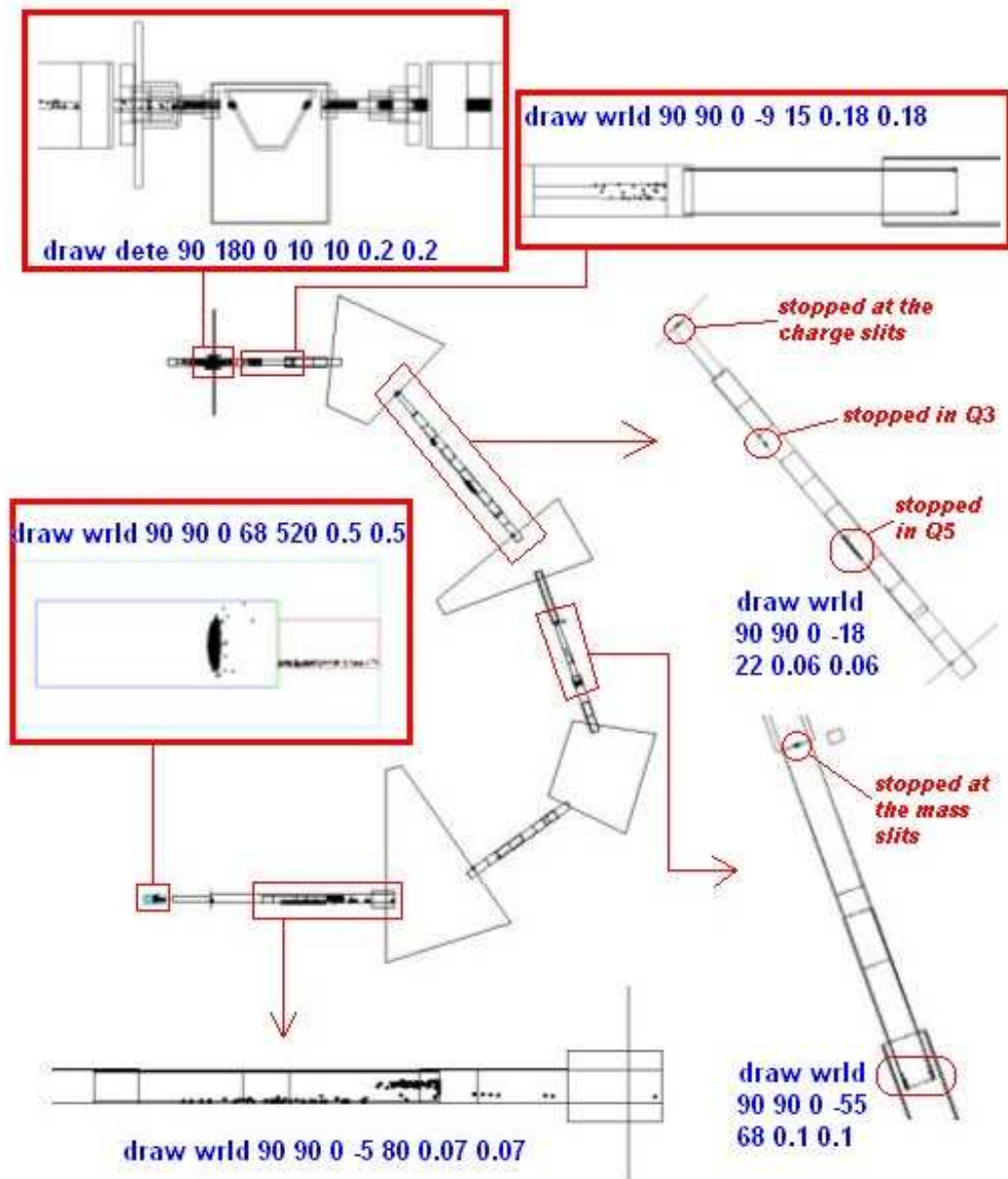


Figure 59: Blow-up diagrams of the 'hits' around the DRAGON after run 60. Run 60 was set to trigger 50000 events (normal runs were 5000), and was left as a perfect tune.

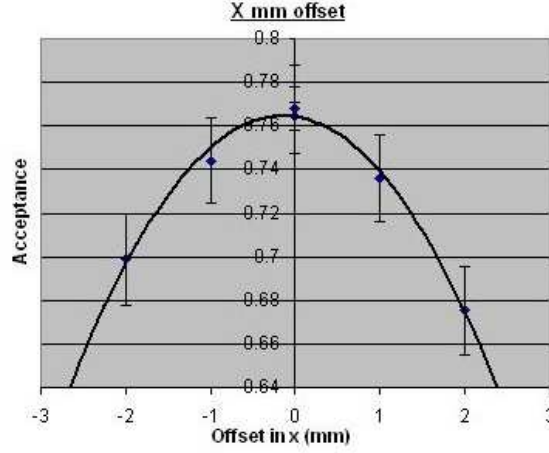


Figure 60: Results for the acceptance through the DRAGON, from the GEANT simulation of the $^{13}\text{C}(\text{p},\gamma)^{14}\text{N}$ reaction, by mistuning the reference tune in the x position. Maximum acceptance when reference tune is **not** mistuned.

(ΔA), was given as the statistical error, as shown in Eq. 46).

$$\Delta A = A \left(\left[\frac{\sqrt{E_{final}}}{E_{final}} \right]^2 + \left[\frac{\sqrt{E_{recoil}}}{E_{recoil}} \right]^2 \right)^{1/2} \quad (46)$$

The results from simulations mistuned in x and y position show that the reference tune gives the highest acceptance through the DRAGON for the $^{13}\text{C}(\text{p},\gamma)^{14}\text{N}$ reaction (figures 60 and 61). However, the results from the simulations with an energy offset show that a mistune of -0.5% gives the highest acceptance (figure 62).

For the simulations mistuned in x and y angular offsets, the results show that the highest acceptance through the DRAGON is when the reference tune is mistuned at -1.5 mrad in x and -0.5 mrad in y (figures 63 and 64).

The results from the mistunes of the reference tune in x and y position show steep peaks, and therefore are a conclusive result that the reference tune gives the maximum acceptance. However for the results from the angular x and y offsets of the reference tune, the peaks are not so steep, and hence the highest acceptance may not

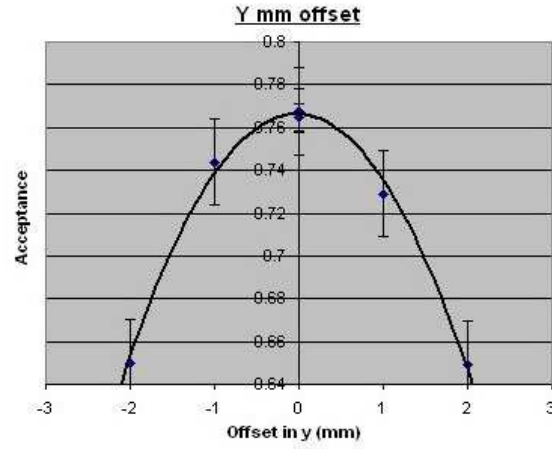


Figure 61: Results for the acceptance through the DRAGON, from the GEANT simulation of the $^{13}\text{C}(p,\gamma)^{14}\text{N}$ reaction, by mistuning the reference tune in the y position. Maximum acceptance when reference tune is **not** mistuned.

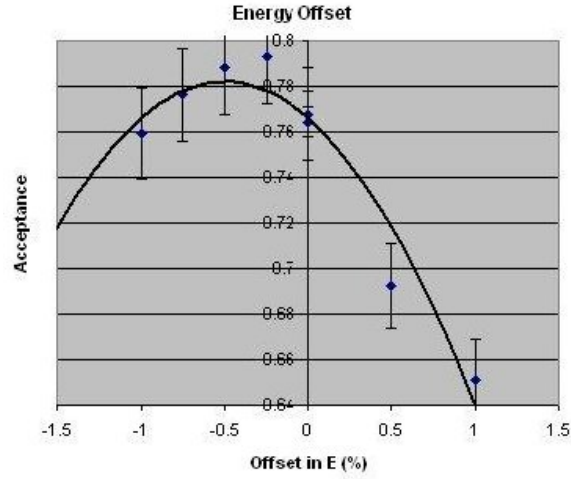


Figure 62: Results for the acceptance through the DRAGON, from the GEANT simulation of the $^{13}\text{C}(p,\gamma)^{14}\text{N}$ reaction, by mistuning the reference tune in percentage of energy. Maximum acceptance when reference tune is mistuned by -0.5% in energy.

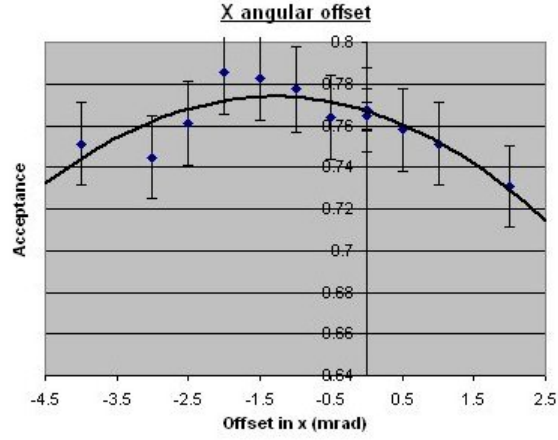


Figure 63: Results for the acceptance through the DRAGON, from the GEANT simulation of the $^{13}\text{C}(p,\gamma)^{14}\text{N}$ reaction, by mistuning the reference tune in the x angle. Maximum acceptance when reference tune is mistuned by -1.5 mrad in x angular position.

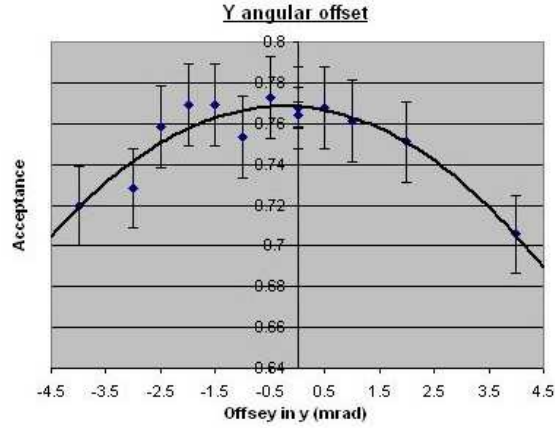


Figure 64: Results for the acceptance through the DRAGON, from the GEANT simulation of the $^{13}\text{C}(p,\gamma)^{14}\text{N}$ reaction, by mistuning the reference tune in the y angle. Maximum acceptance when reference tune is mistuned by -0.5 mrad in y angular position.

be a peaks at -1.5 mrad and -0.5 mrad respectively, but rather plateaus around the reference tune.

From all five of these different mistunes to the reference tunes, not only does the reference tune not give the maximum acceptance, but the graphs of these mistunes (figures 60 - 64) show that the maximum acceptance of the DRAGON for this reaction, is only around 78-79%.

8 Conclusions

To conclude, studying the $^{13}\text{C}(\text{p},\gamma)^{14}\text{N}$ reaction is important for the DRAGON facility in their future analysis of the $^{13}\text{N}(\text{p},\gamma)^{14}\text{O}$ reaction, not only due to the similar properties of ^{13}N and ^{13}C , but also as a good test of the DRAGON due to the fact that the $^{13}\text{C}(\text{p},\gamma)^{14}\text{N}$ reaction has been measured before.

Early analysis of the $^{13}\text{C}(\text{p},\gamma)^{14}\text{N}$ reaction data collected by DRAGON, showed that not all the ^{14}N recoils make it through the DRAGON separator to the end detector, because they are being clipped in the gas target box and beam pipes leaving the target, due to a large cone angle for this reaction, calculated to be approximately 19 mrad (3 mrad larger than the design limit of the DRAGON).

A GEANT simulation of DRAGON was used to simulate the $^{13}\text{C}(\text{p},\gamma)^{14}\text{N}$ reaction so that it could be compared to see what fraction of the recoils were being lost within the DRAGON, and also to see where the clipping occurred.

Initial simulations of the $^{13}\text{C}(\text{p},\gamma)^{14}\text{N}$ reaction, showed a 1.5 MeV difference in coincidence recoil energy compared with the actual data from DRAGON. The reason for this was later discovered to be because there was no ionization chamber in the GEANT simulation of DRAGON, which was known to lose roughly this amount of energy from recoils, as they pass through its mylar window.

Initial simulations of the ionization chamber proved to be very difficult to get right. The main problem was the simulation of the ionization chamber's mylar window. The thickness of the mylar window proved to be too thin for GEANT to recognize it even existed in the simulation. Through trial and error, it was found that the window had to be 30 times thicker for GEANT to recognize it. Making the mylar

window 30 times less dense (as well as 30 times as thick) than the original proved to yield the same energy loss, from SRIM simulations of the two different types of mylar window.

Two regions of recoils were discovered to form in the ionization chamber, from batch simulations of the $^{13}\text{C}(\text{p},\gamma)^{14}\text{N}$ reaction. This produced a trough in the coincidence recoil energy peak (forming a two-peaked structure), which was observed from the actual data from the DRAGON analysis. Further SRIM simulations proved that the difference in distance between the two regions of recoils in the ionization chamber, corresponded to the difference in energy between them (from the final energy histogram).

These two regions of recoils were later discovered to be caused from a few more errors in the simulation of the ionization chamber, and were in fact caused by the fact that some of the recoils did not pass through the mylar window, and therefore were not losing energy, and were entering the anode region of the ionization chamber with the incorrect energy.

With the ionization chamber updated with the relevant changes and finalised, the simulations of the $^{13}\text{C}(\text{p},\gamma)^{14}\text{N}$ reaction continued, with the testing of the DRAGON's acceptance, using different mistunes of the DRAGON's reference tune, in x and y position, x and y angle, and percentage of energy.

These mistunes showed that the maximum acceptance for DRAGON is achieved when the beam is not mistuned in x and y position, but mistuned to -0.5% of the energy, and -1.5 mrad and -0.5 mrad in the x and y angular position respectively (although, for the angular mistunes, if more results find a plateau for the highest acceptance, then this may mean that the DRAGON is not sensitive to small changes in the angular tune of the beam).

The 40+ GEANT simulations, for the $^{13}\text{C}(\text{p},\gamma)^{14}\text{N}$ reaction, with different mis-tunes, has shown that there is a large acceptance loss (acceptance is only 78-79%), and that the data from this reaction (and the future $^{13}\text{N}(\text{p},\gamma)^{14}\text{O}$ reaction) will need to be corrected for it to be used.

The creation and addition of the ionization chamber into the DRAGON simulation will not only aid the DRAGONeers in distinguishing the different elements in their future $^{13}\text{N}(\text{p},\gamma)^{14}\text{O}$ data, but also help in the analysis of future reaction studies when the ionization chamber is used. It also means that future reactions requiring the ionization chamber can be done before DRAGON starts new experiments.

Appendix A - 'c13pg.dat' input file

```
# Input namelist for 13C(p,g)14N reaction
# A.Bebington 31.07.2003
# Note: All mass excesses in GeV
#   All widths in MeV
#   All elevels in MeV
$params
  life = 15*1000.
  level = 15*0.
  beamtyp = '13C'
  rectyp = '14N'
  zbeam = 6.
  abeam = 13.
  atarg = 1.
  ztarg = 1.
  zprod = 7.
  beamlifetime = 1000.
  beam_mass_excess = 3.125E-3
  recoil_mass_excess = 2.863E-3
  resenerg = 0.511
  part_width = 0.038
  gam_width = 0.0000099
  spin_stat_fac = 0.75
  ell = 0.0
  rstate = 11
  level( 0) = 0.0
  level( 1) = 2.312798
  level( 2) = 3.94810
  level( 3) = 4.9151
  level( 4) = 5.10589
  level( 5) = 5.69144
  level( 6) = 5.83425
  level( 7) = 6.2035
  level( 8) = 6.44617
  level( 9) = 7.02912
  level(10) = 7.9669
  level(11) = 8.0620
  life( 0) = 1000.
  life( 1) = 6.8E-14
```

```
life( 2) = 4.8E-15
life( 3) = 5.3E-15
life( 4) = 4.35E-12
life( 5) = 1.1E-14
life( 6) = 8.3E-12
life( 7) = 1.11E-13
life( 8) = 4.3E-13
life( 9) = 3.7E-15
life(10) = 2.63E-16
life(11) = 2.86E-19
br(1,1) = 100.
md(1,1) = 0
br(2,1) = 96.06
md(2,1) = 1
br(2,2) = 3.94
md(2,2) = 0
br(3,1) = 0.49
md(3,1) = 2
br(3,2) = 0.99
md(3,2) = 1
br(3,3) = 98.52
md(3,3) = 0
br(4,1) = 0.72
md(4,1) = 2
br(4,2) = 19.41
md(4,2) = 1
br(4,3) = 79.87
md(4,3) = 0
br(5,1) = 63.90
md(5,1) = 1
br(5,2) = 36.10
md(5,2) = 0
br(6,1) = 78.68
md(6,1) = 4
br(6,2) = 21.32
md(6,2) = 0
br(7,1) = 76.92
md(7,1) = 1
br(7,2) = 23.08
md(7,2) = 0
```



```
br(8,1) = 3.71
md(8,1) = 6
br(8,2) = 6.52
md(8,2) = 4
br(8,3) = 19.69
md(8,3) = 2
br(8,4) = 70.08
md(8,4) = 0
br(9,1) = 0.90
md(9,1) = 2
br(9,2) = 0.49
md(9,2) = 1
br(9,3) = 98.61
md(9,3) = 0
br(10,1) = 45.05
md(10,1) = 2
br(10,2) = 54.95
md(10,2) = 0
br(11,1) = 3.53
md(11,1) = 5
br(11,2) = 0.25
md(11,2) = 4
br(11,3) = 1.86
md(11,3) = 3
br(11,4) = 12.68
md(11,4) = 2
br(11,5) = 1.40
md(11,5) = 1
br(11,6) = 80.28
md(11,6) = 0
$[end]
```

Appendix B - subroutine 'ugmate.f'

```

C.      SUBROUTINE ugmate
C.
*****
*
*          Routine to define tracking material
*
*****
C.
      IMPLICIT none
C.
      INTEGER i
C.
      INTEGER n_mat
      PARAMETER (n_mat = 12) ! # of created new materials
C.
      INTEGER i_mat(n_mat)
      DATA i_mat/ 17, 18, 19, 20, 21, 22, 23, 24, 25, 50, 60, 61/
C.
      CHARACTER*20 name_mat(n_mat)
C.
      DATA name_mat/
*          'SCINTILLATOR      ',
*          'BARIUM FLORIDE BAF2 ',
*          'CESIUM FLORIDE CSF  ',
*          'SODIUM IODIDE NAI:TL',
*          'CESIUM IODIDE CSI:TL',
*          'BGO      BI4GE3012 ',
*          'LSO      LU2(SI04)O:CE ',
*          'MGO (POWDER)      ',
*          'GLASS              ',
*          'SILICON            ',
*          'ISOBUTANE          ',
*          'MYLAR              '/
C.
      INTEGER nl_mat(n_mat)
      REAL a_mat(5,n_mat),z_mat(5,n_mat),w_mat(5,n_mat),dens_mat(n_mat)
      REAL radl_mat(n_mat),absl_mat(n_mat)

```

C.

```

      DATA a_mat/                                ! Atomic weights of constituents
*      12.01,   1.01,   0.0 ,   0.0 ,   0.0,
*      137.3,  19.0 ,   0.0 ,   0.0 ,   0.0,
*      132.9,  19.0 ,   0.0 ,   0.0 ,   0.0,
*      23.0, 126.9 ,   0.0 ,   0.0 ,   0.0,
*      132.9, 126.9 ,   0.0 ,   0.0 ,   0.0,
*      209.0,  72.6 , 16.0 ,   0.0 ,   0.0,
*      175.0,  28.1 , 16.0 ,   0.0 ,   0.0,
*      24.3,  16.0 ,   0.0 ,   0.0 ,   0.0,
*      12.01,   1.01,   0.0 ,   0.0 ,   0.0,
*      28.08,   0.0,   0.0 ,   0.0 ,   0.0,
*      12.01,   1.01,   0.0 ,   0.0 ,   0.0,
*      16.00,  12.01, 1.01 ,   0.0 ,   0.0/

```

C.

```

      DATA z_mat/                                ! Atomic numbers of constituents
*      6.0,   1.0,   0.0, 0.0, 0.0,
*      56.0,  9.0,   0.0, 0.0, 0.0,
*      55.0,  9.0,   0.0, 0.0, 0.0,
*      11.0, 53.0,   0.0, 0.0, 0.0,
*      55.0, 53.0,   0.0, 0.0, 0.0,
*      83.0, 32.0,   8.0, 0.0, 0.0,
*      71.0, 14.0,   8.0, 0.0, 0.0,
*      12.0,  8.0,   0.0, 0.0, 0.0,
*      6.0,   1.0,   0.0, 0.0, 0.0,
*      14.0,  0.0,   0.0, 0.0, 0.0,
*      6.0,   1.0,   0.0, 0.0, 0.0,
*      8.0,  6.0,   1.0, 0.0, 0.0/

```

C.

```

      DATA dens_mat/                            ! density
*      1.032 ,
*      4.890 ,
*      4.640 ,
*      3.670 ,
*      4.510 ,
*      7.130 ,
*      7.400 ,
*      1.870 ,
*      1.032 ,
*      2.330 ,

```

```

*      0.000267 ,
*      1.39 /
C.
      DATA nl_mat/                ! >,< 0 => WMAT: proportions by mass, atoms
*      -2 ,
*      -2 ,
*      -2 ,
*      -2 ,
*      -2 ,
*      -3 ,
*      -3 ,
*      -2 ,
*      -2 ,
*      0 ,
*      -2 ,
*      -3 /
C.
      DATA w_mat/                ! proportions of elements in the mixture
*      1.0 , 1.1 , 0.0 , 0.0 , 0.0 ,
*      1.0 , 2.0 , 0.0 , 0.0 , 0.0 ,
*      1.0 , 1.0 , 0.0 , 0.0 , 0.0 ,
*      1.0 , 1.0 , 0.0 , 0.0 , 0.0 ,
*      1.0 , 1.0 , 0.0 , 0.0 , 0.0 ,
*      4.0 , 3.0 , 12.0 , 0.0 , 0.0 ,
*      2.0 , 1.0 , 5.0 , 0.0 , 0.0 ,
*      1.0 , 1.0 , 0.0 , 0.0 , 0.0 ,
*      1.0 , 1.1 , 0.0 , 0.0 , 0.0 ,
*      1.0 , 0.0 , 0.0 , 0.0 , 0.0 ,
*      4.0 , 10. , 0.0 , 0.0 , 0.0 ,
*      2.0 , 5.0 , 4.0 , 0.0 , 0.0 /
C.
      DATA radl_mat/             ! radiation length;  if 0 GEANT will calc.
*      42.40 ,
*      2.05 ,
*      0.0 ,
*      2.59 ,
*      0.0 ,
*      1.12 ,
*      0.0 ,
*      0.0 ,

```

```

*      42.40 ,
*      2.70  ,
*      0.0   ,
*      0.0   /
C.
DATA abs1_mat/ (n_mat)*0.0 / ! absorption length; if 0 GEANT will calc.
C.
Do i = 1, n_mat
  If (nl_mat(i).eq.0)then
    CALL gsmate(i_mat(i), name_mat(i), a_mat(1,i), z_mat(1,i),
*          dens_mat(i), radl_mat(i), abs1_mat(i), 0, 0)
  Else
    CALL gsmixt(i_mat(i), name_mat(i), a_mat(1,i), z_mat(1,i),
*          dens_mat(i), nl_mat(i), w_mat(1,i))
  Endif
Enddo
C.
CALL ugmate_trgt
C.
RETURN
END
C.

```

Appendix C - subroutine 'ugstmed.f'

```

C.      SUBROUTINE ugstmed
C.
*****
*
*          Routine to define tracking media
*
*****
C.      IMPLICIT none
C.
C.      include 'geometry.inc'          !local
C.
C.      INTEGER i
C.
C.      INTEGER n_med
C.      PARAMETER (n_med = 22)  ! # of created tracking media
C.
C.      CHARACTER*20 name_med(n_med)
C.
C.      INTEGER nmed_mat(n_med), isvol_med(n_med), ifield(n_med)
C.      REAL fieldm(n_med), tmaxfd_med(n_med), dmaxms_med(n_med),
*      deemax_med(n_med), epsil_med(n_med), stmin_med(n_med)
C.
C.      REAL ubuf_med(n_med)
C.
C.      DATA name_med/
*          'VACUUM -> no field ', ! 1
*          'VACUUM -> ifield = 1', ! 2 ! sensitive
*          'VACUUM -> ifield = 2', ! 3 !sensitive
*          'VACUUM -> ifield = 3', ! 4 !sensitive
*          'COPPER', ! 5 !sensitive
*          'ALUMINUM', ! 6
*          'LEAD', ! 7
*          'ATMOSPHERE (AIR)', ! 8
*          'SCINTILLATOR', ! 9 !sensitive
*          'BARIUM FLORIDE BAF2 ', ! 10 !sensitive
*          'CESIUM FLORIDE CSF ', ! 11 !sensitive

```

```

*          'SODIUM IODIDE NAI:TL', ! 12 !sensitive
*          'CESIUM IODIDE CSI:TL', ! 13 !sensitive
*          'BGO      BI4GE3O12 ', ! 14 !sensitive
*          'LSO      LU2(SIO4)O:CE ', ! 15 !sensitive
*          'MGO (POWDER)      ', ! 16
*          'GLASS              ', ! 17 !sensitive
*          'TUNGSTEN           ', ! 18
*          'SILICON            ', ! 19 !sensitive
*          'STAINLESS STEEL    ', ! 20
*          'ISOBUTANE          ', ! 60 !sensitive
*          'MYLAR              '/ ! 61 !sensitive

C.
  DATA nmed_mat/
                                ! index of these materials
*    16, 16, 16, 16, 11,
*    9, 13, 15, 17, 18, 19, 20, 21, 22, 23, 24, 25, 12, 50,
*    26, 60, 61/

C.
  DATA isvol_med/
                                ! 0 if not a sensitive medium
*    0, 1, 1, 1, 1,
*    0, 0, 0, 1, 1, 1, 1, 1, 1, 1, 0, 1, 0, 1, 0, 1, 1/

C.
  DATA tmaxfd_med/ n_med*10.0 / ! max. angle due to field in one step

C.
  DATA dmaxms_med/ n_med*-1.0 / ! max. displace for mult scatt. in one step

C.
  DATA deemax_med/ n_med*-1.0 / ! max. fractional energy loss in one step

C.
  DATA epsil_med/
                                ! tracking precision
*    5*0.001, 2*0.001, 0.1, 14*0.001 /

C.
  DATA stmin_med/ n_med*-1.0 / ! min. step due to energy loss or m. s.

C.
  DATA ifield / 0, 1, 2, 3, 0,
*              0, 0, 0, 0, 0, 0, 0, 0, 0, 0, 0, 0, 0, 0,
*              0, 0 /

C.
                                ! magnetic field flag =1 GRKUTA
C.
                                =2 GHELIX
C.
                                =3 GHELX3
C.

  DATA fieldm / 0., 100., 100., 100., 0.,

```

```

*          0., 0., 0., 0., 0., 0., 0., 0., 0., 0., 0., 0.,
*          0., 0., 0., 0., 0./
C.          ! max. field value [kGauss]
C.          or magn. field for GHELX3
C.
C.          *****
C.          *** GEANT will recalculate negative variables of ***
C.          *          dmaxms,deemax,stmin          *
C.          *** as long as you don't run with IAUTO=0 card ***
C.          *****
C.
C.          INTEGER ipckov, npckov
C.          REAL ppckov, absco, effc, rindex
C.          REAL absco_scnt, effc_pmt, rindex_scnt
C.
C.          PARAMETER (npckov = 32)
C.
C.          DIMENSION ppckov(npckov), absco(npckov)
C.          DIMENSION effc(npckov), rindex(npckov)
C.          DIMENSION absco_scnt(npckov), effc_pmt(npckov)
C.          DIMENSION rindex_scnt(npckov)
C.
C.          DATA ppckov / 2.038E-9, 2.072E-9, 2.107E-9, 2.143E-9, 2.181E-9,
&          2.220E-9, 2.260E-9, 2.302E-9, 2.346E-9, 2.391E-9,
&          2.438E-9, 2.486E-9, 2.537E-9, 2.590E-9, 2.645E-9,
&          2.702E-9, 2.763E-9, 2.825E-9, 2.891E-9, 2.960E-9,
&          3.032E-9, 3.108E-9, 3.188E-9, 3.271E-9, 3.360E-9,
&          3.453E-9, 3.552E-9, 3.656E-9, 3.767E-9, 3.884E-9,
&          4.010E-9, 4.144E-9 /
C.
C.          DATA absco_scnt / 344.8, 408.2, 632.9, 917.4, 1234.6, 1388.9,
&          1515.2, 1724.1, 1886.8, 2000.0, 2631.6, 3571.4,
&          4545.5, 4761.9, 5263.2, 5263.2, 5555.6, 5263.2,
&          5263.2, 4761.9, 4545.5, 4166.7, 3703.7, 3333.3,
&          3000.0, 2850.0, 2700.0, 2450.0, 2200.0, 1950.0,
&          1750.0, 1450.0 /
C.
C.          DATA rindex_scnt / 1.82, 1.82, 1.82, 1.82, 1.82, 1.82, 1.82,
&          1.82, 1.82, 1.82, 1.82, 1.82, 1.82, 1.82,

```



```

&          1.82, 1.82, 1.82, 1.82, 1.82, 1.82, 1.82,
&          1.82, 1.82, 1.82, 1.82, 1.82, 1.82, 1.82,
&          1.82, 1.82, 1.82, 1.82 /
C.
CCC      DATA effic_pmt / 0.005,0.01, 0.02, 0.03, 0.04, 0.05, 0.06, 0.07,
CCC      &          0.08, 0.09, 0.10, 0.115,0.13, 0.15, 0.16, 0.18,
CCC      &          0.195,0.22, 0.23, 0.24, 0.25, 0.255,0.26, 0.265,
CCC      &          0.26, 0.25, 0.24, 0.215,0.175,0.14, 0.085, 0.0 /
C.
      DATA effic_pmt / 0.02, 0.025,0.03, 0.035,0.04, 0.05, 0.075,0.09,
&          0.12, 0.14, 0.15, 0.175,0.185,0.20, 0.21, 0.22,
&          0.25, 0.26, 0.27, 0.28, 0.30, 0.30, 0.295,0.29,
&          0.285,0.28, 0.26, 0.20, 0.175,0.10, 0.05, 0.0 /
C.

      Do i = 1, n_med
C.
      CALL gstmed(i, name_med(i), nmed_mat(i), isvol_med(i),
*          ifield(i), fieldm(i), tmaxfd_med(i),
*          dmaxms_med(i), deemax_med(i),
*          epsil_med(i), stmin_med(i), ubuf_med(i), 1)
C.
      If(i.ge.9.and.i.le.15)then ! dielectric - scintillator
C.
      CALL ucopy(absco_scnt,absco,npckov)
      CALL vfill(absco,npckov,bulk_absorption)
      CALL ucopy(effic_pmt,effic,npckov)
      CALL ucopy(rindex_scnt,rindex,npckov)
      CALL gsckov(i,npckov,ppckov,absco,effic,rindex)
      Elseif(i.eq.8.or.i.eq.1)then ! dielectric - air and vacuum
      CALL vzero(effic,npckov)
      CALL vfill(absco,npckov,1.e10)
      CALL vfill(rindex,npckov,1.00)
      CALL gsckov(i,npckov,ppckov,absco,effic,rindex)
      Elseif(i.eq.17)then ! dielectric - glass
      CALL vzero(effic,npckov)
      CALL vfill(absco,npckov,10.0)
      CALL vfill(rindex,npckov,1.50)
      CALL gsckov(i,npckov,ppckov,absco,effic,rindex)
      Elseif(i.eq.6.or.i.eq.16)then ! metal - Al and MgO
      CALL vzero(effic,npckov)

```

```
        CALL vzero(rindex,npckov)
        CALL vfill(absco,npckov,paint_absorption)
        CALL gsckov(i,npckov,ppckov,absco,effic,rindex)
    Endif
Enddo
C.    CALL ugstmed_trgt
C.
    RETURN
END
C.
```

Appendix D - subroutine 'gustep_mitr ay.f'

```

C.      SUBROUTINE gustep_mitray
C.
C.      IMPLICIT none
C.
C.      include 'gcbank.inc'          !geant
C.      include 'gcflag.inc'          !geant
C.      include 'gckine.inc'          !geant
C.      include 'gctrak.inc'          !geant
C.      include 'gcking.inc'          !geant
C.      include 'gcvolu.inc'          !geant
C.      include 'gctmed.inc'          !geant
C.      include 'gconst.inc'          !geant
C.      include 'gccuts.inc'          !geant
C.      include 'gcnum.inc'           !geant
C.      include 'gcunit.inc'          !geant
C.      include 'gcsets.inc'          !geant
C.
C.      include 'geom_dipole.inc'      !local
C.      include 'geom_edipol.inc'     !local
C.      include 'geom_mpole.inc'       !local
C.      include 'geom_sole.inc'        !local
C.
C.      include 'mitray_diag.inc'      !local
C.      include 'diagnostic.inc'       !local
C.      include 'ukine.inc'            !local
C.      include 'beamcom.inc'
C.      include 'dsssd.inc'
C.      include 'rescom.inc'
C.      include 'uevent.inc'
C.
C.      INTEGER i, j, k, irot, kstop, ihit
C.      INTEGER JPAA,JPAB,JDKA,JDKB
C.      REAL radius, dr, theta, xlo, xhi, trec, hits(5)
C.
C.      CHARACTER*20 chtmed

```

```

      CHARACTER* 4 cname_nlevel
      CHARACTER* 4 chcase
      CHARACTER* 1 kdname
C
      INTEGER in_new_vol, name_old, number_old, ntmult_old
      DATA name_old / 0 /, number_old / 0 /, ntmult_old / 0 /
C.
      REAL xm(3), xd(3), xd_endv(3), xdd_endv(3)
C.
      REAL amugev, tlast
      amugev = 0.93149432E+00
      kstop = 0
C.
C *** Because INWVOL = 1 can mean either that a new volume has been
C *** entered or that a new track has been started, define a new
C *** variable IN_NEW_VOL which specifically indicates a new volume.
C.

      in_new_vol = 0
      If(inwvol.eq.1)then
        If(name_old .ne.names(nlevel).or.
&      number_old.ne.number(nlevel))then
          If(ntmult.eq.ntmult_old)in_new_vol = 1
        Endif
      Endif
C.

      CALL uhtoc(natmed(1),4,chtmed,20)
      CALL uhtoc(names(nlevel),4,cname_nlevel,4)
C.      CALL uhtoc(kcase,4,chcase,4)
C.
      If(sleng.gt.len_max)then
        istop = 6
        goto 999
      Endif
C
C *** Change beam particle charge state to the same as the recoil
C
c      If(ipart.eq.80) then

```

```

c      JPAA = LQ(JPART-IPART)  !! pointer to beam particle
c      print*, Q(JPAA+10), FKINE(2)
c      Q(JPAA+10) = FKINE(2)
c      Endif

C
C *** Calculate recoil (or beam) kinetic energy
C
      If(ipart.eq.irecoil) then
        If(in_new_vol.eq.1)then
          tlast = 1000.*(sqrt(prodm**2+vect(7)**2)-prodm)
        Endif
        trec = sqrt( prodm**2 + vect(7)**2 ) - prodm
      Else If(ipart.eq.80) then
        trec = sqrt( beammass**2 + vect(7)**2 ) - beammass
      Endif
      trec = trec*1000.

C
C
C *** If particle is escaped beam
C
      If(ipart.eq.80 .and. cname_nlevel.eq.'D1 '
+ .and. inwvol.eq.2 ) then
        CALL hfill(503,1.,0.0,1.0)
      Endif

C
C *** If recoils are stopped
C
      If(ipart.eq.irecoil .and. (istop.eq.1 .or. istop.eq.2) .and.
+  cname_nlevel.ne.'ENDV') then
        CALL hfill(504,vect(3),vect(1),1.0)
c      print*, 'recoil disappeared!', vect(1), vect(2), vect(3)
        write(4,*) vect(1), vect(2), vect(3), tlast
      Endif

C.
C *** If particle is in ENDV volume
C.

```

```

      If(chname_nlevel.eq.'ENDV' .and. in_new_vol.eq.1 )then

C.
      CALL ucopy(vect(1),xm(1),3)
      CALL gmtod(xm,xd_endv,1)
      CALL ucopy(vect(4),xm(1),3)
      CALL gmtod(xm,xdd_endv,2)

C.
      If(iswit(8).eq.1)nevent = ievent

C.
      If(xdd_endv(1).ne.0.0.or.xdd_endv(3).ne.0.0)then
        xdd_endv(1) = 1000.*atan2(xdd_endv(1),xdd_endv(3))
      Else
        xdd_endv(1) = 0.0
      Endif
      xdd_endv(2) = 1000.*asin(xdd_endv(2))

C.
      hits(1) = vect(1)
      hits(2) = vect(2)
      hits(3) = vect(3)
      hits(4) = 0.
      hits(5) = trec

C.
      CALL gsahit(iset,idet,itra,numbv,hits,ihit) C.
      radius = sqrt(xd_endv(1)**2+xd_endv(2)**2)
      dr = sqrt(1.-vect(6)**2)

C.
      theta = 0.0
      If(dr.ne.0.0.or.vect(6).ne.0.0)then
        theta = 1000.*atan2(dr,vect(6))
      Endif

C.
C.
      DSSSD hit-pattern
      nstrip = 16
      pitch = 0.3
      do i = 1, nstrip
        xlo = -(float(nstrip)/2.)*pitch + float(i-1)*pitch
        xhi = -(float(nstrip)/2.)*pitch + float(i)*pitch
        if (xd_endv(1).ge.xlo.and.xd_endv(1).lt.xhi) then

```

```

        CALL hfill(401,float(i),0.0,1.0)
    endif
    if (xd_endv(2).ge.xlo.and.xd_endv(2).lt.xhi) then
        CALL hfill(402,float(i),0.0,1.0)
    endif
enddo

C.
    CALL hfill(11, xd_endv(1),0.0,1.0)
    CALL hfill(12, xd_endv(2),0.0,1.0)
    CALL hfill(13,xdd_endv(1),0.0,1.0)
    CALL hfill(14,xdd_endv(2),0.0,1.0)
    CALL hfill(15,trec,0.0,1.0)
    CALL hfill(19,gekin*1000.,0.0,1.0)

C.
    CALL hfill(111, xd_endv(1), xd_endv(2),1.0)
    CALL hfill(112,xdd_endv(1),xdd_endv(2),1.0)
    CALL hfill(113, xd_endv(1),xdd_endv(1),1.0)
    CALL hfill(114, xd_endv(2),xdd_endv(2),1.0)

C.
    CALL hfill(115,radius,theta,1.0)

If(iswit(7).eq.2)then
C.
    kstop = 1
    istop = 100

C.
Elseif(iswit(7).eq.3)then
C.
    idevt = idevt + 1

    WRITE(lout,111)jevent,
&          xd_endv(1),xdd_endv(1),
&          xd_endv(2),xdd_endv(2),
&          100.*(vect(7)/recoilmom*1000.-1.0),xd(3)
111  FORMAT(1X,I7,F10.6,F10.4,F10.6,F10.4,F12.8,F12.6)

C.
    kstop = 1
    istop = 200

C.
Elseif(iswit(7).eq.1)then

```

```

C.
c$$$      write(lout,*)' x_final: ',xd_endv(1),
c$$$      &      ' y_final: ',xd_endv(2)
c$$$      write(lout,*)' theta_final: ',xdd_endv(1),
c$$$      &      ' phi_final: ',xdd_endv(2)
          kstop = 1
          istop = 200
C.
      Endif
C.
      goto 999
C.
      Elseif(chtmed.eq.'COPPER'          ')then
C.
C *** If particle is in COPPER (jaws, slits)
C.
      jslit = 1
C.
      If(iswit(7).eq.1)then
          CALL hfill(16,sleng,0.0,1.0)
          kstop = 1
          istop = 5
          goto 999
      Endif
C.
      Endif
C.
      If(chname_nlevel.eq.'ENDV')goto 1111
      If(chname_nlevel.eq.'STRV')goto 1111
C.
C *** Check collimators in all RAYTRACE elements
C.
      If(in_new_vol.eq.1.or.inwvol.eq.2)then
          If(in_new_vol.eq.1)j = 1
          If( inwvol .eq.2)j = 2
          k = number(nlevel)
          CALL uhtoc(names(nlevel),4,kdname,1)
          CALL ucopy(vect(1),xm(1),3)
          CALL gmtod(xm,xd,1)
          If(kdname.eq.'D')then

```



```

        irot = irot_dipole(k)
        CALL gitran(xd,dx_dipole(1,k),irot,xd)
        If(in_new_vol.eq.1)then
            If(jcol_dipole(j,k).eq.1)then
                If((xd(1)-xcol_dipole(j,k))**2/dxcol_dipole(j,k)**2 +
&                (xd(2)-ycol_dipole(j,k))**2/dycol_dipole(j,k)**2.gt.1.0)
&                                                                istop = 3
            Else
ccc                If(abs(xd(1)-xcol_dipole(j,k)).gt.dxcol_dipole(j,k))istop=3
                    If(abs(xd(2)-ycol_dipole(j,k)).gt.dycol_dipole(j,k))istop=3
                Endif
            Else
                If(abs(xd(2)-ycol_dipole(j,k)).gt.dycol_dipole(j,k))istop=3
            Endif

        Elseif(kdname.eq.'Q')then
            irot = 0
            CALL gitran(xd,dx_mpole(1,k),0,xd)
            If(jcol_mpole(j,k).eq.1)then
                If((xd(1)-xcol_mpole(j,k))**2/dxcol_mpole(j,k)**2 +
&                (xd(2)-ycol_mpole(j,k))**2/dycol_mpole(j,k)**2.gt.1.0)
&                                                                istop = 3
            Else
                If(abs(xd(1)-xcol_mpole(j,k)).gt.dxcol_mpole(j,k))istop=3
                If(abs(xd(2)-ycol_mpole(j,k)).gt.dycol_mpole(j,k))istop=3
            Endif
        Elseif(kdname.eq.'S')then
            irot = 0
            CALL gitran(xd,dx_sole(1,k),0,xd)
            If(jcol_sole(j,k).eq.1)then
                If((xd(1)-xcol_sole(j,k))**2/dxcol_sole(j,k)**2 +
&                (xd(2)-ycol_sole(j,k))**2/dycol_sole(j,k)**2.gt.1.0)
&                                                                istop = 3
            Else
                If(abs(xd(1)-xcol_sole(j,k)).gt.dxcol_sole(j,k))istop=3
                If(abs(xd(2)-ycol_sole(j,k)).gt.dycol_sole(j,k))istop=3
            Endif
            CALL gmtod(xm,xd,1)
        Endif
    Endif

```



```

C.          If(chcase.eq.'DCAY')then
              iflgk(i) = 1
          Endif
C.          If(gkin(5,i).eq.4)iflgk(i) = -1
C.          Enddo
C.          CALL gsking(0)
C.          Endif
C.          999 Continue
C.
C *** Debug/plot event
C.          CALL gdebug
C          If(itrtyp.eq.8)Call gdebug C.
          If(jstop.ne.0)then
              istop = 1
              kstop = 1
              CALL hfill(16,sleng,0.0,1.0)
              write(6,*)' *** Problem!!! *** '
          Endif
C          If(kstop.eq.0.and.istop.ne.0)then
          If(istop.ne.0 .and. iswit(1) .eq. 1)then
              write(6,*)' Whats stopping me??? '
              write(6,*)' istop: ',istop,' Volume: ',chname_nlevel
          Endif
          jstop = 0
C.          ngkine = 0
C.          name_old   = names (nlevel)
          number_old = number(nlevel)
          ntmult_old = ntmult
C.          RETURN
          END

```

Appendix E - subroutine 'uhinit.f'

```

C.
      SUBROUTINE uhinit
C.
*****
*
*      Defines HBOOK histogram/scatterplot definitions
*
*****
C.
C.
      IMPLICIT none
C.
      include 'gcflag.inc'          !geant
      include 'gcunit.inc'          !geant
C.
      include 'geometry.inc'        !local
      include 'u_geom.inc'          !local
      include 'gbox_info.inc'       !local
C.
      include 'uggeom.inc'          !local
      include 'higamcoinc.inc'      !local
      include 'res.inc'             !local
      include 'beamcom.inc'         !local
      include 'rescom.inc'          !local
      include 'history.inc'
C.
      REAL sig, lm1, lm2, angdist
      EXTERNAL sig, angdist
C.
      INTEGER i, n, istat, nstrip
      CHARACTER*32 wfile
      character*11 strip
      character*2 num(16)
      character*8 chtags(NVAR10)
      data chtags/ 'GML0', 'GML1', 'GML2', 'GML3', 'GML4', 'GML5', 'GML6',
&    'GML7', 'GML9', 'GML10', 'GML11', 'GML12', 'GML13', 'GML14', 'GML15',

```

```

&  'GML16','GML18','GML19','GML20','GML21','GML22','GML23','GML24',
&  'GML25','GML27','GML28','GML29',
&  'HML0','HML1','HML2','HML3','HML4','HML5','HML6',
&  'HML7','HML8','HML9'/
  data num/'01','02','03','04','05','06','07','08','09',
&          '10','11','12','13','14','15','16'/
C.
C -->   Open a HBOOK direct access file
C.
      CALL namfil('dragon',idrun,'.hbook',wfile)
C
      CALL HROPEN(lunits(4),'HBOOK',wfile,'N',1024,istat)
C.
      If(istat.ne.0)then
        WRITE(lout,*)' Error: Bad return from HROPEN! '
        STOP
      Endif
C.
C -->   Initialize user HBOOK histograms and scatterplots
C.
      n = 0
C.
      CALL hbook1(n+ 1,' Initial - x - ',100,-2.0,2.0,0.0)
      CALL hbook1(n+ 2,' Initial - y - ',100,-2.0,2.0,0.0)
C.
      CALL hbook1(n+ 3,' Initial - dx - ',100,-100.0,100.0,0.0)
      CALL hbook1(n+ 4,' Initial - dy - ',100,-100.0,100.0,0.0)
C.
      CALL hbook1(n+ 5,' IniFin - x - Stops ',100,-2.0,2.0,0.0)
      CALL hbook1(n+ 6,' IniFin - y - Stops ',100,-2.0,2.0,0.0)
C.
      CALL hbook1(n+ 7,' IniFin - dx - Stops',100,-100.0,100.0,0.0)
      CALL hbook1(n+ 8,' IniFin - dy - Stops',100,-100.0,100.0,0.0)
C.
      CALL hbook1(n+ 9,' Initial Momentum ',100,-5.0,5.0,0.0)
      CALL hbook1(n+10,' Momentum spread (%) ',100,-5.0,5.0,0.0)
C.
      CALL hbook1(n+11,' Final - x - ',16, -2.4, 2.4,0.0)
      CALL hbook1(n+12,' Final - y - ',16, -2.4, 2.4,0.0)

```

```

CALL hbook1(n+13,' Final - dx - ',100,-100.0,100.0,0.0)
CALL hbook1(n+14,' Final - dy - ',100,-50.0,50.0,0.0)
C.
CALL hbook1(n+15,' Final Energy ',4000,0.,20.0,0.0)
C.
CALL hbook1(n+16,' Stop Length (cm) ',2000,0.0,2000.0,0.0)
CALL hbook2(n+17,' X vs Stop Length (cm) ',50,-20.,20.,
&          200,0.,2000.,0.)
C.
n = 20
C.
CALL hbook1( n+1,' True photon energy      ', 200, 0., 20., 0.)
CALL hbook1( n+2,' True photon pol. angle ', 200, 0., 200., 0.)
CALL hbook1( n+3,' Photon conv. module    ', 29, 1., 30., 0.)
CALL hbook2( n+4,' Photon creation time vs z_react',
&    600,0.,300., 300,-15.,15.,0.)
CALL hbook2( n+5,' Photon detection time vs z_react',
&    600,0.,300., 300,-15.,15.,0.)
C.
CALL hbook1(n+11,' No. of Modules hit ', 10, 0., 10., 0.)
CALL hbook1(n+12,' Total energy dep. ', 200, 0., 20., 0.)
CALL hbook1(n+13,' x-coordinates of hit', 60, -15., 15., 0.)
CALL hbook1(n+14,' y-coordinates of hit', 80, -20., 20., 0.)
CALL hbook1(n+15,' z-coordinates of hit', 100, -20., 20., 0.)
CALL hbook1(n+16,' Energy dep. in module ', 200, 0., 20., 0.)
CALL hbook1(n+17,' Energy dep. in 1. module ', 200, 0., 20., 0.)
CALL hbook1(n+18,' Energy dep. in 2. module ', 200, 0., 20., 0.)
CALL hbook1(n+19,' Energy dep. in 3. module ', 200, 0., 20., 0.)
CALL hbook1(n+20,' Energy dep. in 4. module ', 200, 0., 20., 0.)
C.
CALL hbook1(n+21,' Energy dep. in crystal ', 200, 0., 20., 0.)
C.
CALL hbook1(n+26,' True conversion z ', 100, -20., 20., 0.)
CALL hbook1(n+27,' Energy weighted z ', 100, -20., 20., 0.)
C.
CALL hbook1(n+28,' Distance: conv. and max-energy dep. (xy) ',
&          , 100, 0., 1., 0.)
CALL hbook1(n+29,' Distance: conv. and max-energy dep. ( xyz) ',
&          , 100, 0., 1., 0.)
CALL hbook1(n+30,' Distance: PMT and max-energy dep. (xy) '

```

```

&          , 100, 0., 20., 0.)
C.
  CALL hbook1(n+31,' Number of photons detected in PMT '
&          , 200, 10., 10000., 0.)
  CALL hbook1(n+32,' Photons in 1. PMT '
&          , 2000, 0., 10000., 0.)
  CALL hbook1(n+33,' Photons in 2. PMT '
&          , 100, 0., 1000., 0.)
  CALL hbook1(n+34,' Photons in 3. PMT '
&          , 100, 0., 1000., 0.)
  CALL hbook1(n+35,' Photons in 4. PMT '
&          , 100, 0., 1000., 0.)
C.
  CALL hbook1(n+36,' Number of PMTs hit above threshold'
&          , 20, 0., 20., 0.)
  CALL hbook1(n+37,' Total Number of photons det. in PMTs > thrsl d '
&          , 2000, 0., 10000., 0.)
C.
  CALL hbook1(n+40,' Reconstructed x-position '
&          , 120, -30., 30., 0.)
  CALL hbook1(n+41,' Reconstructed y-position '
&          , 120, -30., 30., 0.)
  CALL hbook1(n+42,' Reconstructed z-position '
&          , 120, -30., 30., 0.)
C.
  CALL hbook1(n+50,' Number of photons max. '
&          , 100, 0., 15000., 0.)
  CALL hbook1(n+51,' Number of photons generated '
&          , 100, 0., 5000., 0.)
  CALL hbook1(n+52,' Number of photons lost LABS '
&          , 100, 0., 5000., 0.)
  CALL hbook1(n+53,' Number of photons lost REFL '
&          , 100, 0., 5000., 0.)
  CALL hbook1(n+54,' Number of photons lost ds < e '
&          , 100, 0., 1000., 0.)
  CALL hbook1(n+55,' Number of photons lost N > 1000 '
&          , 100, 0., 1000., 0.)
  CALL hbook1(n+56,' Number of photons unable to reflect '
&          , 100, 0., 1000., 0.)
  CALL hbook1(n+57,' Number of photons with error from GLISUR '

```

```

&          , 100, 0., 1000., 0.)
C.
CALL hbook1(n+61,' Number of steps taken to PMT '
&          , 100, 0., 200., 0.)
CALL hbook1(n+62,' Total track length to PMT '
&          , 100, 0., 100., 0.)
C.
CALL hbook1(n+70,' Number of photon clusters ',10, 0., 10., 0.)
CALL hbook1(n+71,' Energy of Cluster #1 ', 200, 0., 20., 0.)
CALL hbook1(n+72,' Energy of Cluster #2 ', 200, 0., 20., 0.)
CALL hbook1(n+73,' Energy of Cluster #3 ', 200, 0., 20., 0.)
CALL hbook1(n+74,' Energy difference #1 ', 80, -2., 2., 0.)
CALL hbook1(n+75,' Energy difference #2 ', 80, -2., 2., 0.)
CALL hbook1(n+76,' Energy difference #3 ', 80, -2., 2., 0.)
CALL hbook1(n+77,' Dir. diff. [deg] #1 ', 90, 0., 90., 0.)
CALL hbook1(n+78,' Dir. diff. [deg] #2 ', 90, 0., 90., 0.)
CALL hbook1(n+79,' Dir. diff. [deg] #3 ', 90, 0., 90., 0.)
C.
n = 100
C.
CALL hbook2( n+1,' Initial - y - vs - x - ',
&          100,-2.5,2.5,100,-2.5,2.5,0.0)
CALL hbook2( n+2,' Initial - dy - vs - dx - ',
&          100,-100.0,100.0,100,-100.0,100.0,0.0)
CALL hbook2( n+3,' IniFin - y - vs - x - ',
&          100,-2.0,2.0,100,-2.0,2.0,0.0)
CALL hbook2( n+4,' IniFin - dy - vs - dx - ',
&          100,-100.0,100.0,100,-100.0,100.0,0.0)
CALL hbook2( n+5,' Initial - dx - vs - x - ',
&          100,-2.0,2.0,100,-100.0,100.0,0.0)
CALL hbook2( n+6,' Initial - dy - vs - y - ',
&          100,-2.0,2.0,100,-100.0,100.0,0.0)
CALL hbook2( n+7,' IniFin - dx - vs - x - ',
&          100,-2.0,2.0,100,-100.0,100.0,0.0)
CALL hbook2( n+8,' IniFin - dy - vs - y - ',
&          100,-2.0,2.0,100,-100.0,100.0,0.0)
C.
CALL hbook2(n+11,' Final - y - vs - x - ',
&          16,-2.4,2.4,16,-2.4,2.4,0.0)
CALL hbook2(n+12,' Final - dy - vs - dx - ',

```



```

&          100,-100.0,100.0,100,-50.0,50.0,0.0)
  CALL hbook2(n+13,' Final - dx - vs - x ',
&          100,-2.5,2.5,100,-100.0,100.0,0.0)
  CALL hbook2(n+14,' Final - dy - vs - y ',
&          100,-3.0,3.0,100,-50.0,50.0,0.0)
C.
  CALL hbook2(n+15,' Final theta vs radius ',
&          100,0.0,2.0,100,0.0,100.0,0.0)
C.
  n = 120
C.
  CALL hbook2( n+1,' True conversion position '
&          , 60, -15., 15., 80, -20., 20., 0.)
  CALL hbook2( n+2,' Energy weighted position '
&          , 60, -15., 15., 80, -20., 20., 0.)
  CALL hbook2( n+3,' Reconstructed position '
&          , 60, -15., 15., 80, -20., 20., 0.)
  CALL hbook2( n+4,' True conversion xy fngr-coordinates '
&          , 60, -15., 15., 80, -20., 20., 0.)
  CALL hbook2( n+5,' True conversion zx fngr-coordinates '
&          , 60, -15., 15., 80, -20., 20., 0.)
  CALL hbook2( n+6,' True conversion zy fngr-coordinates '
&          , 60, -15., 15., 80, -20., 20., 0.)
C.
  CALL hbook2(n+11,' Max loop = 1 ',29, 1., 30., 100, 0., 10., 0.)
  CALL hbook2(n+12,' Max loop = 2 ',29, 1., 30., 100, 0., 10., 0.)
  CALL hbook2(n+13,' Max loop = 3 ',29, 1., 30., 100, 0., 10., 0.)
  CALL hbook2(n+14,' Max loop = 4 ',29, 1., 30., 100, 0., 10., 0.)
  CALL hbook2(n+15,' Max loop = 5 ',29, 1., 30., 100, 0., 10., 0.)
  CALL hbook2(n+16,' Max loop = 6 ',29, 1., 30., 100, 0., 10., 0.)
  CALL hbook2(n+17,' Max loop = 7 ',29, 1., 30., 100, 0., 10., 0.)
  CALL hbook2(n+18,' Max loop = 8 ',29, 1., 30., 100, 0., 10., 0.)
  CALL hbook2(n+19,' Max loop = 9 ',29, 1., 30., 100, 0., 10., 0.)
  CALL hbook2(n+20,' Max loop = 10 ',29, 1., 30., 100, 0., 10., 0.)
C.
  n = 200
C.
  CALL hbook1(n+ 1,'Z-Stops in all col',1000,-TLrms,TLrms,0.)
  CALL hbook1(n+ 2,'R-Stops in targ entrance col',50,0.,Rrms/2.,0.)
  CALL hbook1(n+ 3,'R-Stops in targ exit      col',50,0.,Rrms/2.,0.)

```

```

      CALL hbook1(n+ 4,'TOF to TEND',200,0.,2.,0.)
      CALL hbook1(n+ 5,'Reaction z-pos',1000,-3*targetl,3*targetl,0.)
      CALL hbook1(n+ 6,'Beam Stops in target',1000,-TLrms,TLrms,0.)
      CALL hbook2(n+11,'stop/exit dist',
&                200,-TLrms,TLrms,20,0.,Rrms/2.,0.)
      CALL hbook2(n+12,'stop dist      ',
&                200,-TLrms,TLrms,20,0.,Rrms/2.,0.)
      CALL hbook2(n+13,'Reaction position R-pos vs z-pos ',
&                50,-3*targetl,3*targetl,50,0.,1.,0.)
      CALL hbook2(n+14,'Exit spot',
&                50,-Rrms/2.,Rrms/2.,50,-Rrms/2.,Rrms/2.,0.)
      CALL hbook2(n+15,'cosx vs X',
&                100,-Rrms/2.,Rrms/2.,100,-.02,.02,0.)
      CALL hbook2(n+16,'cosy vs Y',
&                100,-Rrms/2.,Rrms/2.,100,-.02,.02,0.)
      CALL hbook2(n+17,'cosx vs Xtarg',
&                100,-1.,1.,100,-.02,.02,0.)
      CALL hbook2(n+18,'cosy vs Ytarg',
&                100,-1.,1.,100,-.02,.02,0.)
C.
C.
      CALL hbook1(n+ 21,' Ini - x - Recoils ',100,-2.0,2.0,0.0)
      CALL hbook1(n+ 22,' Ini - y - Recoils ',100,-2.0,2.0,0.0)
C.
      CALL hbook1(n+ 23,' Ini - dx - Recoils',100,-100.0,100.0,0.0)
      CALL hbook1(n+ 24,' Ini - dy - Recoils',100,-100.0,100.0,0.0)
      CALL hbook1(n+ 25,' Momentum spread (%) -Recoils',100,-5.0,5.0,0.0)
C.
C.  Strip detector separate spectra
C.    n = 300
C.    nstrip = 16
C.    do i = 1, nstrip
C.      strip = 'x-strip('//num(i)//')'
C.      CALL hbook1(n+i,strip,16,0.,16.,0.0)
C.      strip = 'y-strip('//num(i)//')'
C.      CALL hbook1(n+nstrip+i,strip,16,0.,16.,0.0)
C.    enddo
C.
C.  Strip detector hit patterns
C.    n = 400

```

```

C.      nstrip = 16
C.      CALL hbook1(n+1,'x-strip hit pattern',16,0.,16.,0.0)
C.      CALL hbook1(n+2,'y-strip hit pattern',16,0.,16.,0.0)

C.      user defined angular distribution

C.      CALL hbfun1(250,'ang. dist.',1000,-1.,1.,angdist)

C.      cross-section function and probability density
      lm1 = (1.-0.005)*beamo*m2/(m1+m2)
      lm2 = (1.+3.*(emax/beamenerg))*beamenerg*m2/(m1+m2)
      print*, m1, m2, beamenerg, beamo, el
      CALL hbfun1(500,'capture cross-section',1000.,lm1,
+               lm2,sig)
      CALL hcopy(500,501,'')

C.      CM energy distribution
      CALL hbook1(502,'CM energy distribution',1000,beamo*(1.-0.01),
+               beamenerg*(1.+0.01),0.0)

C.      Beam caught after D1, scaler
      CALL hbook1(503,'Caught beam',1,1.,2.,0.0)

C.      Recoils which don't make it to ENDV
      CALL hbook2(504,'Stopped recoil pos.',100,-2000.,1000.,100,
+               -1000.,100,0.0)

C.
C.--> New ntuples 07.07.03
C.
C 'History' ntuple
      CALL HBNT(1000,'HISTORY',' ')
      CALL HBNAME(1000,'HISTORY',E_int,'E_int:R,E_rec:R,E_g(15):R,' //
+               'E_gp(15):R,cost_g(15):R,phi_g(15):R,' //
+               'cost_gp(15):R,cost_r:R,cosp_r:R,' //
+               'Nodec:I,' //
+               'react:I,x_r:R,y_r:R,z_r:R')

C --> Define other ntuples

```

```

C.
      If(iswit(9).eq.2)then
C Gamma -HI coincidence ntuple
      CALL HBOOKN (100,'Gamma-HI',nvar10,'//HBOOK',1024,CHTAGS)
C.
C.-->   Setup parameters - filled once at the end of UGINIT
C.
      CALL HBNT(998,'GBOX Geant Setup Ntuple',' ')
      CALL HBNAME(998,'U_GEOM',x1_fngr,CH_U_GEOM)
C.
C.-->   Event variables - filled every event at the end of GUDIGI
C.
      CALL HBNT(999,'GBOX Geant Event Ntuple',' ')
      CALL HBNAME(999,'GBOX_INF',melem_gbox,CH_GBOX_INFO)
C.
      Endif
C.
      RETURN
      END
C.
      SUBROUTINE namfil(wstart,inum,wend,wfile)
C.
C-----
C      Subroutine to create a file name containing a number inbedded
C
C      Input arg :      wstart  - Character string to be placed at the
C                             start of the file name.
C
C                             inum   - I*4 to be converted to ASCII character
C                             and appended to 'wstart' in file name.
C                             No blanks or zeroes will be placed
C                             before the number.
C
C                             wend   - Character string to terminate the file
C                             name.
C
C      Output arg:      wfile   - Character string containing the file
C                             name. The calling program must have
C                             defined 'wfile' big enough to contain
C                             all characters.

```

```
C
C-----
C.
      IMPLICIT none
C.
      INTEGER inum, ifin, indexn
C.
      CHARACTER *(*) wstart, wend, wfile
      CHARACTER*10  wnum
C.
      Write(wnum,10)inum
10 Format(I10)
C.
      ifin = indexn(wnum)
C.
      wfile = wstart//wnum(ifin:10)//wend
C.
      RETURN
      END
C.
```

Appendix F - subroutine 'ugeo_ionc'

```

      SUBROUTINE ugeo_ionc(pos,irot)
C.
*****
*
*           Define simple ion chamber
*
*****
C.
C.
      IMPLICIT none
C.
      INTEGER ivol, irot
C.
      REAL shape(3), pos(3), p1, p2, p3
C.
      shape( 1) = 8.7
      shape( 2) = 6.78
      shape( 3) = 20.05
      p1 = pos(1)
      p2 = pos(2) + 0.75
      p3 = pos(3)
      CALL gsvolu ('ICAC', 'BOX ', 6, shape, 3, ivol)
      CALL gsatt('ICAC','SEEN',1)
C.
      shape(1) = 4.5
      shape(2) = 5.25
      shape(3) = 12.6
      CALL gsvolu('ICGB', 'BOX ', 21, shape, 3, ivol)
      CALL gsatt('ICGB','SEEN',1)
C.
      shape(1) = 0.
      shape(2) = 2.5
      shape(3) = 5.25
      CALL gsvolu('ICVT', 'TUBE', 1, shape, 3, ivol)
      CALL gsatt('ICVT','SEEN',1)
C.
      shape(1) = 4.5
      shape(2) = 5.25

```

```

      shape(3) = 0.1
      CALL gsvolu('ICDL', 'BOX ', 21, shape, 3, ivol)
      CALL gsatt('ICDL','SEEN',1)
C.
      shape(1) = 0.
      shape(2) = 2.5
      shape(3) = 0.00141
      CALL gsvolu('ICMW', 'TUBE', 22, shape, 3, ivol)
      CALL gsatt('ICMW','SEEN',1)
C.
      CALL gspos('ICMW',1,'ICVT',0,0,-5.24859,irot,'ONLY')
      CALL gspos('ICDL',1,'ICGB',0,0,12.5,irot,'ONLY')
      CALL gspos('ICGB',1,'ICAC',0,0,3.05,irot,'ONLY')
      CALL gspos('ICVT',1,'ICAC',0,-0.75,-14.8,irot,'ONLY')
      CALL gspos('ICAC',1,'WRLD',p1,p2,p3,irot,'ONLY')
C.
      999 RETURN
      END
C.

```

Appendix G - subroutine 'rescale.f'

```
Subroutine Rescale(Id1,Id2,X1,X2,Nbin,Bw,Chtitl2)
Character*32 Chtitl, Chtitl2
Logical Hexist
Call Hgive(Id1,Chtitl,Ncx,Xmin,Xmax,Ncy,Ymin,Ymax,Nwt,Loc)
If(Hexist(Id2)) Call Hdelet(Id2)
Call Hbook1(Id2,Chtitl2,Nbin,X1,X2,0.)
Do I=1,Ncx
  Call Hix(Id1,I,X)
  XI = X + Bw
  W = Hx(Id1,XI)
  CALL Hfill(Id2,XI,0.,W)
Enddo
End
```


Bibliography

- [1] Ruiz, C, **Aspects of Nuclear Phenomena Under Explosive Astrophysical Conditions**, PhD thesis, University of Edinburgh (2003)
- [2] Laird, A, **An investigation on the $d(^{18}\text{Ne}, ^{19}\text{Ne}^*)p$ reaction and its astrophysical relevance**, PhD thesis, University of Edinburgh (2000)
- [3] Schombert J, <http://zebu.uoregon.edu/~js/ast122/lectures/lec11.html>, CNO Cycle
- [4] Champagne, A, and Wiescher, M, *Ann. Rev. Nucl. Part. Sci.* **42** (1992) 39
- [5] Laird, A, private communication (2003)
- [6] www.triumf.ca/welcome/about.html, About TRIUMF
- [7] Kost, C, and Jones, F, www.triumf.info/public/about/background.html, TRIUMF Backgrounder, (2003)
- [8] www.triumf.ca/isac/bluepost1.pdf, The ISAC Radioactive Beam Facility in Canada: Progress and Plans
- [9] Chen, A, www.triumf.ca/isac/chenweb.pdf, ISAC: Radioactive Beams at TRIUMF
- [10] Kost, C, and Jones, F, www.triumf.info/public/about/isac.html, The Isotope Separation and ACceleration (ISAC) facility, (2003)

- [11] Neish, C, <http://www.triumf.ca/dragon/system.html>, The DRAGON System, (2003)
- [12] Neish, C, **Novae in a test-tube: Investigating the $^{21}\text{Na}(p,\gamma)^{22}\text{Mg}$ reaction at TRIUMF's ISAC facility**, Final report (internal), (2003)
- [13] Hutcheon, D et al., Nuclear Instruments and Methods in Physics Research A **498** (2003) 190-210
- [14] Gigliotti, D, **Calibration and Simulation of a Gamma Array for DRAGON at ISAC**, Master's thesis, University Of Northern British Columbia (in preparation) (2004)
- [15] Wrede, C, **A Double Sided Silicon Strip Detector as an end detector for the DRAGON recoil mass separator**, Master's thesis, Simon Fraser University (2003)
- [16] Frisch, O, British Atomic Energy Report **BR-49** (1944)
- [17] Knoll G, Radiation Detection And Measurement, 3rd Edition, page 152-3, (2000 John Wiley and Sons Inc.)
- [18] Dale, C, **The DRAGON Detectors**, Final report (internal),(1998)
- [19] Lamey, M, private communication (2003)
- [20] Hutcheon, D, http://www.triumf.ca/dragon/sep_hardware.html, User's Manual for DRAGON Separator Hardware, (2003)
- [21] Hutcheon, D, http://www.triumf.ca/dragon/sep_tuning.html, User's Manual for Tuning the DRAGON Separator, (2003)
- [22] Amaudraz, P, <http://pierre.triumf.ca/midas/intro.html>, What is MIDAS?

- [23] Rogers, J, http://www.triumf.ca/dragon/MIDAS_analyzer.html, The DRAGON/MIDAS Analyser, (2003)
- [24] Ruiz, C, private communication (2003)
- [25] King, J et al., Nuclear Physics A 567 (1994) 354-376
- [26] Apostolakis, J, <http://wwwasd.web.cern.ch/wwwasd/geant/>, GEANT - Detector Description and Simulation Tool
- [27] www2.bnl.gov/ton/cgi-bin/nuclide?nuc=C13
- [28] www2.bnl.gov/ton/cgi-bin/nuclide?nuc=N14
- [29] Nuclear Physics A 523
- [30] <http://physics.nist.gov/cgi-bin/Star/compos.pl?matno=222>
- [31] http://www.handsonplastics.com/hands_on_plastics/intro_to_plastics/teachers.html, Common Plastic Resins Used in Packaging: Polyethylene Terephthalate (PET or PETE)
- [32] <http://www.hychill.com/pdf/chemiso.pdf>, Chemical Properties of Isobutane
- [33] <http://www.geocities.com/thesciencefiles/carbon/compounds.html>, Hydrocarbons
- [34] <http://www-collider.physics.ucla.edu/cms/cmsim/cmsim/manual/www/cms113/node199.html>, Examples of Material Mixtures, (1998)
- [35] Bishop, S, private communication (2003)
- [36] Jewett, C, PhD thesis, Colorado School Of Mines, (in preparation) (2004)
- [37] Sprenger, H, private communication (2003)

- [38] Gumplinger, P, private communication (2003)
- [39] CERNlib, http://wwwasd.web.cern.ch/wwwasd/cernlib/download/2003_source/src/geant-321/gtrak/granor.F
- [40] CERNlib, <http://wwwasd.web.cern.ch/wwwasd/cgi-bin/listpawfaqs.pl/14>, How to re-scale an histogram?